meteorology research, inc. • 2420 n. lake ave. • altadena, calif.

STUDY & MODIFICATION OF CONVECTIVE STORMS

Report No. 2
Contract No. DA 36-039 SC-89066

Order No. 265-62, Project Code No. 8900
Dept. of the Army Project 3A99-27-005-06

Final Report Covering the Period
April 1, 1962 - March 30, 1963

U. S. Army Electronic Research & Development Laboratory
Fort Monmouth, New Jersey

Study and Modification of Convective Storms

Final Report, Report No. 2

Contract No. DA-36-039 SC-89066

ARPA order No. 265-62

Dept. of the Army Project No. 3A99-27-005-06

Project Code No. 8900

Final Report, covering the period April 1, 1962 to March 30, 1963

Object of the Research: To obtain a quantitative understanding of the physical mechanisms involved in convective storms (nucleation, hydrometeor development, electrification, cloud and storm dynamics), both for natural storms and storms which have been artificially modified.

This report prepared by: Dr. P. B. MacCready, Jr.
Dr. T. B. Smith
Mr. C. J. Todd
Dr. Chen-Wu Chien
Miss Betsy Woodward

TABLE OF CONTENTS

PURPOSE

This basic research program is directed toward obtaining a quantitative and qualitative understanding of the physical mechanisms involved in natural and modified convective storms. The various phases of the convective phenomena are considered from a balanced, integrated viewpoint. The aim is to investigate and understand critical factors such as: nucleation, hydrometeor development, electrification, cloud dynamics, environmental effects, and the complex interrelations between all these separate items. The research technique is built around the concept of an outdoor cloud laboratory, treating the clouds and storms in the simplest possible real situations. Seeding is used as a diagnostic research tool to permit observations of direct and secondary effects on hydrometeor development, electrification, and cloud dynamics.

The program necessarily has entailed the development of some equipment and field study techniques. Success of the field program relies on an extensive coordinated effort using radar, other ground observations, and light aircraft systems. These tools must be coordinated so they can probe the dominant factors simultaneously. Certain critical subjects have received special emphasis up to the present time and the future course of the program will be to focus even more sharply on the specific areas which are now being shown to be critical.

The first year of this two-year program is divided into four phases: (1) the planning, preparations, and instrumentation techniques development; (2) the field program itself; (3) the data analysis; and (4) the initial preparations for the 1963 field season. The details of phase (1) and much of phase (2) were contained in Interim Report No. 1. This present report discusses phase (1) only briefly, continues the presentation of phase (2), and covers phases (3) and (4). Data reduction is included in phases (2) and (3).

ABSTRACT

This final report describes the first year of progress under the contract. The work consists of the development of field research and analysis techniques and a basic research investigation of cloud physics, cloud dynamics, and related cloud modification, based on a summer field program at Flagstaff, Arizona. The report describes the over-all field research system, the instrumentation details, data handling and analysis methods, and the research results of the various studies which go to make up the whole program. Data summaries and field work organization, given in the first Interim Report, are not covered here.

During the six-week field program the sub-cloud layer and representative cumulus clouds of all sizes were investigated using a coordinated system of two instrumented aircraft, two ground radars, and a ground network. There were cases of small and large cloud seeding by dry ice drops and by silver iodide from ground and from an additional aircraft. The investigations were coordinated with the studies of USAERDL, which used three aircraft, a limited ground network, and several lightning study stations, for probing lightning development and characteristics, IR measured ground temperatures, condensation nuclei and seeding with condensation nuclei apparatus and chaff.

The following subjects are covered in this report:

1. Field program and analysis. The coordinated ground-air field research system worked well to meet the project aims. The new measurement techniques and instrumentation proved appropriate for the specific studies, and the analysis techniques have been advanced to where they are satisfactory for a program of such broad scope.

2. Daily analyses. Cloud particle types, concentrations, and sizes have been studied for a number of seeded and unseeded clouds, in conjunction with the analysis of records from the camera network, radar, and the aircraft probing flights. The studies pertaining to flights on four days are presented. They show a) Under some conditions the ice crystals nucleated by seeding could be identified by location, concentration, and type of crystal with certainty. b) Natural ice crystals formed either higher in the cloud or in a mature neighboring cloud, could descend in downcurrents and produce observable ice crystal concentrations to near the 0C level. c) The water droplet concentrations in the undiluted parts of the cumulus cloud were high, usually 300 to 700/cm^3 . d) In most cumulus observed the droplets were small (less than 20μ in diameter) indicating no tendency towards coalescence precipitation in the water

phase. e) There were substantial regions of undiluted updraft cores at heights of several thousand feet above cloud base, and f) The effect of glaciation on buoyancy could be detected.

3. Cell dynamics. Aircraft measurements of the temperature, moisture, and flow regimes in and around the cumulus clouds are compared with measurements of the cloud developments as observed from time-lapse cameras. Buoyancy calculations from the aircraft data are related to rate of growth theory derived from laboratory models, and reasonable agreement is achieved. Details are given for a) August 15, with light winds at all levels, when cells with moderate buoyancy emerged at medium rise rates from the cloud mass and persisted in their rise rates, and b) July 27, with strong wind shear aloft, when strongly buoyant cells emerged rapidly but decayed quickly in the strong shear. On July 27 a cell seeded with dry ice rose faster than unseeded cells, and left an ice anvil while unseeded cells did not.

4. Mountain wake studies. Aircraft and ground mesoscale measurements demonstrated a distinct wake effect of the San Francisco peaks on days with moderate winds. Beginning in mid-morning the wake flow pattern in the wake helps to collect the heat supply from the lower layers into a localized convergent area downwind of the peaks, where a near-continuous updraft may exist for several hours. The wake effect exists initially in stable conditions when the strong upper flow is dynamically somewhat disconnected from the low level flow immediately downwind of the mountains. Surface heating in the lee of the mountain emphasizes the convergence flow but promotes vertical convective mixing which finally destroys the wake effect. In the afternoon as the upwind air becomes more stable the wake flow may be re-established, again promoting continuous cumulus development in the lee of the peaks.

5. Slope studies. Airflows up the mountain slopes and into cumulus clouds were investigated by aircraft traverses, surface measurements, the motions of balloons tethered at 1000 feet, and time-lapse photographs. Consistent, identifiable, large updraft areas were found which lasted for long periods and drifted slowly upslope. These regions became more extensive and better organized as the morning progressed and the slope heating increased.

6. Atmospheric electricity. Data from ground-based potential gradient units were supplied for USAERDL studies. Also aircraft measurements of hydrometeor charge and other electrification variables were made in conjunction with the ARG-NSF program. It was found that a) the charge on ice hydrometeors was predominantly positive, both in the early stages

of development within the supercooled clouds and in later stages below the clouds, b) the hydrometeors switched rather abruptly to negative in the last stages of their melting below cloud, and c) the maximum charge magnitudes in ice and water were apparently limited by hydrometeor size. Subsequent laboratory studies on charging during melting showed a reproducibly smaller effect of the wrong sign.

Recommendations are presented for more critical studies during the second year of the program. The field studies will then be materially benefited by the availability of an M-33 dual tracking and search radar, and from the technique developments evolving from the first year, as well as from advances in basic understanding of the interactions between cloud dynamics and cloud microphysics for seeded and unseeded situations.

PUBLICATIONS, LECTURES, REPORTS, & CONFERENCES

There have been no publications as yet under this contract.

An informal memorandum report, "MRI and ARC Memorandum on 1962 Flagstaff Cumulus Project, June 9, 1962" was circulated to all people related to the program to facilitate coordination of the field phase.

An informal report "Informal Interim Report on Continuous Cloud Particle Sampler Research," August 27, 1962, by C. J. Todd and E. E. Hindman II was submitted to ONR and NRL. It covers theoretical and laboratory development as well as the field tests conducted at Flagstaff.

Interim Report No. 1, "Study and Modification of Convective Storms", April 1 to September 30, 1962 was submitted in October, 1962. This report described the summer field program, cataloged the data collected, and included preliminary conclusions from the data which had been analyzed.

P. MacCready and H. Selvidge of MRI held three conferences with Dr. Weickmann of USAERDL pertaining to this program. The first, an unofficial one prior to the official start of the project, was at Flagstaff on February 18 and 19, 1962, for the purpose of checking the field site and for preliminary planning and coordination of the whole program. The next was at USAERDL, Belmar, N. J., April 30, 1962. Its subject was further detailed planning of the extensive coordinated program. The third conference was at Belmar on September 17, 1962, and involved a review of the first field season, together with planning for the analysis phase of the program. A fourth visit by H. Selvidge on November 28, 1962, included a discussion of the preliminary results of the field data. Dr. H. Weickmann and Dr. H. Kasemir visited MRI's main office at Altadena from December 11 to December 13, 1962 to discuss further the field data and to arrange for data exchanges. Additional informal conferences occurred when principal investigators met at general scientific meetings.

At Flagstaff during July and August there was a series of seven semi-formal meetings attended by all interested members of the MRI-ARG and USAERDL groups and by visitors. All meetings were held in the conference room of the Research Center of the Museum of Northern Arizona. One meeting, the first, was solely a general coordination and planning conference. In most of the other meetings there would be some project business plus technical or general interest talks by investigators and visitors. The following gave presentations:

Dr. H. Weickmann, USAERDL - Greenland Meteorology
Dr. V. Schaefer, NYSU - The Special Student Program at the Atmospheric Science Center, N. Y. State University
Dr. P. Squires, NCAR - Convection Models, and NCAR
Mr. D. Sartor, NCAR - Electrification by Drop Induction
Mr. B. McLean, AMS - Educational Science Films
Mr. D. M. Fuquay, USFS - The USFS Cloud Electrification Modification Program
Mr. Taylor, USFS - Lightning Damage to Trees
Mr. R. G. Baughman, USFS - Statistical Results of the USFS Seeding Program
Dr. T. B. Smith, MRI - Aircraft Wakes
Mr. G. Ettenheim, MRI - (as of 10-1-62) The Arcata Fog Modification Program
Dr. C. E. Anderson, Douglas Aircraft - Douglas Programs and Convection
Dr. R. Koenig, Douglas Aircraft - Cumulus Glaciation on the University of Chicago Seeding Project

DISCUSSION

A. Introduction

This report summarizes MRI activities during the first year of Project Baton support of the investigation at Flagstaff. Various conclusions can be drawn at this stage of the program, but perhaps the development of the techniques by which the ultimate program goals can be realized should be considered as the main result. The study and modification of convective storms is necessarily a program of broad scope. Both meteorological results and the research system developed are presented here.

It has been necessary to divide this report into various sections so that the subjects could be presented with sufficient clarity. Since no one part of the report can be completely separated from the rest of the program, many of the MRI personnel have contributed to each part. The primary responsibility for writing certain of the sections is as follows:

Instrumentation: P. B. MacCready, Jr.
Data Reduction: C. J. Todd
Daily Analyses: C. J. Todd and C. W. Chien
Cell Dynamics: B. Woodward
Mountain Wake: T. B. Smith
Slope Studies: T. B. Smith
Atmospheric Electricity: P. B. MacCready, Jr.

Analysis of data collected during the summer of 1962 will continue, even though the 1963 data will be added in the near future. Each analysis adds new information and helps to complete or clarify the total picture. Plans for the 1963 field program and analysis program are implicit in the following sections. Since techniques are in a constant state of development or evolution, the preparations in instrumentation, field procedures, and analysis are subject to change as a result of new concepts and changing needs.

In the written report the study of seeding has been emphasized. A particular attempt has been made to stress physical concepts of cloud modification rather than the applications of cloud seeding. Deliberate attempts have been made to study what, when and where physical changes occur inside clouds as a result of various types, amounts and techniques of seeding.

A comprehensive 20-minute movie is also part of the final report. The movie is intended to demonstrate the instrumentation, field operations, and data handling in the field. It is not intended to show results from the research effort.

The report will cover such techniques and results as using a cloud as a natural cold box for experimentation with AgI generators, spirals up 9000 feet inside clouds showing non-dilution of the cloud core, and measuring heat buoyancy due to glaciation.

Much of the information concerning instrumentation, field techniques, and analysis procedures has been reported in the Interim Report No. 1 covering the period April 1 - September 30, 1962 and will not be repeated in the final report.

B. History and Acknowledgments

On April 1, 1962 Meteorology Research, Inc. began final preparations for the summer field program "Study and Modification of Convective Storms" under Army contract at Flagstaff, Arizona.

MRI has had previous background and experience in studying Flagstaff storms. These earlier experiences proved invaluable in organizing and preparing for the field program and the analysis program which followed.

MRI first worked at Flagstaff with the U. S. Forest Service on Project Skyfire in 1956, and in 1958 worked on a study of cloud electrification at Flagstaff under an AEC contract. During the summer of 1959 and 1960 MRI participated in the GRD-USAF "Hi-Cue" program of convective storm studies. Since 1959 ARG, an MRI affiliate, has worked on cumulus cloud studies at Flagstaff under NSF sponsorship. This program was continued through the summer of 1962. These studies are to be reported on shortly in a report to NSF.

Other groups and organizations have cooperated extensively in the 1962 field program, and MRI wishes to recognize and thank those who contributed in the past and present to the success of this program.

The U. S. Air Force, AFCRL, made a U-2 available to the project on four days in cooperation with their studies of the summer monsoon in the southwest United States.

The Fire Research Laboratory of the U. S. Forest Service in Missoula, Montana, provided equipment for massive silver iodide seeding and sent a research group under Mr. D. M. Fuquay to participate in the project.

Dr. Vincent J. Schaefer and eight student members of the NSF-State University of New York Atmospheric Sciences Center participated in the program.

Dr. H. Weickmann and Dr. H. Kasemir of the U. S. Army Electronic Research and Development Laboratory of Fort Monmouth, New Jersey conducted cooperative programs using aircraft, ground atmospheric electricity network, and other surface observations.

The 1963 Flagstaff field program will continue to be supported by most or all of these same agencies and other groups may participate and augment the total field effort.

The NSF study has provided strong complementary support to the ARPA study. Likewise the NSF study has benefited substantially from cooperation with ARPA studies during the 1962 project.

C. Objective and Scope

The over-all aim of the cumulus studies at Flagstaff for Project Baton is to gain a physical understanding of the microphysics and dynamics of convective storms, both natural and artificially modified. As far as possible the physical understanding should be advanced to yield a quantitative picture of the interrelationship of dominant factors. One long range aim of such work is the eventual modification of such clouds for practical purposes. Cloud seeding is being used now as a research tool; the eventual practical utilization must be built on the framework of adequate physical understanding bolstered by the sort of quantitative data which can make modification a true engineering science.

The present Flagstaff studies form a link in the long chain of cloud investigations there by MRI and the affiliated Atmospheric Research Group. The program philosophy has always followed the plan of obtaining a physical understanding of dominant mechanisms. In the first years only small clouds were studied. As techniques, understanding, and resources grew, it was possible to study the larger, more complex, clouds profitably. The program accent has now evolved more toward studying the cloud dynamics, while still simultaneously considering the more specialized subjects emphasized in previous years.

Flagstaff is considered as an outdoor cloud laboratory. The isolated San Francisco Peaks form an orographic and heat source feature which helps emphasize certain meteorological factors and also helps concentrate repeatable cloud developments in one spot where they can be intensively studied. The numerous complex variables cannot be duplicated in proper interrelationsh in a confined laboratory. Thus the laboratory gear is brought to Flagstaff. The apparatus required is extensive because no potentially-dominant factor can be ignored. The program constitutes the most detailed investigation ever made on the details of cumulus development. In spite of the completeness of the program, nature's complexity still makes it very difficult to derive definitive answers.

This report describes the most productive year so far in the Flagstaff studies.

D. Instrumentation

General

One aim of Project Baton is to develop practical field investigation techniques, another aim is to use the techniques for various cloud physics, cloud dynamics, and cloud modification projects. Thus the instrumentation description is both of the equipment which was used in the 1962 field program, and, briefly, the improved equipment to be used in the summer of 1963.

The whole instrument system (instruments and the techniques of their use) is necessarily a compromise between the type of research projects to be undertaken, the state of the instrument art, and the time and money available for the equipment development and checking. In 1962 many instrumentation short cuts were required because of the project timing, and some development and debugging was required in the field. Gaps in the data and inaccuracies in some instances necessitated extra analysis effort subsequently. Nevertheless, the instrumentation system did prove to serve for the primary research tasks. The feasibility of the whole coordinated aircraft-radar-ground network system was demonstrated.

1962 System

The instrumentation system was designed to describe adequately the basic parameters pertaining to the development of small and moderate cumulus clouds and small thunderstorms, and to probe the microphysics of hydrometeor and electrification development. MRI provided two instrumented aircraft, a supercharged Aero-Commander (called Metro II) for seeding with dry ice pellets, and a more heavily instrumented Cessna 180 (called Metro I) for general studies. Two MRI 3.2 cm (Model MR-4) radars were employed, one for RHI cloud physics studies, the other for PPI use, especially for tracking the aircraft. The aircraft tracking with the PPI pencil beam was awkward but, with technique development, generally proved to be practical. The ground system included a network of time-lapse cameras, some with parabolic reflectors for whole sky use, and miscellaneous potential gradient, temperature, and wind recorders. The detailed list of items is given in the Interim Report. Fig. D-1 shows the geographical location of the main system elements.

Fig. D-2 depicts the isolated San Francisco Peaks as seen from the radar control headquarters at the Flagstaff Airport. Fig. D-3 shows the RHI radar, and Fig. D-4 pictures one of the whole sky camera stations, one of which was adjacent to the RHI radar. In Fig. D-5 is shown a zero lift balloon launching, typical of the measurement techniques involved in the special slope-effects study.

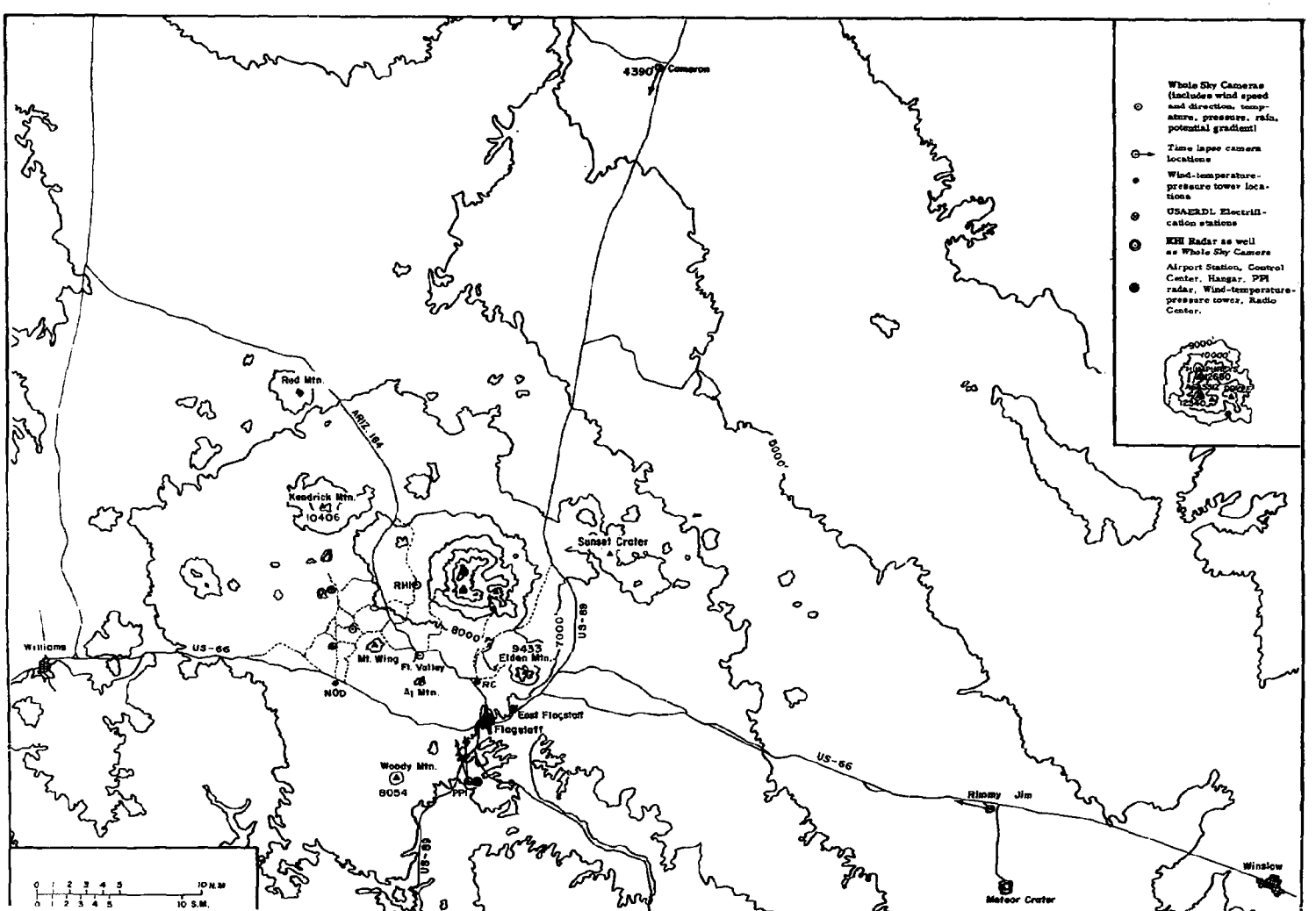
Whole Sky Cameras (includes wind speed and direction, temperature, pressure, rain, potential gradient)
Time lapse camera locations
Wind-temperature-pressure tower locations
USAERDL Electrification stations
KHI Radar as well as Whole Sky Camera
Airport Station, Control Center, Hangar, PPI radar, Wind-temperature-pressure tower, Radio Center.
4390
Cameron
Red Mtn.
ARIZ. 164
Kendrick Mtn.
10406
RHI
Sunset Crater
8000'
7000'
US-89
Williams
US-66
Mt. Wing
Ft. Valley
9433
Elden Mtn.
RC
NOD
A1 Mtn.
East Flagstaff
Flagstaff
Woody Mtn.
8054
PPI
US-89
US-66
Rimmy Jim
Winslow
Meteor Crater
0 1 2 3 4 5 10 N.M.
0 1 2 3 4 5 10 S.M.

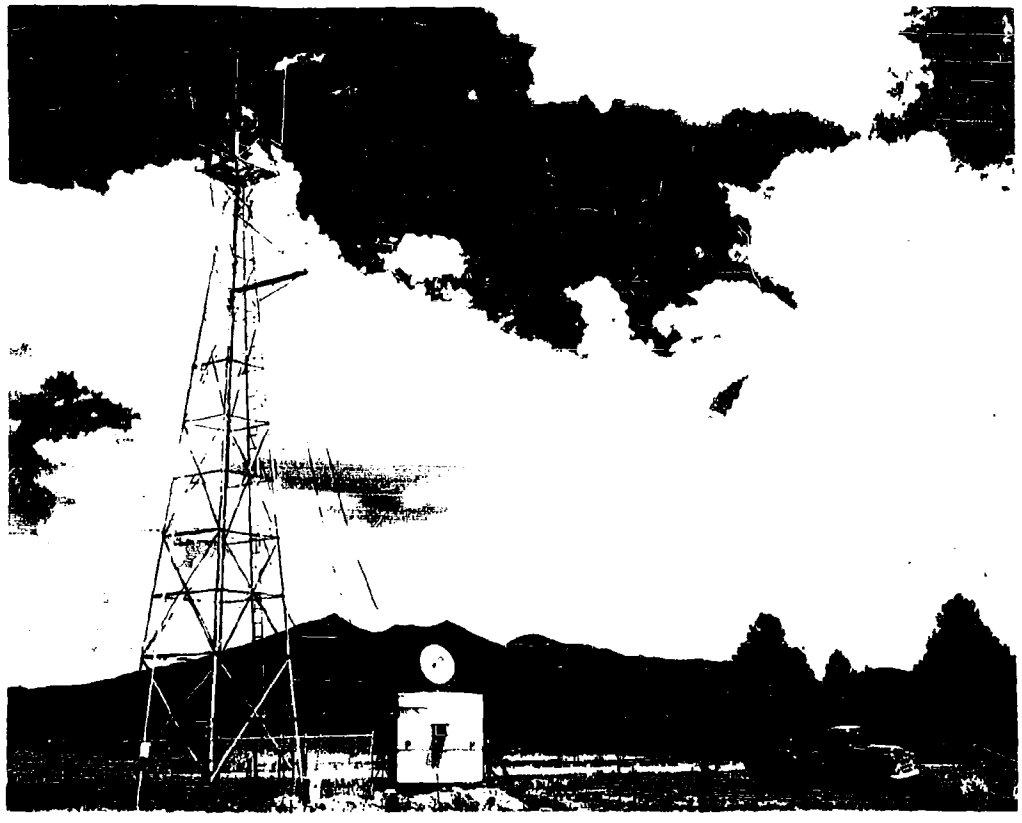

Fig. D-2. THE SAN FRANCISCO PEAKS

Looking north from the Flagstaff Airport. In the foreground are the radio beacon tower and the radar-trailer serving as control headquarters.

Fig. D-3. THE RHI RADAR

The trailer and pibal station were positioned on a knoll on the west skirt of the Peaks.

Fig. D-4. WHOLE SKY CAMERA SYSTEM

In addition to sky cover the camera photographs time, temperature, wind direction (A), and counts from the wind speed sensor (B). Potential gradient from probe (C) is recorded on a strip chart recorder.

Fig. D-5. SLOPE ZERO LIFT BALLOON RELEASE

Fig. D-6. SEMINAR AT THE RESEARCH CENTER

There were regular seminars held at the Research Center of the Museum of Northern Arizona to discuss Project Baton plans and results, and to hear about other interesting research by project personnel and visiting scientists. The seminar list is given in the Interim Report. Fig. D-6 shows one of the seminars.

Fig. D-7 shows a portion of the hangar used for data reduction and analysis. The dry ice crusher, Fig. D-8, is in another section of the hangar.

Special studies of mountain wakes and slope effects utilized the standard aircraft and ground network, but also required special measurements by simple balloon and ground observer techniques. These measurements are described in the appropriate sections.

1963 System

The fundamentals of the coordinated ground-air system is the same for 1963, but there are significant improvements. Instead of two instrumented aircraft only one will be employed, a supercharged Piper Apache This permits a considerably refined instrumentation package, which includes hydrometeor sizing apparatus, IR remote temperature equipment, and extra atmospheric electricity units, as well as improvements in the 1962 variables. The Apache has silver iodide pellet seeding apparatus.

An instrumented Cessna 180 will be used occasionally for seeding with silver iodide. Aircraft tracking and general monitoring will be done automatically with an M-33 radar, greatly improving tracking reliability, permitting faster operations, greatly reducing data reduction time, and facilitating balloon tracking. The other MRI radar will be exclusively used for cloud studies. The ground network will be similar to 1962, but refined.

Aircraft and Their Research and Seeding Operations

The unsupercharged Cessna 180, (see Fig. D-9, 13) with the most complete instrument system, was used for cloud penetrations up to true altitudes of about 24,000 feet, as well as subcloud studies. Its maximum practical operating altitude was in the 19,000-20,000 foot range; the higher operations came in spirals up within up-currents. The gas load was always kept at a minimum to conserve weight. The Cessna carried a continuous droplet sampler (Fig. D-16, 17), and a complete console-recorder system (Fig. D-14, 15) with a 2-pen Brush recorder cycled for multi-channel use. A magnetic tape recorder was attached for recording notes of the observer. Dry ice pellets were occasionally carried for dispensing out of the window by the observer. On a few flights the pilot flew solo and also served as the observer. The Cessna 180

Fig. D-7. FIELD ANALYSIS

Preliminary analysis and data handling area in the hangar at the airport.

Fig. D-8. DRY ICE CRUSHER

The dry ice crusher and sizing chute operating in the hangar.

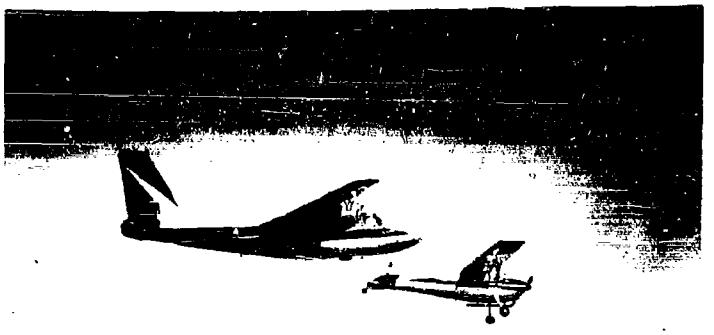

Fig. D-9. AERO-COMMANDER AND CESSNA 180

Fig. D-10. USFS AgI GENERATOR

U.S. Forest Service silver iodide generators mounted on each side of the wing of a Cessna 180.

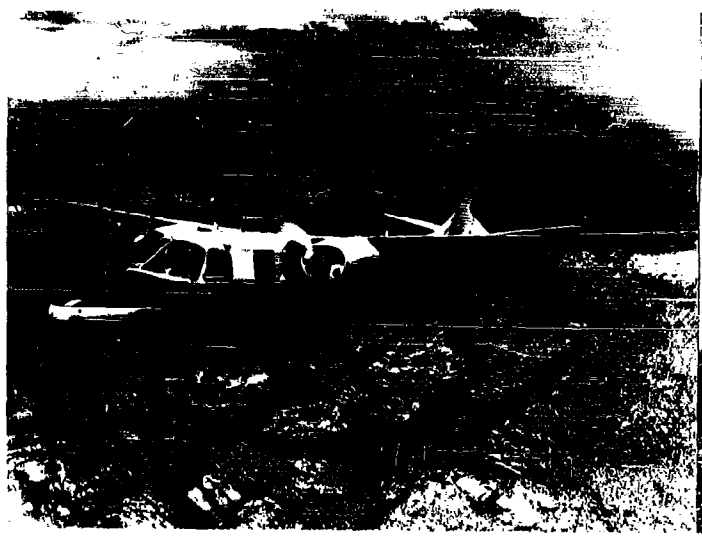

Fig. D-11. AERO-COMMANDER

The dry ice dispenser can be seen mounted through the main door of the Aero-Commander.

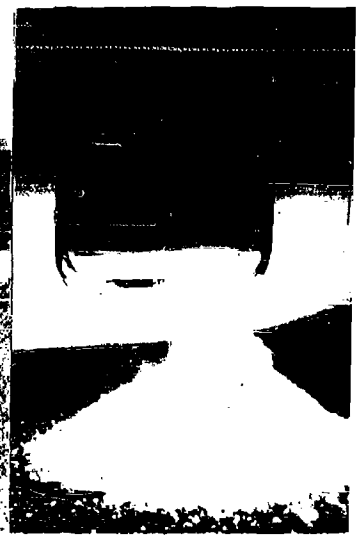

Fig. D-12.
DRY ICE DOOR OPEN

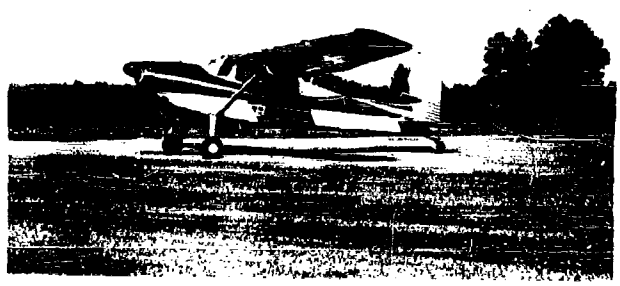

Fig. D-13. CESSNA 180

Sensors (see D-19) and the long exhaust tube of the smoke generator are shown.

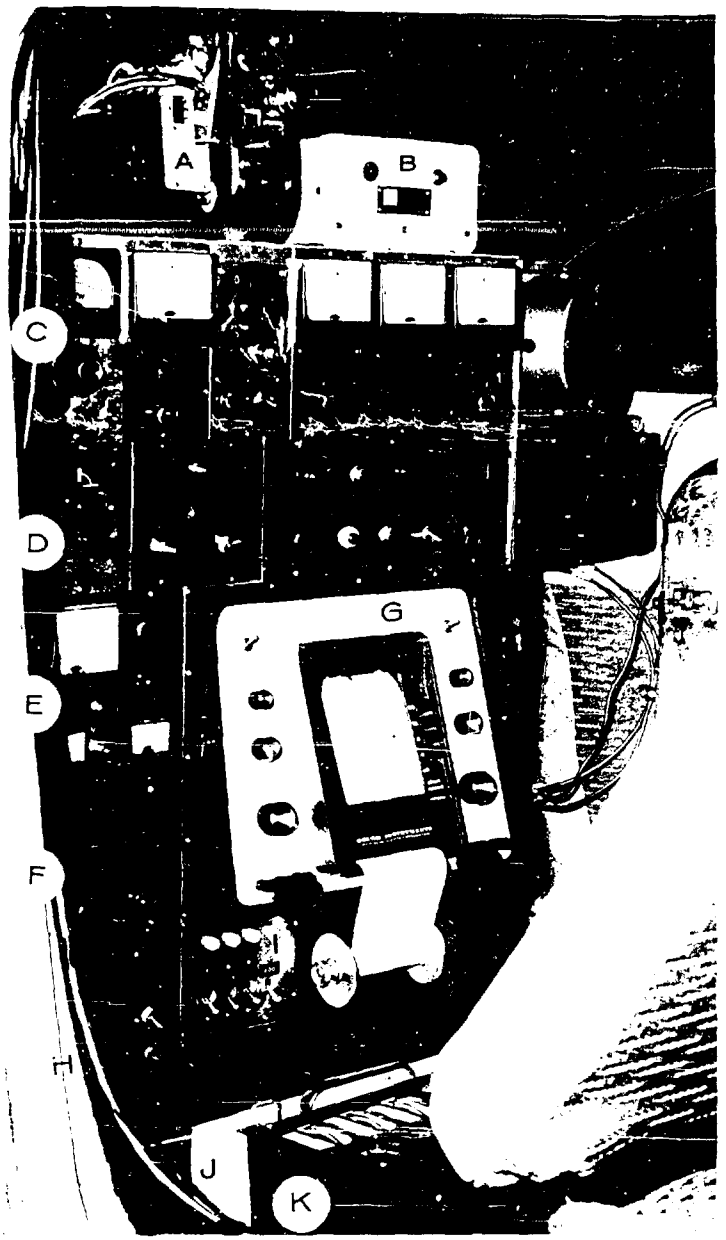

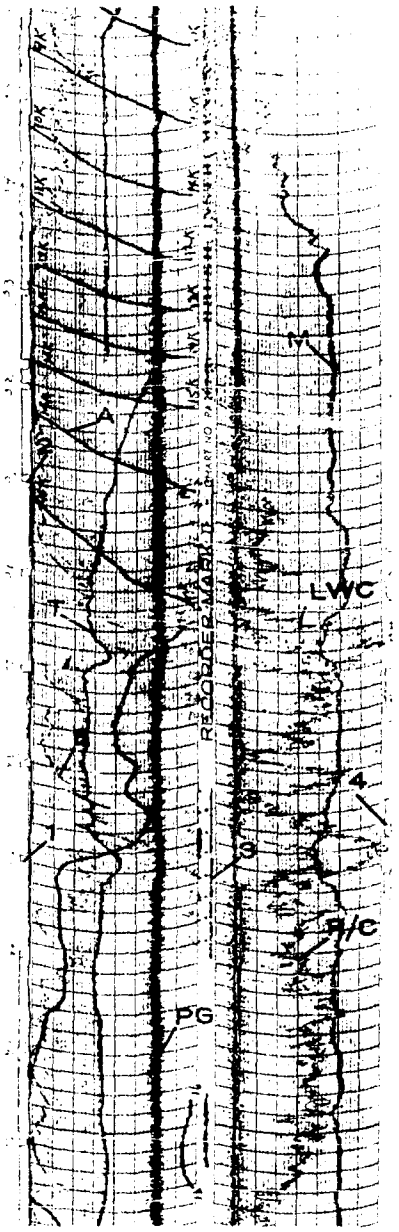

Fig. D-14. CESSNA 180 INSTRUMENT CONSOLE

Time-lapse camera (A),
Aircraft charge generator (B).
Row (C) left to right, liquid water content, aircraft charge, altimeter follower, potential gradient, turbulence, temperature.
Row (D) time, cycling controls, event controls.
Mixing ratio (E), rate of climb (F), Brush recorder (G), drop charge (H), power controls (I), time-lapse control (J), droplet sampler temperatures (K).

Fig. D-15. SAMPLE RECORD

KEY

LWC	liquid water
A	altitude
PG	pot. gradient
E	turbulence
T	temperature
M	mixing ratio
R/C	climb rate
1	minute mark
2	in cloud
3	droplet frame
4	event mark

could dispense an oil fog through an extended exhaust stack. This turned out to constitute a good indicator of turbulence in sub-cloud convection studies.

The Cessna demonstrated a reliable, all-weather capability in these studies. It was operated without damage in soft hail of moth-ball size, and, in slow flight, in extremely severe turbulence situations. Parachutes were always used. The plane was equipped with quick release doors for emergency exit. It had a constant flow re-breathing oxygen system.

The supercharged Aero-Commander (Fig. D-9, 11) would fly to altitudes of about 28,000 feet. It contained a continuous droplet sampler (Fig. D-18), a 6-channel Brush recorder system, and a magnetic tape voice recorder.

In addition to being used for a cloud probing aircraft, the Aero-Commander served for massive dry ice seeding. A large metal box in the midsection of the fuselage held dry ice pellets which had been crushed on the ground by the crusher shown in Fig. D-8. This GFE crusher was modified by MRI by adding an appropriate power motor, and removing the sizing screen which had caused excessive powdering of the dry ice. Some large pellets would come out of the crusher: they were reprocessed. Powder was removed by a sieving process. 1000 pounds of 50-pound blocks of dry ice would make about 500 pounds of pellets suitable for seeding. The pellets were released from a small door with longitudinal hinge set at the bottom of the main fuselage door opening, as shown in Fig. D-11, 12. The rate of release could be controlled crudely by carefully controlling the door opening handle. It was often necessary for the observer to use a shovel to move the dry ice from the far corner of the box toward the door. The pilot could help this by flying in a slipping attitude. Maximum amounts of somewhat over 500 pounds were released, in flight intervals varying from about 10 to 40 seconds.

Silver iodide seeding was conducted with two USFS generators (see Fuquay, 1960), from a Cessna 180 leased by MRI. This is shown in Fig. D-10. Silver iodide solution was consumed at a rate of approximately 4 gal/hr from each generator.

The roles of the non MRI-ARG aircraft, the U-2, the AD5, the R4D, and the C47, are covered in the Interim Report. That Report also describes some of the coordination procedures for the aircraft operation. Positioning even one aircraft at the correct time and place relative to a particular transient cloud development is difficult; handling the coordination of two or more is of course even more difficult. In general,

the more control that can be exerted from ground headquarters the better, but the different perspective on the clouds which the pilots and observers have dictates that much of the detailed flight planning rests in their hands. Coordination of two aircraft is best done by having them in visual contact before cloud penetrations. This was facilitated by establishing about a dozen prominent ground features over which the aircraft could rendezvous. It is presumed that the aircraft coordination in 1963 will be considerably eased because of the availability of an M-33 radar. In addition to providing automatic tracking of any individual target, the radar is equipped with a fan beam which can continually keep track of all aircraft and the precipitation echoes.

In 1963 a single supercharged Piper Apache is to be used as the instrumented research airplane, and a Cessna 180 as before for silver iodide seeding. The Apache combines the altitude range of the Aero-Commande with the slow speed and spiraling capability of the Cessna 180. It is to carry a 6-channel Brush recorder, cycled for 15-channel operation, appropriate instrument modules, cameras, continuous droplet collector, Naval Ordnance Test Station silver iodide "Roman candle" type generators for seeding from high altitude (the burning pellets will descend about 5000 feet), and a capability of minor dry ice seeding.

Continuous Droplet Collector 1962

This device is an important development of the long range MRI-ARG Flagstaff cumulus studies. It was developed primarily to provide a tool by which the presence of a few ice crystals in a supercooled water cloud could be established. It has attained this goal, and handled many additional jobs, too.

The collector or sampler continuously exposes a liquid plastic coating on a moving transparent film to cloud particles which impinge through a slit. The plastic covers over the droplets or crystals, and quickly hardens to make a permanent casting or replica of the particle. Small ice crystals are viewed in their exact size and shape; small liquid droplets are spherical, but with a replica diameter somewhat larger than the original droplet diameter. The particle record can be observed with 16 mm projection devices. The principle and some results are discussed by Todd(1961) and MacCready (1962) and detailed results from this past summer are given elsewhere in this report. The development of this technique has been furthered primarily through help from NSF and with recent NRL support, and the present USAERDL sponsorship has necessarily also contributed to the technique. (Appendix A discusses "Sampling Error and Calibration of the Continuous Cloud Particle Sampler".)

The method is still to be considered developmental, although useful results are obtained with it even in its present stage. In 1962 two types

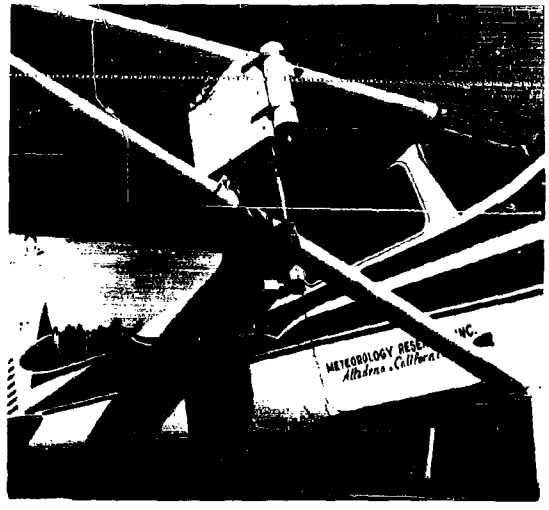

Fig. D-16. DROPLET COLLECTOR

Continuous droplet collector on the Cessna 180. Bottom potential gradient probe (A) and aircraft charge probe (B) are shown.

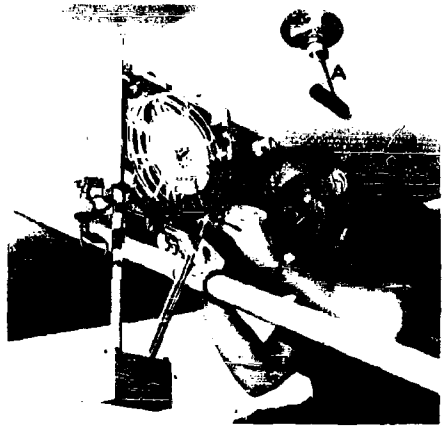

Fig. D-17. DROPLET COLLECTOR

Cover off collector on the Cessna 180. Arrow points to film exposure slit. Liquid water content probe (A) is shown.

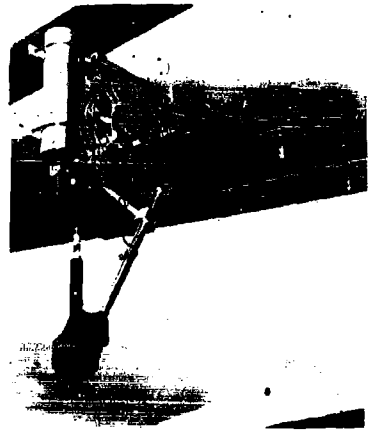

Fig. D-18. DROPLET COLLECTOR

Cover off the collector on the Aero-Commander.

of samplers or collectors were used. The one shown mounted on the Aero-Commander, Fig. D-18, uses a film precoated with the plastic Formvar. This film is dipped in a solvent tank containing chloroform or ethylene dichloride, shown at the bottom of the device in the photograph, which makes the plastic liquid. The film continues up the vertical tube, is momentarily exposed as it goes past the exposure slot, and is rewound on a takeup reel after passing through the extended drying tube. The unit shown on the Cessna 180, Fig. D-16 and 17, uses an alternate method. Uncoated film is used. It is coated with Formvar-solvent solution by a roller wheel in a coating tank which substitutes for the solvent tank of the Aero-Commander unit. Each method has special advantages and disadvantages pertaining to the physics and the engineering of the system. Details will be forthcoming in a report to NRL in June, 1963.

On several occasions the droplet collector was in operation in clouds seeded by USAERDL with chlorosulfonic acid. The droplet records showed distorted shapes which are presumably the result of some physical or chemical interaction between the acid and the Formvar solution; the droplet apparently spread on the Formvar, rather than vice versa as conventional. The records for these seedings have been provided to USAERDL so the seedings are not discussed in this report.

Continuous Droplet Collector 1963

The new unit is to be mounted within the Apache fuselage, and provision for immediate viewing of the replica film in flight is being made. The new design incorporates all the improvements arising out of the recent NRL sponsored droplet collector development program and cooperative NRL-MRI field tests.

The Recording Console

Fig. D-14 shows the instrument console mounted in place of the rear seat in the Cessna 180. All of the different instrument modules are indicated in the photograph. Each module is removable with two screws. A plug on the rear of each one fits into a socket and connects the module to the aircraft power system (12 volts), the sensor for the module, and the recorder cycling switch.

Each variable can be put continuously on one channel of the 2-channel recorder, or it can be cycled with other variables onto one channel. The usual chart speed is 1 inch per minute. Non-cycling operation is used during calibration and for hydrometeor charge measurements where high frequency pulses must be observed. Routinely the observer manually cycles through each variable on the chart to simplify the problem of later

identifying the individual chart traces (occasionally there is ambiguity in interpreting the overlapping traces). This manual cycling also includes zero and full scale calibrations.

Time marks are placed on the recorder chart at one minute intervals by a one minute clock triggering a side marker pen. Special event marks also appear on a side marker, controlled by pushbutton. Counts from the film movement monitoring counter in the continuous droplet sampler also appear on the chart record, as dots near the center.

Whenever the magnetic tape voice recorder is on, another event mark appears on the chart. The length of each transmission can be observed on the chart, and can also be found for each tape transmission. With random transmission lengths, it turns out to be simple to correlate which transmission goes with which position on the chart.

The photograph of Fig. D-14 was taken late in the project after a time lapse camera had been installed to show clouds, the aircraft instrument panel (so manifold pressure and turn gyros could be monitored), and an extra meter pertaining to simulated hydrometeor charging for which no recorder channel was available. Time lapse photography was at 10 seconds/frame regularly, and 1 second/frame for cloud penetrations.

The console in the Aero-Commander used identical modules, but did not require cycling because fewer variables were measured and because a 6-channel recorder was available.

For 1963 a cycled 6-channel recorder is to be used for up to 15 variables. (On some flights certain atmospheric electricity and hydrometeor size records will alternately be made on a separate, faster moving, 2-channel Brush recorder). Cycling is to be by means of reed relays controlled by a solid state timer system rather than by mechanical magnetic movement as was employed in 1962.

Altitude 1962

A standard high grade sensitive altimeter is used as the altitude sensor. The position of the most sensitive needle, 1000 feet per revolution, is sensed by a potentiometer keyed to the needle by a "light follower". A light bulb and photocell servo arrangement is used which positions a pointer on the potentiometer arm always over the needle. Thus no friction is put on the altimeter needle itself. The module can be seen on Fig. D-14. Full scale on the chart represents each 1000-foot increment of altitude, 0-1000 feet, 1000-2000 feet, etc. The altimeter time constant is on the order of 1 to 2 seconds. The altimeter is always set at 29.92" so as to read the standard atmosphere pressure, for ready conversion to

millibars, and the aircraft's altimeter is set the same way to simplify coordination between verbal directions and the chart record.

Altitude 1963

The same unit is employed, but it includes a vibrator on the altimeter to decrease lag and hysteresis which can otherwise occasionally amount to about ±50 feet, and temperature compensation is incorporated in the photocell system to minimize the need for any in-flight adjustment.

Compass Deviation 1963

A light follower, identical to that on the altimeter, is positioned on the face of a remote reading compass.

Temperature 1962

Temperature is sensed by a Veco #41A5 thermistor. The thermistor is set in an axial flow vortex housing to provide speed compensation for dynamic heating and to protect the thermistor somewhat from cloud moisture. The thermistor time constant is about 0.08 seconds. The vortex housing is a plastic replica of the unit developed by the Naval Research Laboratory. The housing can be seen in Fig. D-19 and 20. The unit has nine overlapping scales of 14C each, centered at -35, -25, -15, -5, +5, +15, +25, +35, and +45C. The thermistor is set in a Wheatstone bridge circuit, and balanced for zero output at the center temperature. The bridge nonlinearity and the thermistor nonlinearity interact in such a way that the bridge voltage output is a rather linear function of temperature for a range of about 15C below balance and 6C above balance; thus each of the ± 7C scales are essentially linear. The resistance-temperature curve is obtained with the thermistor set in oil baths of various temperatures. Then the balance and sensitivity of each scale is set to this curve with the aid of a resistance decade box.

The amplifier is a Philbrick P-65 used as an operational amplifier. The amplifier gain is set about 10, from ±80 millivolts from the bridge to ± 0.8 volts output. The feedback puts the input impedance in the multi-megohm range, which keeps the bridge from being loaded down even at the lowest temperature scale where the thermistor resistance is in the range of 10^5 ohms.

The vortex housing is adjusted experimentally to give perfect speed correction of temperature. In smooth air, the aircraft is flown at high speed at a certain altitude, and then throttled back but kept at the same altitude and hence at the same temperature. If the vortex temperature correction is right, the indicated temperature will not vary with

speed. If it does vary, the size of the front restrictor knob on the vortex housing is made smaller or larger, and the test is repeated.

Temperature 1963

The unit is fundamentally identical to that of 1962, except the scales are switched automatically instead of manually, and there are 12 overlapping scales of 8C each centered every six degrees from -30 to +36C. The 8C scale conveniently matches the chart paper which is divided into eight sections.

Humidity 1962

Humidity is sensed as mixing ratio in grams of water vapor per kilogram of air with the MRI Model 901 Mixing Ratio Indicator. The operation and features of the unit are described in detail by MacCready (1963a). Air is drawn at about 5cc/min through an electrolyzing tube which is internally coated with phosphorous pentoxide. Current flows between two wires in the tube which is exactly proportional to the rate of water vapor entering the tube. The mass rate of flow of air is kept constant by monitoring the mass flow with a temperature-controlled hot thermistor sensor and controlling the pump to keep the mass flow constant. The instrument has a time constant as short as 1 second, the exact value depending on temperature and coating thickness. On the aircraft the sensor is put in a box or location where ambient air blows past it slowly at a pressure close to that of the cockpit air and where the sensor is shielded from large water droplets. For simplicity a single scale was used throughout the summer, 0 to 11 gms/kg.

Humidity 1963

The same unit is being employed, differing only in having a later version of temperature compensation on the mass flow sensor, and having five overlapping automatic switching scales, 0-2, 1.5-4, 3-8, 6-16, and 12-32 gms/kg.

Liquid Water Content

This variable is measured by a Johnson-Williams hot wire sensor. The sensor can be seen in Fig. D-17. One heated wire is transverse to the airflow and the other is parallel to the airflow. The wires are in a bridge circuit with zero output in still air. In a cloud, the droplets impinge on the transverse wire and are evaporated, cooling the wire. At the airspeed for which it is calibrated, the instrument output is linearly proportional to liquid water content provided the droplets are less than about 50 microns in diameter. Evaporation of larger droplets is incomplete.

Thus, the instrument is of greater quantitative value for clouds with small droplets which is generally the case at Flagstaff.

The instrument requires rezeroing before starting a cloud penetration. Even after a zero has been established, there tends to be a systematic drift within cloud. It has not yet been established whether the drift is continuous or is concentrated at the cloud entry or the exit. The sensor is heated for de-icing, but the heat is only applied before a cloud penetration, not during it, and this is not involved in the drift. It is felt that these drift characteristics can be quantitatively understood after making a series of systematic tests in a simple cloud. Some rough quantitative data are now obtainable with the device, as will be shown in subsequent sections of this report. The instrument has a fast response time of about one second, and so is of considerable use in showing the spacial variation of liquid water content. The instrument has limitations, but it is simple; it has considerable value in physical cloud studies, and no other suitable technique is available, so it will be used in 1963.

Turbulence 1962

An early version of the MRI Universal Turbulence Indicator was used. This instrument measures an intensity level from which any of the statistical properties of the turbulence at wavelengths under about 200 or 300 meters are derivable; it is related to the turbulence dissipation rate, the rate of conversion of turbulence energy into heat by the tiniest eddies. The theory and instrumentation techniques are given by MacCready (1963). The main feature of the device is that it measures the most basic turbulence quantity simply and continuously, and independently of the aircraft speed or type. The sensor of this particular embodiment is a fast response 4 inch diameter propeller, having a response distance of about three feet. The sensor can be seen in Fig. D-19 and 20. By a DC tachometer generator a voltage is produced proportional to true airspeed. The voltage fluctuations are processed by a filter and averaging circuit, the gain of which is automatically adjusted according to a particular function of the mean airspeed. The meter output is proportional to $\epsilon^{1/3}$, where ϵ is the turbulent dissipation rate.

The 1962 unit was not calibrated, but calibration within a factor of two can be achieved by comparing pilot reports of turbulence severity with other pilot reports where complete spectra were measured. The meter reading can be calibrated in the laboratory in terms of $C_2^{1/2} \epsilon^{1/3}$, where C_2 is a dimensionless constant. Dr. Hans Panofsky* finds that the best value of C_2 is 0.14. Taking pilot reports for research flights where the turbulence spectra are known (and hence $C_2^{1/2} \epsilon^{1/3}$ is known), it turns out (MacCready,

*Private communication.

Fig. D-19. CESSNA 180 SENSORS

Some sensors are shown including turbulence propeller (A), temperature vortex tube (B), drop charge tunnel (C), and simulated drop charge housing (D).

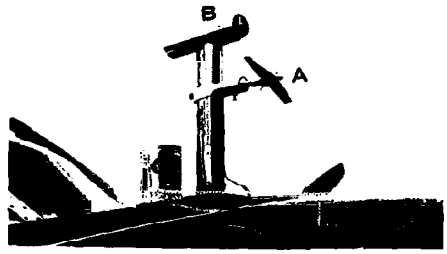

Fig. D-20. AERO-COMMANDER SENSORS

Turbulence (A), temperature (B), and mixing ratio (C)

1963b) that the following approximate relative categories can be established for aircraft flying at moderate speeds (moderate considering the aircraft type):

Description	$C_2 \epsilon^{2/3}$ ($cm^{4/3}$ sec^{-2})	$\epsilon^{1/3}$ ($cm^{2/3}$ sec^{-1})
Negligible	< 0.04	< .54
Light	0.04 - 0.33	.54 - 1.5
Moderate	0.33 - 1.75	1.5 - 3.5
Heavy	1.75 - 9.3	3.5 - 8.2
Extreme	> 9.3	> 8.2

Turbulence 1963

The instrument fundamentals are the same, but this later generation unit features a light chopper and frequency to analog converter to produce the true airspeed voltage, has more stable electronics, a sharper filter shape, and is calibrated in absolute terms.

True Airspeed 1962

The turbulence sensor true airspeed signal was put on an expanded scale instrument on the aircraft instrument panel of each plane so as to facilitate aircraft speed coordination when the planes were at different heights. The devices were rarely used because this precision in aircraft operation proved inappropriate in 1962.

True Airspeed 1963

The true airspeed signal is to be recorded on one cycled channel of the Brush recorder, as general reference information, and as data from which longitudinal wind speed can be derived when coupled to the M-33 radial speed indicator.

Rate of Climb 1962, 1963

With the plane flown at a known climbing rate or sinking rate with respect to the air, vertical air velocity can be computed from aircraft rate of climb data. Rate of climb can be (and is often) found from altimeter information, but it turns out to be convenient to have it appear as a separate variable with a faster response sensor. A Crossfell electric variometer is therefore incorporated into the instrument system (see Fig. D-14). By a hot thermistor principle, the rate at which air moves in or out of a one liter flask is measured. The device is linear with vertical velocity, and the zero point holds well, but the gain calibration changes somewhat with altitude and temperature. Sometimes as with sailplanes a "total energy" compensator is added to the system, to

compensate for the rate of change of horizontal airspeed which can be introduced by the pilot and otherwise confuse the rate of climb versus air vertical velocity relationship. This correction is of great help at the very slow sailplane speeds, but the "contamination" by air turbulence produces a larger noise effect in higher speed aircraft. The compensator has been used in Flagstaff studies, but its use in the future is not recommended.

With the rate of climb indicator and with reasonable attention to maintaining the aircraft attitude constant, vertical air velocity can be obtained with reasonable accuracy for cloud dynamics studies for horizontal scales exceeding about 400 feet. In rough air the errors become large, but the significant values to be measured are still larger and so the errors are not relatively severe.

Infrared 1963

A Barnes Model IT-1,14-312 Optitherm infrared unit is being incorporated into the 1963 aircraft instrument package. It records radiation temperature in the 8 to 13 micron band, over the temperature range from +20 to +100F. Beam width is 2°. The sensor is pointed straight down. The unit has proven to be valuable in MRI diffusion studies. Here it is to serve for ground temperature surveys pertaining to convective cell formation, and to give in-cloud and cloud top data.

Hydrometeor Size 1963

An experimental hydrometeor size device is being prepared for 1963 to provide data in the size range of 1 mm to 10 mm diameter. The principle of operation is that the capacitance change in a parallel plate condenser turns out to be directly proportional to the volume (mass) of a droplet between the plates. Recent advances in capacitance change measurements make this seem to be a feasible measurement technique for in-flight data. Calibration of this method for liquid droplets has worked very well; calibration has not been performed for ice hydrometeors. Pulses are to appear on an uncycled Brush channel, the pulse height denoting the hydrometeor volume. A cube root circuit will make pulse height proportional to radius rather than volume.

Icing 1962, 1963

Both the instrument sensors and the aircraft would ice up during spirals or several passes through a cloud at subfreezing temperatures. The only research instrument sensors being de-iced were the continuous cloud droplet collector and the liquid water content sensor, the latter being heated only outside clouds so as to minimize bias effects during

operation. By the time other sensors were excessively iced up the aircraft was also generally iced up enough so it was expedient to descend and melt off the ice. The turbulence sensor would go out first, as the propeller iced in a way which effectively feathered the propeller.

Icing causes negligible trouble during a few short traverses followed by descents for melting. It is a problem during long upward spirals, or very long or repeated traverses. It can be cured for most sensors by standard electric heating. For some sensors, such as temperature, the heating can interrupt the action of the sensor and so can only be done intermittently or outside clouds before traverses.

In summary, enough de-icing is used so that, with the type of operation taking place at Flagstaff, the instruments are effective until about the time when icing of the aircraft requires temporary termination of the probings. It would be desirable and straightforward to de-ice all the sensors electrically, at least intermittently, but this does not have a sufficiently high priority to warrant doing it for 1963.

Atmospheric Electricity Parameters

The airborne atmospheric electricity studies during the 1962 Flagstaff season were primarily the responsibility of the NSF portion of the work. Therefore the airborne electrification instrumentation will be reviewed here rather briefly. More complete details will be found in the forthcoming NSF final report by Atmospheric Research Group. This instrumentation was only employed in the latter stages of the field program, in August.

Vertical potential gradient was recorded on each aircraft. The voltage difference was measured between two radioactive probes, one on the top of the fuselage, the other underneath. The probes are visible in Figs. D-16 and 13. The electrometer was electrically floating (insulated) so that its reading depended only on the voltage difference rather than on the plane charge. The signal was translated to the grounded recorder by converting it to AC, and passing it through a highly insulated transformer, and reconverting to DC. A corona current generator was used to calibrate the balance of the probes; with the generator the plane was artificially charged in flight to verify the balance, i.e., to see that the plane charge would not register as a vertical gradient. The correct relative position of the probes was experimentally established this way. Aircraft charge itself was measured on the Cessna by another probe-electrometer, with the probe situated on the fuselage side under the wing so as to be virtually unaffected by vertical gradients. The potential gradient instrumentation was deemed crude, and did not receive much attention in the field, but was nevertheless adequate to establish gross effects.

For 1963 a much more quantitative system has been developed, utilizing separate operational amplifier electrometers for a top probe and a bottom probe, and balancing in flight by simply turning a potentiometer in the unit. The voltage difference yields the vertical gradient (relative to the airplane vertical), and the voltage sum is proportional to the aircraft charge. To refine the gradient instrumentation much beyond this point would require an unwarranted dilution of project effort.

The most important measurement was that of hydrometeor charge. As a hydrometeor passed through an open ended Faraday cage mounted under the wing of the Cessna 180 (see Fig. D-19) its charge was momentarily observed by an electrometer system and translated into a pulse on the recorder, the pulse height being proportional to charge. The pulse duration was electronically lengthened to permit the millisecond pulses to be observed on the Brush recorder. The equipment was quite satisfactory. A somewhat refined version is available for 1963, featuring nonlinear sensitivity to eliminate manual scale switching, and using a rectangular pulse shape instead of an exponential decay shape. The units handle charges in the range 1 to 2000 picocoulombs.

Charge on a "simulated" hydrometeor was sometimes monitored by observing the current by electrometer from a wire, 1/8 inch diameter by 6 inches long, set in the airstream but shielded from potential gradients. The probe is just visible in Fig. D-19. As the wire rimed, the charging was noted. Since the instrument also serves qualitatively as a hydrometeor charge sensor, it is only used before many hydrometeors are present. The data from the device seem significant, but of such complexity that their interpretation is not complete. A similar device will be used in 1963.

Space charge was measured by a larger, more sensitive version of the Faraday cage hydrometeor charge sensor, with a Keithley 600A electrometer used in an operational amplifier mode with a three second time constant. The simple unit would show relative effects, detect charged smoke rising from the ground, and indicate apparent charges around and in cloud edges. An improved version is being made for 1963.

Conductivity is to be recorded continuously on the ground and measured occasionally in flight with standard vibrating reed conductivity units (Applied Physics Laboratory type).

In 1962, in a tiny wind tunnel laboratory, studies were conducted on charging during ice hydrometeor melting. The significance of the results warrants performing the identical experiments in 1963 in the aircraft where natural hydrometeors can be caught and processed in a more representative natural environment.

E. Data Reduction

General

Data reductions for the general purposes of the project have been systematized. Special investigations may have special needs requiring greater accuracy and more detail, or consideration of second-order factors; some of these are described in the following sections of this report dealing with the individual studies. The general system, though, combines five subsystems into one system of cloud depiction.

It is desirable to make a rough evaluation of all data to see which situations will produce the most complete and useful final cloud depictions. This is done by cataloging of all data. Then, when the situations for study have been chosen, each of the subsystems is reduced to a form compatible with the system.

The subsystems are:

1. The airborne continuous cloud particle collection.
2. The general aircraft observations.
3. The cloud electrification observations.
4. The ground-based observations made by radar and time-lapse cameras.
5. Miscellaneous observations such as U. S. W. B. radiosonde and surface observations and also special surface observations taken by the project personnel.

Cloud Particle Data

At the end of the 1962 field program there was still much to learn about the interpretation of the cloud particle sampler data. This instrument replicates cloud particles in a fresh Formvar solution coated on clear polyester 16 mm movie film. The Formvar hardens rapidly after collecting the cloud particles in the free airstream below the aircraft wing. The replicas show concentrations, sizes of particles, and whether these particles are water, ice, or other airborne particles. The size relationship of the droplet to the replica was not well understood, until a theoretical study of this was undertaken under an NRL contract. A theoretical relationship was worked out which shows that the replica diameter must be a function of the thickness of the Formvar coating. (See Appendix A, p. 71). During the summer of 1962, this thickness factor

was not carefully controlled; therefore, the size data is not as quantitative as it might be. An attempt will be made to control this problem for the 1963 summer field program.

Many forms of ice crystals are clearly and distinctly recognizable. However, complications arise in the interpretation of replicas left by graupel which smashes when it is soft. Hard hail leaves a skid mark. Rimed ice may be quite irregular and can be confused with parts of a broken graupel. Ice crystals crack if they are larger than about 150μ and they break apart if they are larger than 250μ.

The cloud sampler records may be studied in a microscope, but since the film footage exceeded 2 miles for the summer of 1962, this was hopelessly slow. A system of projecting the film by a 16 mm stop-motion picture projector has been developed. The replicas in the clear Formvar plastic bend the light and produce shadows which are clearly seen in projection. Various examples are shown later in this report. A 100 X magnification of the whole frame is achieved with a 5/8-inch projection lens at a distance of 45 inches. A 1000 X magnification is achieved with a microscope lens system adapted to fit the projector. Here a 20 X eye piece and a 10 X objective lens are used.

With this projection system it was found that resolving power of light is achieved. Records can be scanned at 24 frames per second, which is about twice the rate the film was exposed during flight. At this projection speed it is possible to recognize: 1) one graupel replica in hundreds of frames of water cloud, 2) one ice crystal against a background of water droplets, 3) variations in the size and concentration of water droplets, etc.

Quantitative analysis is done by counting, sizing droplets into distributions, and classifying representative frames of water droplets. This can be accomplished rapidly and efficiently by making an unordered classification and size scatter of the particles on a clear plastic sheet. To do this a reference line is drawn on the left side of the sheet. The sheet is moved so the reference line is tangent to the left side of the projected replicas. A mark is made at the right side of the replica. The mark's position indicates the diametric width of the replica and the type of mark indicates the classification (water, ice needle, etc.).

This is done for all droplets in the sample. This unordered scatter is turned into an accumulated probability distribution by making an accumulating size count from the left to the right. This is plotted as it is being counted on cumulative probability paper. Finally, the mean and standard

deviations are read from the cumulative probability plot.

The output (400 feet or so of record taken during a flight) shows the time variation of the cloud particle type, concentration, and size distribution. All of the above can be plotted along the same time scale where plots are made for the aircraft-observed altitude, temperature, liquid water, mixing ratio, turbulence, and electrification parameters, in addition to the changes in cloud top height. This has been accomplished by sampling. Counts are made of a few frames to represent each homogeneous section, points are then plotted on a time graph. The points are connected by eye, averaging variations on the intervening record.

It has been suggested that the cloud sample records be analyzed by a flying spot scanner linked with a pattern recognition computer. It is believed that MRI's system of data reduction is more suitable for its particular needs. The problems involved using an electronic pattern recognition system are:

1. The replicating technique is not yet uniform enough to adapt to a reasonably simple recognition system.

2. The recognition of differences between water, ice, broken ice, graupel, and dust through a wide range of sizes presents a major problem.

At the present time, a detailed summary of the significant parts of only four flights made during the last field season has been completed, but a rough catalog of all flights has been compiled. During this analysis program the cloud particle analysis technique has been greatly improved to the point where, now, obtaining detailed summaries for each day of a field program is not impractical.

General Aircraft Data

The main flight records come off a multi-channeled Brush recorder, on which the information is recorded using rather arbitrary scales. The record is made by pivoting pens so the vertical is curved. A drawing machine was constructed especially for this project which allows the Brush recorder records to be transformed for easier analysis. This linear pantagraph is shown in Fig. E-1. The transformation preserves the time scale, but takes curvature out of the trace and amplifies the vertical scale as desired. Thus, the ability to make easily compared time graphs of flight records is possible. The transformation allows a more useful compatible representation of the data.

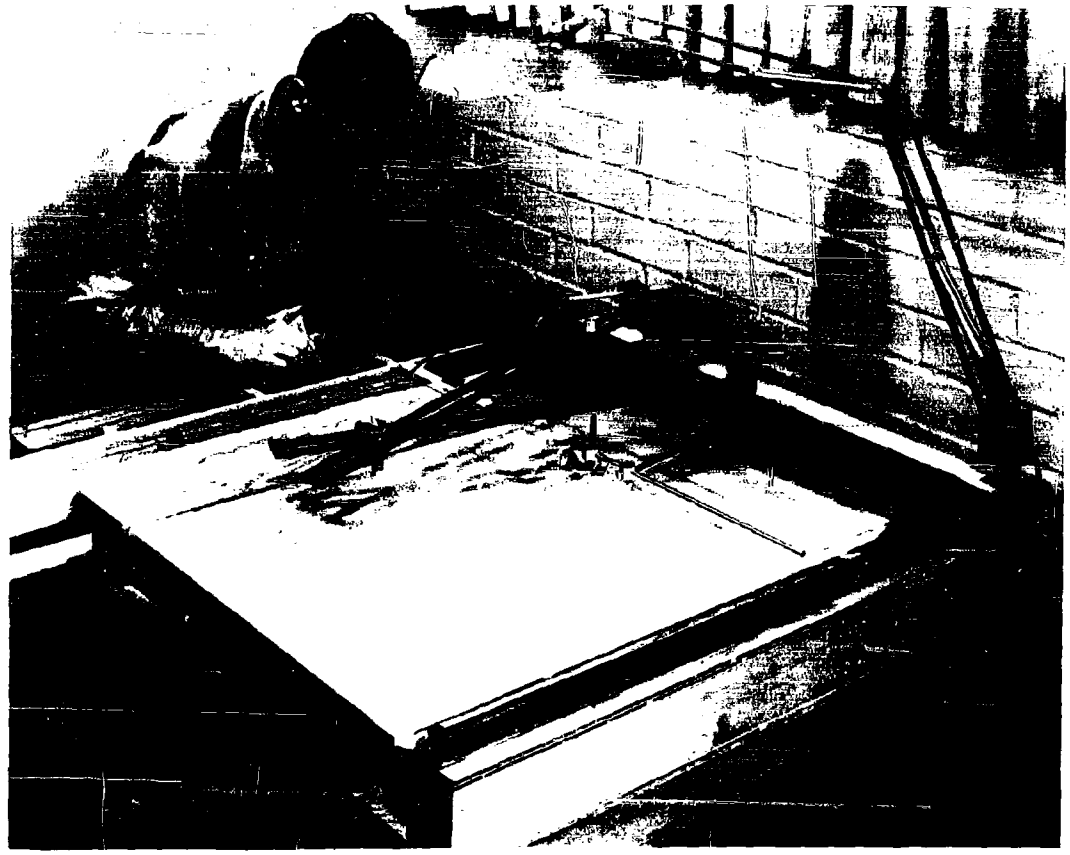

Fig. E-1. LINEAR PANTOGRAPH

Colored marker pen (A) traces a variable from the recorder chart (B) in an appropriate expanded amplitude scale on an acetate sheet. The time scale remains identical to that on the recorder chart. The operator advances the pantograph assembly along the time axis of chart (B) by rotating wheel (C). The operator moves handle (D) to keep the cross hair (E) always on top of the appropriate variable on the chart. Chart curvature is taken care of by using a curved line on the transparent time mark grid. Adjustment of the amplification factor is made by positioning pivot (F) along the slotted "scissors" members.

The development of the analog aircraft data reduction system required a great deal of time and effort; however, it is now operational. With further development it might be speeded up by a factor of three. It would be practicable to have a technician reduce all useful flight data from a field program.

1. Altitude

On the original record the altitude trace crosses the chart once for each 1000-foot change in pressure altitude. It automatically switches back to the other side of the chart when it crosses the limit of the chart edge. Hence, a long ascent or descent is characterized by lines crossing and recrossing the chart. The record is further distorted by curvature of the chart. This is transformed into a time-height graph by the tracing machine (distortions of the record are eliminated), adjustments are made for zero shift or scale change on the original charts, and with the altitude ascending and descending rather than cycling.

2. Comments Made from Logs

Observers' comments are made on the tape during flight and comments made at the ground control center are written at their appropriate time location on the chart. Special marks are made to indicate the times of seeding.

3. Temperature

Stability conditions are determined by temperatures at varying altitudes. For ease of comparison and interpretation of temperatures at differing altitudes the data is transformed to potential temperature. Below cloud base the dry adiabat is used. In the cloud and above cloud base the moist pseudo-adiabat is used to calculate the reference, the dry and moist, adiabatics. If the temperature and altitude traces are identical the potential temperature cloud base will be the same also. When the potential temperature is colder than the cloud base the altitude trace is above the temperature trace. The opposite holds true when the potential temperature is warmer than cloud base. By comparing relative departures of the temperature trace from the altitude trace, one can compare the relative buoyancies of air parcels the plane passes through.

Below cloud base the air that is buoyant enough to rise into the cloud will have a temperature trace on or below the altitude trace. In a cloud the moist adiabat will follow the altitude trace where there is relatively little mixing of air in the cloud. If the moist adiabatic temperature curve falls below the altitude trace when the plane is flying in

the cloud, heat is being added to surrounding air by the release of the latent heat of fusion as cloud particles turn to ice. In this manner, the relative departure of the temperature trace from the altitude trace is indicative of the dynamic processes in and below the cloud.

4. Mixing Ratio

A parcel of air lifted adiabatically will condense at a specific pressure (altitude). This altitude can be determined from the mixing ratio, temperature, and altitude of the flight record. In this study an approximation of the potential is used. It is assumed that the potential temperature of the cloud base is the same, or very nearly so, as the potential temperature of an air parcel. On the basis of this multiplicative function of the potential temperature of the dominant cloud base, it is possible to transform recorded mixing ratios in convective condensation levels for a parcel. For close analysis the correction for the parcel potential temperature may be computed by eye integration.

5. Turbulence

Turbulence records are transcribed in the same amplitude as they are recorded on the flight record. The trace height is proportional to the RMS value of the turbulent energy in small eddies.

6. Drop Sampler

One dot is plotted to represent 10 frames of the sampler operation. A dotted line is thus produced. Following each 100 frames, there is a dot superimposed on the line above the record line. This, along with the fact that there is a unique marking on the sampler each time it stops, allows for the location of each frame of cloud sample at its proper time and relates it to the altitude temperature and turbulence. A digest of the droplet sampler record is then put on the master flight time section.

Radar and Time-Lapse Cloud Photographs

During the 1962 season the MRI radar at control was used for tracking aircraft as well as observing precipitation echoes. During much of the time the aircraft tracks are easily followed from the radar tracks. However, at some very important times the aircraft tracks are lost or are ambiguous because two or more aircraft are operating in the same cloud area. During the 1963 season it is planned to record aircraft heading and true airspeed on the flight record to help overcome this difficulty. Also, efforts are being made to have the M-33 radar operational as an aircraft tracker. With the flight record and either the MRI

radar or the M-33, it should be possible to resolve virtually complete aircraft tracks.

The plan position of the precipitation echoes and aircraft track is taken from the radar by projecting on a map table at 1 inch = 2 miles. On this map the 16 mm time-lapse projectors are placed at their proper map location. The projection is done through the same lenses used on the cameras during the field operations. The cloud projections are in true scale of 1 inch = 2 miles when the screen is located over the map position of the cloud. If a cloud can be identified from two cameras, then it can be located. Clouds from photographs and radar echoes can be related in a quantitative manner. Cloud plan positions have been drawn by use of the oblique views of the cloud bases. This is performed by attaching a pen to a small projection screen. A vertical line on the screen comes up from where the pen touches the horizontal paper. A cross line intersects the vertical line at the height of the cloud base. The screen is moved sideways and forward and back so that the cross point follows around the cloud base as projected on the vertical screen. The pen then draws a plan position of the cloud base on the horizontal map.

Radar and time-lapse photographs were the last elements to be incorporated into the system. Some further development is required before it will be possible to use the full potential of our radar and time-lapse photographs from all of the seven locations. The data reduction so far indicates that the system has real potential in allowing the analyst to construct the cloud picture from more points of view than has been possible before.

The composite data reduction system is developed to the point where it has the capability to provide the project scientist with most of the useful routine data from the field program in an easily usable form. It now is closer to being a routine operation than ever before although personnel must be highly trained. The analyses which follow serve to illustrate the capabilities of the analysis technique.

F. Daily Analysis

Introduction

Illustrative examples from the analysis have been taken from four different days. These illustrations will show: (1) how the data are analyzed, (2) the type and quality of information gained from the field program, and (3) significant findings.

The data chosen for illustration are as follows:

1. July 20, massive dry ice seeding of a small cumulus cloud with a top of 22,000 feet and a short life expectancy.

2. July 24, a small dry ice seeding of a cumulus growing rapidly past 21,000 feet.

3. August 10, silver iodide seeding from an aircraft flying below the base of a large mountain lee wave cumulus.

4. August 15, silver iodide seeding from an aircraft flying below the base of an isolated cumulus cloud.

The accounts in this section will relate cloud particle information to aircraft time-height, temperature and liquid water observations. These will be related either by map or text to information about the cloud physical structure.

Particular attention is given to the distribution of ice particles, both those occurring naturally and those caused by seeding. The concentration and size of water droplets is studied to help understand cloud mixing. The temperature when converted to potential temperature (θ) and psuedo moist adiabatic potential temperature (θ_{sw}) and, compared with the θ and θ_{sw} at cloud base, gives information about the cloud's mixing characteristics. The liquid water measurements are also useful for this purpose. The cloud mixing is analyzed to help explain the origin and development of the ice particles.

The MRI analysis is continuing. The number of cases studied is steadily being increased, as well as the amount and variety of information brought to bear on the individual case. This reporting is illustrative of the present state of the analysis phase of the project.

July 20: Example of Massive Dry Ice Seeding in Small Cumulus

Description of Clouds

On July 20 the low-level wind from the surface to 12,000 feet was roughly 8 knots out of the east. It veered to the southwest by 20,000 feet. Above that level, there was a 10 knot shear per 3000 feet and the wind increased to 18 knots and veered to the west.

The mixing ratio in the lower levels was 7 g/kg and the cloud base was at 14,500 feet with a base temperature of -1.5 C. Cumulus first appeared above the west slopes of the San Francisco Mountains at 0927. Thereafter, clouds continued to build to the west of the peaks. The east side remained clear until after 1200. Smaller clouds, one to two miles in diameter, were limited in vertical growth by shear and seldom penetrated past 21,000 feet. Clouds, three to four miles across, grew to 24,000 feet. Clouds, four to five miles across, reached to 27,000 feet and produced radar echoes.

The first radar echo occurred from a cloud two miles west of Wing Mountain (or 7-1/2 miles west of the San Francisco Peaks) at 1047. Precipitation echoes developed in this area (downwind of the Peaks) during the rest of the day, but were never closer than 3-1/2 miles from the Peaks. The east side was echo-free until approximately 1540 when radar observation stopped.

Cloud Flights

1. The MRI Cessna 180 observation plane (hereafter referred to as Metro I) took off at 1015. It made a spiral ascent into a cloud two miles west of Agassiz Peak. The cloud was two miles in diameter and had a top at 22,000 feet. Metro I was able to stay in the updraft only about half of the time during the spiral. Its rate of climb reached 1,300 feet a minute on occasion. Metro I left the cloud at 16,000 feet (-4 C). The observed water droplet concentration was 500 - 700 per cm^3 in the undiluted portions of the cloud. Individual droplets were as large as 15μ. No ice crystals were recorded.

2. At 1100 Metro I traversed a cloud on the west slopes of the San Francisco Peaks at 15,000 feet. In this cloud the droplet concentration indicated 1000/cm^3. These large concentrations may have been due to airspeeds higher than those assumed in computation. (Metro I was not tracked during this traverse.) Ice crystals of 50μ were found in concentrations of 200 to 800 per liter in parts of the cloud. This cloud had not been seeded but was downwind from the sheared off top of a cloud that was producing a radar echo and reached above 24,000 feet.

3. At 1118:00 - 1118:45 the MRI Aero-Commander (Metro II) seeded a cloud two miles south of Agassiz Peak. This cloud was about 1-1/2 miles in diameter and had a top at 21,000 feet. Seeding consisted of pouring 800 pounds of centimeter-sized dry ice into the top of the cloud from 22,000 feet. Fig. F-1 shows the time flight record of this cloud observational sequence and Fig. F-2 shows the flight tracks and cloud locations.

   Traverse A - Metro I entered the cloud from the north 5 minutes after seeding time (S+5) at 15,500 feet (-4 C) and encountered an updraft of 500 feet per minute. The cloud particle sampler

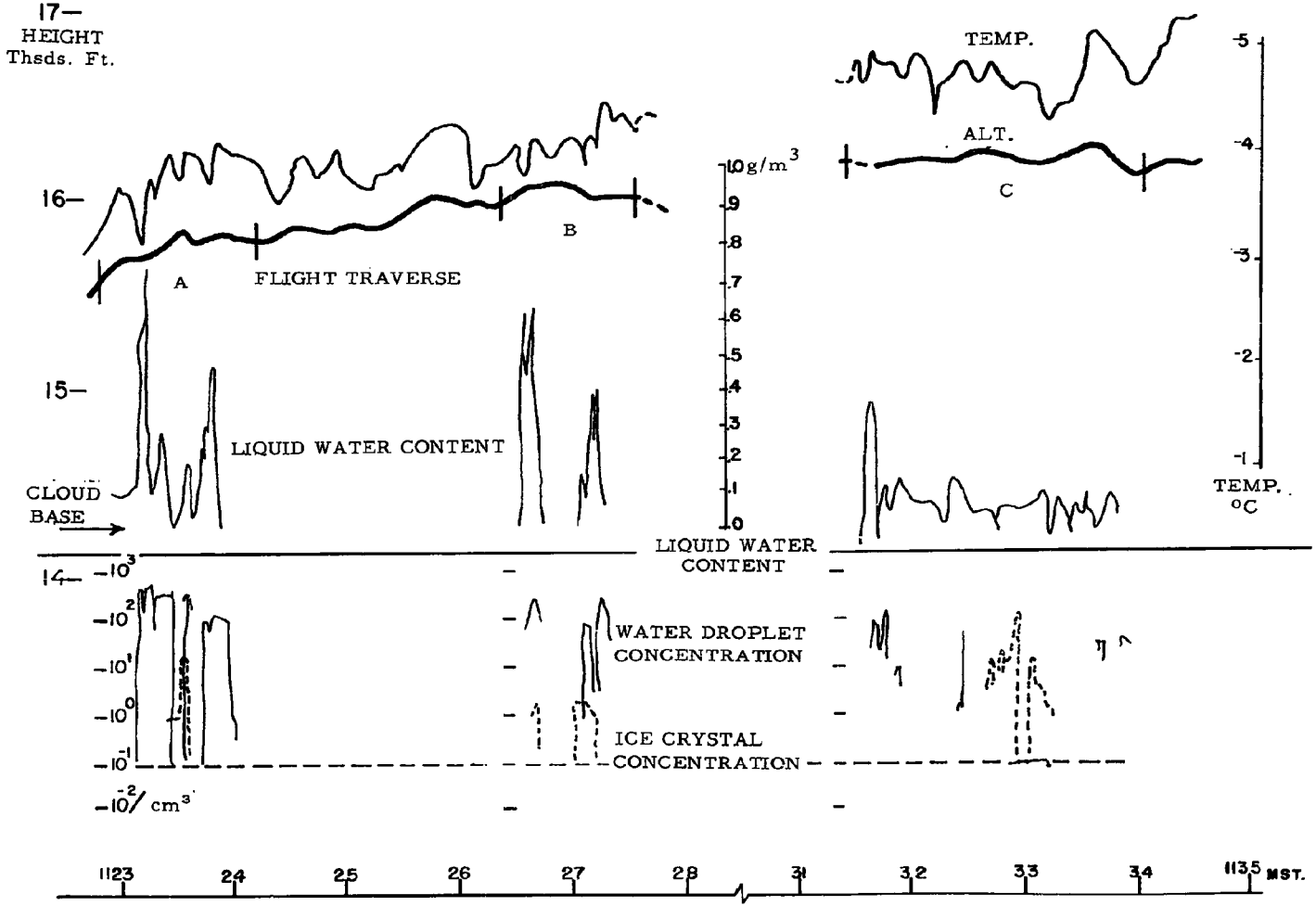

Fig. F-1. FLIGHT TIME SECTION FOR JULY 20.

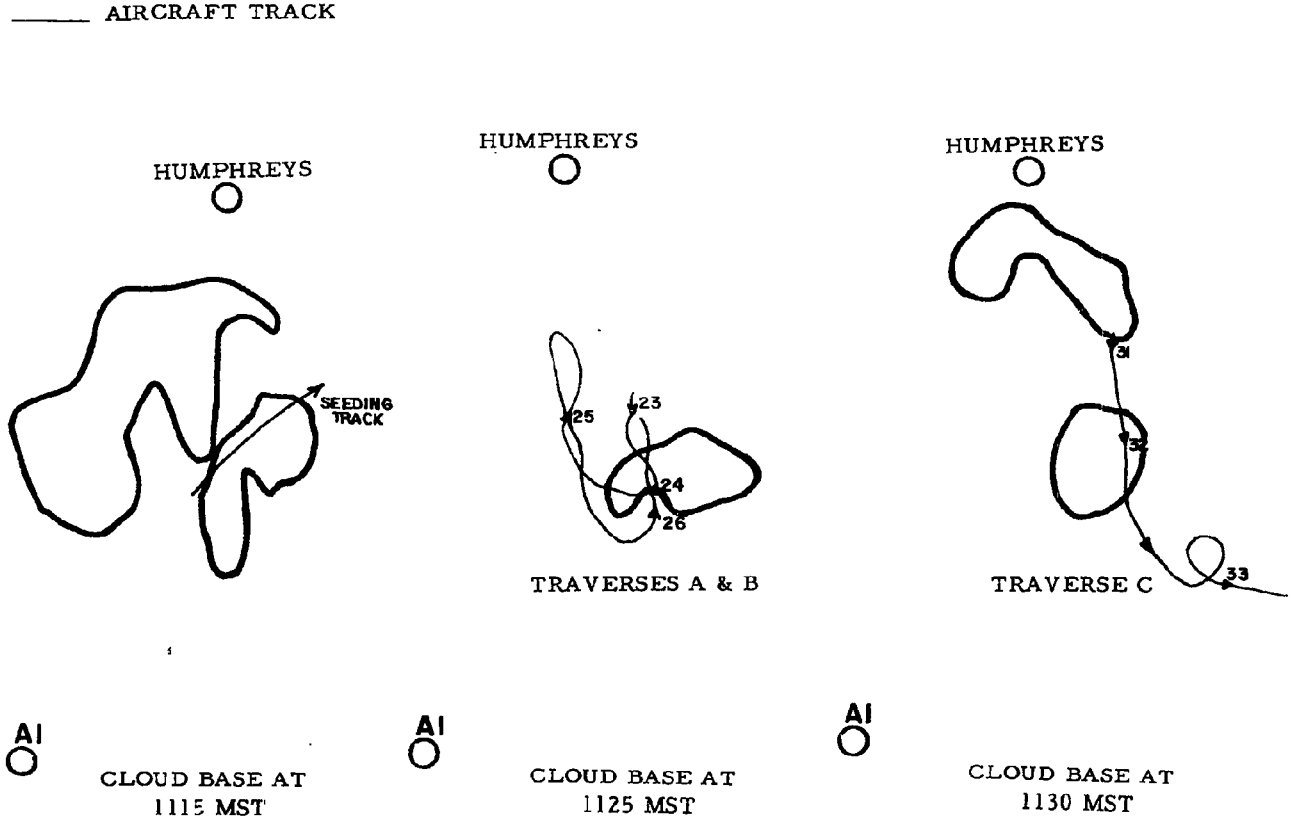

Fig. F-2. AIR PLAN POSITIONS OF CLOUDS AND AIRCRAFT TRACKS, JULY 20.

showed droplet concentrations of 500 to 800 per cm^3 and a burst of 40μ ice needles with a concentration of 8 per cm^3.

Traverse B - At S + 9 Metro I penetrated the seeded cloud again (this time from the south) at 16,200 feet (-5 C), the vertical currents had subsided. For two short portions of the record the droplet concentration was $500/cm^3$. Through one-half mile of the traverse, there were ice crystals, first hexagonal and about 100μ in diameter, and then, some needles of 100 to 300μ length in a concentration of $3/cm^3$.

Traverse C - At S + 15 Metro I, flying from the north, traversed an unseeded cloud over the Peaks and then the seeded cloud south of the Peaks at 16,200 feet (-5 C), without encountering important vertical currents. In the unseeded cloud to the north, the droplet concentration was $100/cm^3$. There were virtually no water droplets left in the seeded cloud. Ice crystals included both hexagonal plates and needles with dimensions to 1000μ Concentrations ranged from 10 to $100/cm^3$.

4. The second dry ice seeding took place in a cloud over Fort Valley at 1140. Metro II dropped 100-150 pounds of dry ice from 20,500 feet into the cloud when the top was at 21,000 feet.

Metro I traversed the cloud from the east at 16,600 feet (-5 C) just after seeding (S + 0 to S + 2). There were 500 feet per minute updrafts in the cloud. The cloud particle sampler showed droplet concentrations of $700/cm^3$ for a two mile stretch. The count then dropped to $300/cm^3$. In some places the cloud's ice crystal count reached 100/liter of 50μ particles. In one region graupel of 1500μ were found in a concentration of $100/M^3$. The dry ice could not have fallen to the flight level at the time of the traverse. Ice crystals and graupel must have come from clouds producing radar echoes two or three miles to the west which reached the 23,000 foot levels where ice crystals might be expected.

By S + 7, Metro I had circled back and made another pass from the east at 17,500 feet (-7 C). At this time the cloud was inactive and had no significant vertical currents. Through one mile of the traverse the cloud droplet concentration was 300 to $500/cm^3$. Ice crystals encountered were irregular plates with diameters of 100 to 200μ in concentrations of 1 to $10/m^3$. During this flight the last half of the record was of no value because of icing of the cloud sampler. No indications of ice concentrations resulting from seeding were obtained in this flight.

July 24: Small Scale Seeding with Dry Ice

Description of Clouds

Winds aloft were generally westerly, increasing from 10 knots in the low levels to 17 knots at mountain top height. Further increases in velocity occurred above 20,000 feet and the direction backed toward the southwest.

Cloud bases were at 15,000 feet and were generally 1 - 3 miles in diameter. First radar echoes were associated with clouds forming in the lee of the mountain. At 1038 there was a radar echo five miles downwind from Kendrick Peak. By 1140 another echo formed on the south slopes of the Peaks. This echo grew to a diameter of five miles as a mountain-lee type of storm.

By 1400 echoes dotted most of the area except for the Peaks region. The high mountain area was no longer a dominant factor in producing rain.

Cloud Flights

1. Cloud A (Seeded) - A cloud, located two miles west of Agassiz Peak and 1-1/2 x 2 miles across the base, was selected for seeding. The top was 21,000 feet and growing at 300 feet per minute.

   Metro I made a spiral ascent in the cloud to 19,500 feet from the base at 15,000 feet. Fig. F-3 shows the time record of the flight. Metro I seeded the cloud as it spiraled up from 16,000 (-5 C) to 18,500 feet (-10 C), with about ten pounds of dry ice. The plane was not able to continue the spiral flight due to weak updrafts. The flight record shows clearly that the ascent rate increased when the other factors indicated that the aircraft was in the undiluted core of the updraft. The temperature curve swung back toward the altitude curve indicating that θ_{sw} was nearly the same as θ_{sw} of the cloud base when the core was undiluted. The liquid water curve approached the altitude curve and indicated that the full amount of liquid water that should be condensed in adiabatic ascent was present. Droplet concentration increased up to a reasonable value for an undiluted cloud (roughly $630/cm^3$ for this cloud). This ascent showed how the various cloud parameters varied as Metro I moved in and out of the cloud.

   Seeding produced just one burst of ice crystals on the cloud particle record. This occurred at 1416 at 18,600 feet. Ice crystal concentrations as high as $536/cm^3$ with no water droplets were recorded. The total length of the path intersecting ice crystals was only 100 meters long. Crystals were plates and prisms with prisms predominant. Sizes ranged from 6 to 47μ in length. These were the only ice crystals recorded by the cloud particle sampler in this spiral flight. This cloud produced an echo at 1420, two minutes after Metro I left the cloud. Fig. F-3 shows the flight track with respect to the cloud top.

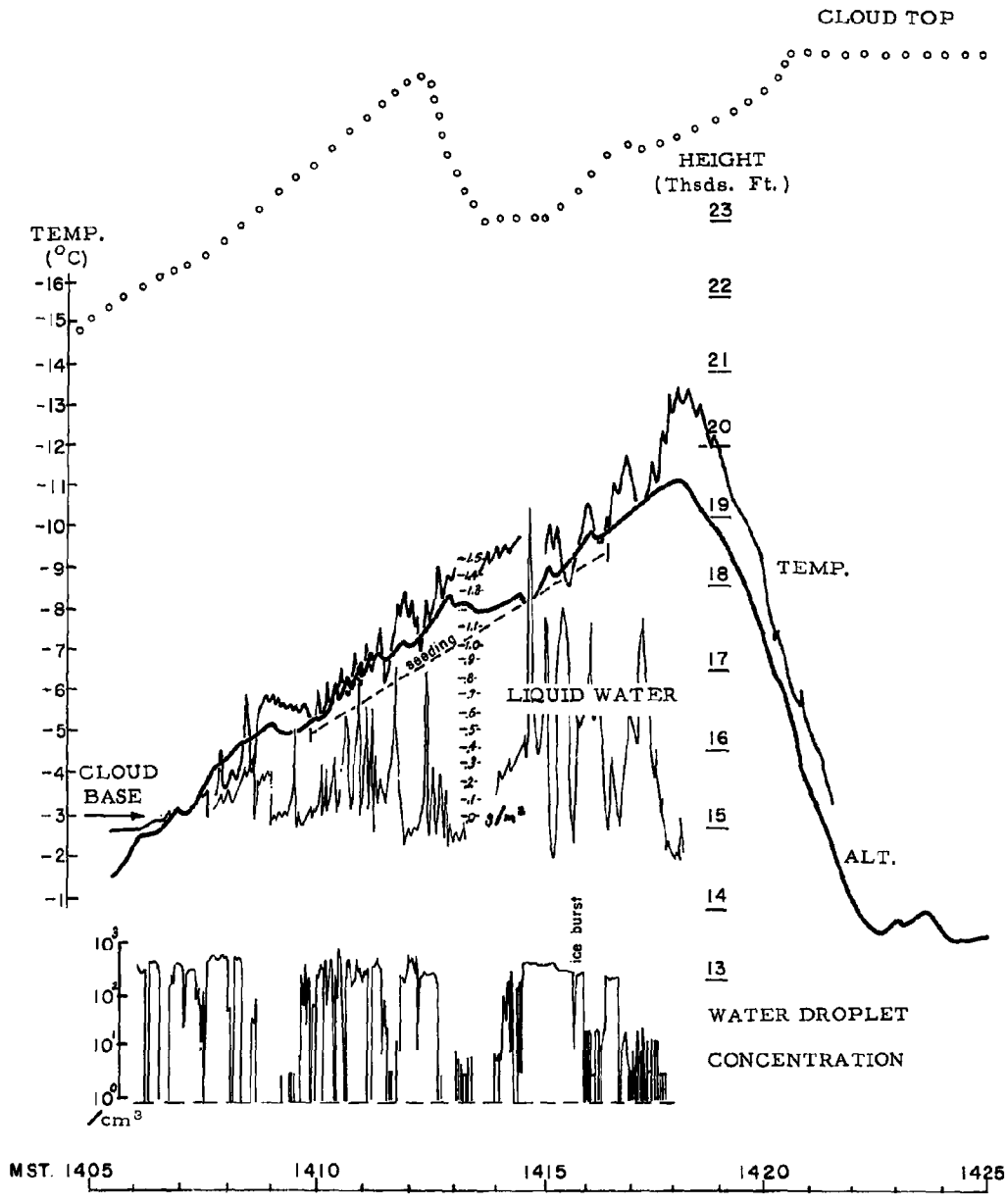

Fig. F-3. FLIGHT TIME SECTION FOR JULY 24, CLOUD A - SEEDED.

It was not certain whether the radar echo was related to the seeding. No additional sampling could be carried out in the cloud due to altitude limitations of the Cessna 180.

2. Cloud B (Unseeded) - The second spiral flight for the day was conducted as a control. A cloud three miles east of the airport was chosen for study. In Fig. F-4 a time section for the flight is shown. This is a good example of an unmixed cloud. Cloud base was 14,700 feet. Metro I ascended 2,000 feet above this level in an undiluted core. Above that level, there were signs of some dilution. The θ_{sw} trace made numerous sharp, cold swings then returned to the θ_{sw} of cloud base. When Metro I left the cloud θ_{sw} dropped to 2.3 C colder than θ_{sw} of the cloud base.

   Because this cloud has such an apparently simple internal structure it is a good case to use to compare various indicators which should be highly correlated. The cloud particle sampler data is smooth and seems to correspond nicely with the θ_{sw} and the altitude curve. No ice crystals were observed in the cloud. The liquid water curve is more variable than expected from the other indications. It does, however, show some agreement in overall characteristics with the large scale features of the cloud. Further study of this instrument is required.

August 10: Silver Iodide Seeding from U. S. Forestry Service Seeding Plane

Description of Clouds

On this day the wind flow was from the southwest at 15 mph at 10,000 feet, 5 mph at 20,000 feet, and 20 mph at 30,000 feet. The cloud base was at 15,000 feet. Clouds formed in the lee of the San Francisco Peaks. The dominant cloud formed just north of O'Leary Peak. This cloud development area was well established about noon and persisted throughout the afternoon. The first radar echo appeared from the area at 1247, and precipitation continued from the cloud system north of O'Leary Peak for the rest of the afternoon. These clouds formed on the southwest end of the development area and grew as they moved northeast with the wind. The horizontal dimensions of the system were three to five miles across wind and five to seven miles down wind. The tops exceeded 30,000 feet in the mature section of the cloud system, but on the south edge the tops were 22,000 to 26,000 feet. The seeding and observing operations were confined to the growing, southwest portion of the system.

Cloud Flights

The AgI seeding was carried out at 12,600 feet by the U. S. Forestry plane (Metro IV) in an area slightly north of O'Leary Peak. Seeding continued throughout the interval. The observation plane was Metro II,

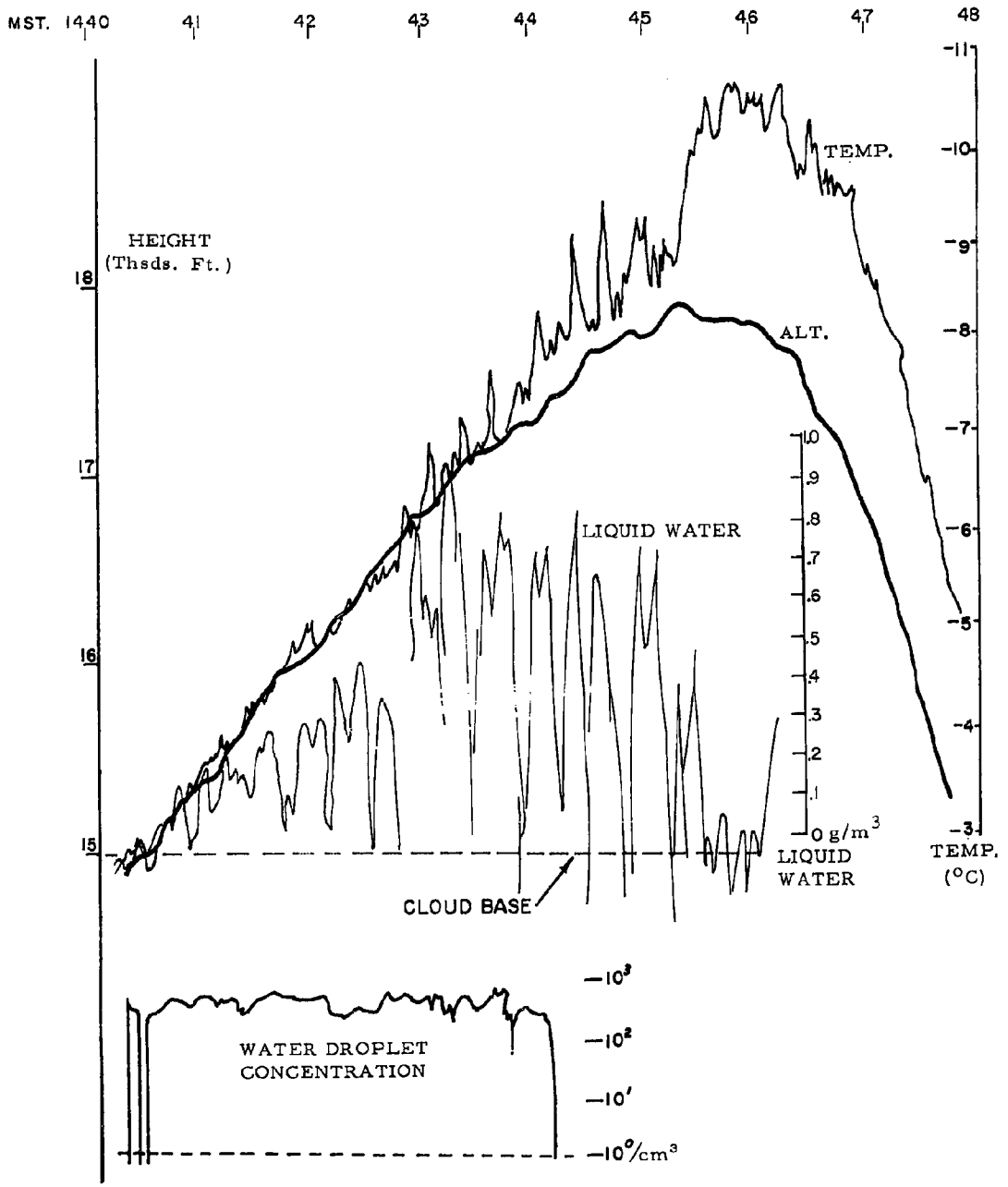

Fig. F-4. FLIGHT TIME SECTION FOR JULY 24, CLOUD B - UNSEEDED.

which carried the cloud particle sampler usually used on Metro I. In this experiment there were 15 cloud traverses of which 5 were control traverses in non-seeded clouds and 10 were in seeded clouds.

1. Fig. F-5 is a time height graph of the first part of the experiment. Metro II was at an altitude of 21,000 feet when Metro IV began seeding from an altitude of 12,600 feet. Metro II verified the location of Metro IV visually to be sure that the right cloud was being observed.

   Traverse A - Metro II then traversed this cloud at 21,500 feet, 3-1/2 minutes after Metro IV had begun seeding. This traverse coincided with the first radar echo from the cloud. On this pass the cloud particle sampler showed a water droplet concentration of 300 to 500/cm^3. There were ice crystals of 10 to 50 μ size in concentrations of 465 per liter on the edges of the cloud. No ice crystals were observed inside the cloud; however, graupel of 1,000 to 3,000μ in a concentration of 1/2 per liter were noted.

   The temperature curve indicates that this cloud must have been diluted by environmental air as θ_{sw} is 2C colder than θ_{sw} for the cloud base. The confidence of the θ_{sw} of cloud base is poor, however, because the aircraft had not flown through the cloud base. Flights through cloud base should be a standard observational procedure in future tests.

   Traverse B - Cloud Traverse B was made at 21,500 feet, 11 minutes after the start of seeding. This was judged to be sufficient time to allow the seeding to be effective 9,000 feet above seeding level. From the temperature curve the cloud has apparently been mixed with the environment since θ_{sw} is 2 C less than θ_{sw} of cloud base. The droplet count shows considerable fluctuation and is generally 200 to 300/cm^3, though in one place it is 500/cm^3. Ice crystals are found at the edge of the cloud as before, but on this traverse they are also found in the cloud cores in concentrations up to 2/cm^3. This concentration is enough to convert the water which was composed of 15 μ droplets to ice if the ice grows to 50 μ. Water is absent where the ice concentration is highest. Ice concentration is 300 times higher than in the cloud before it was seeded. There is a graupel concentration of 1 to 2/liter.

   Traverse C - At S + 14 and at the same altitude as B shows similar results.

   Traverse D - At S + 19 had the same characteristics as B and C, but on this pass there was a strong updraft (800 feet per minute and more than a mile across). It is considered important that there were crystals in this updraft in concentration of from .1 to 2/cm^3.

   Traverse E - Was at 20,000 feet and -11 C. It was similar to Traverses B and C.

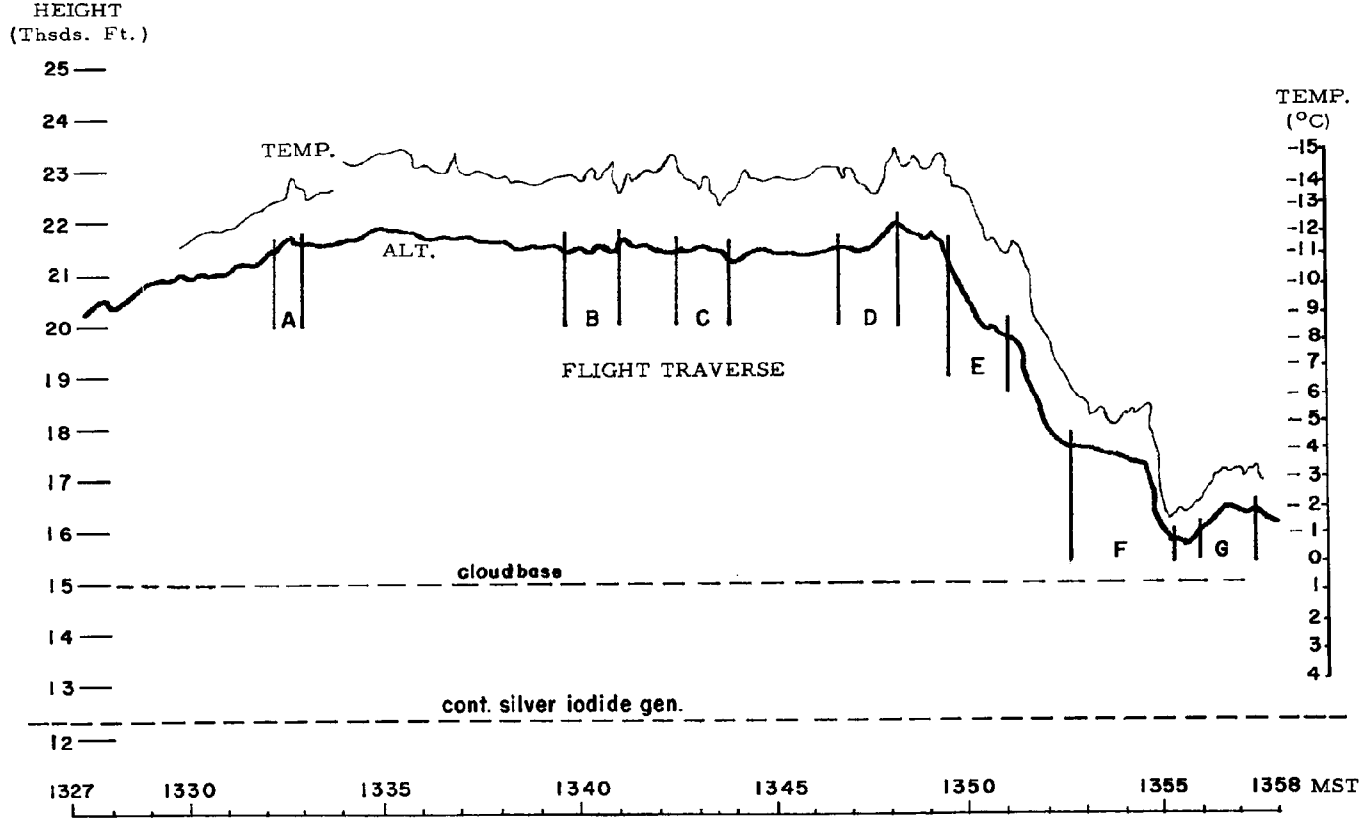

Fig. F-5. FLIGHT TIME SECTION FOR AUGUST 10.

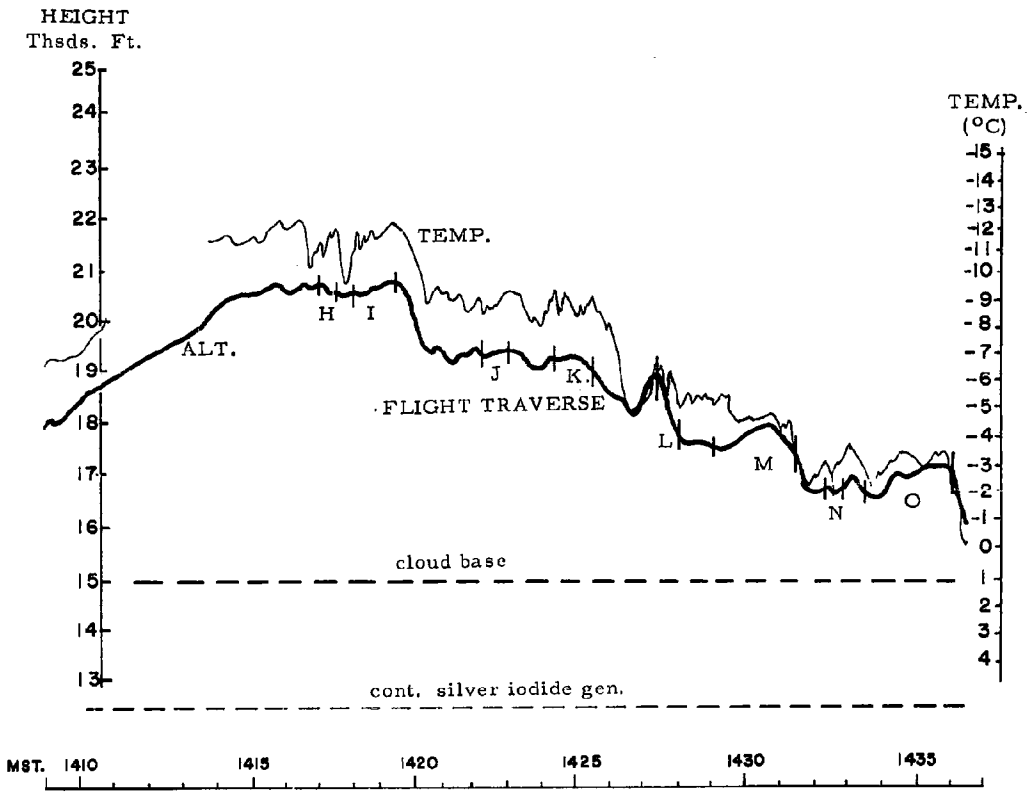

Fig. F-6. FLIGHT TIME SECTION FOR AUGUST 10.

Traverse F - Was at 18,000 feet and -6 C. It still showed ice crystals on the fringes of the cloud and in areas of low water content created by downdrafts within the cloud.

Traverse G - At S + 29 was at 17,000 feet and -4 C. In this pass the water droplet concentration was 300/cm^3, with no ice crystals through a long period of record followed by a region of ice crystals and graupel.

Discussion of Traverses A to G

Ice crystals formed in Traverse D in a strong and broad updraft at -14C apparently were the result of the silver iodide seeding. Concentrations amounted to .1 to 2/cm^3. Extensive areas of ice crystals were also found in other locations within the cloud system and frequently on the cloud boundaries. On the fringes of the cloud, the crystals have probably descended outside the cloud from higher levels. Ice crystals found in Traverse G at -4C indicate substantial descent of air. Natural processes may have played a part in producing the high crystal concentrations at the cloud boundaries since the top of the cloud was high enough for such processes to occur. For these regions of the cloud (outside the primary updraft areas) it is not possible to separate natural and artificial nucleation effects in these traverses.

2. After Traverse G, Metro II de-iced by descending to 12,500 feet. Metro II then ascended to 21,000 feet for another series of observations (Fig. F-6). During this sequence Metro IV seeded from 12,600 feet, flying a race track pattern below cloud base and slightly north of O'Leary Peak. The observational flight procedure was to traverse an unseeded cloud and then a seeded cloud, descend to a new level and repeat the procedure. The first traverse in each case was in the unseeded cloud. This cloud was less mature than the seeded cloud so the observations are not entirely comparable.

Traverses H and I - Were at 21,000 feet (-11C) at 13 minutes after seeding had started for the second time (S + 13). On Traverse H (Unseeded) there were virtually no ice crystals in the water part of the cloud. At the edges of the cloud and outside the cloud, ice crystals were found in concentrations of 10/liter. In Traverse I (Seeded) there were large areas where the water had been transformed to ice. Hexagons of 50 - 70μ were found in concentrations of 1/cm^3. Most of the ice crystals showed signs of riming and the shapes were somewhat irregular.

Traverses J and K - Were flown at 19,000 feet (-9C) at S + 18 minutes. Ice crystal concentrations and distributions were similar to those observed in Traverses H and I. Sizes of the crystals in Traverse K were somewhat smaller than in Traverse I, however, and generally ranged between 40 and 60μ.

Traverses L and M - Were at 18,000 feet (-5C) beginning at S + 23 minutes. The principal feature of interest was a long interval (1.5 miles) in Traverse M (seeded) in which the water droplet concentration was uniformly 300-400 /cm^3. The updraft rate was rather steady at 350 ft/min. No ice crystals were observed in this region and the temperature parameters indicated no mixing with the environmental air. Thus, there appeared to be no seeding effects at this warm temperature. In addition, 50μ ice crystals and graupel were observed at the edge of the cloud and outside the cloud for about 25 seconds of flight time. These ice particles must have descended several thousand feet to reach their observed location.

Traverses N and O - At 17,000 feet (-3C) at S + 28 minutes. Traverse O was quite similar to M. The long interval of uniform water droplet concentrations was interrupted almost in the middle by a burst of graupel and ice crystals. The updraft was also interrupted by a section of downdraft at this point.

Discussion of Traverses H Through O

Principal differences between the seeded and unseeded traverses were observed within the clouds in the updraft areas. At temperatures of -9C or colder ice crystals, apparently from the seeding, were observed within the cloud interior of the seeded cloud. Crystals were also observed at all levels near the edges of the cloud and occasionally somewhat beyond the cloud boundary. It has been suggested that these crystals descended in air outside the cloud from their formation altitude nearer the cloud top. Further evidence of this effect is shown in Traverse O where the updraft was interrupted within the cloud by descending air, containing numerous ice crystals.

August 15: Silver Iodide Seeding from U. S. Forestry Service Seeding Plane

Description Clouds

On August 15 the wind was exceptionally light, to 35,000 feet. The early part of the day was characterized by large cumulus building directly over the San Francisco Peaks. In the afternoon, in the flight sequence to be discussed, cumulus were developing over the desert. The mountain range was no longer a source of suitable clouds for experimentation. The cloud analyzed was seeded with silver iodideby the USFS aircraft. An excellent record of the growth of ice crystals was obtained during an upward spiral through the cloud base. This cloud was about 20 miles east of Flagstaff.

Cloud Flight

The cloud chosen for this seeding experiment was growing vigorously and was in an early stage of development. Its exterior had a firm bulging

appearance and the base was flat and dark. Silver Iodide seeding was done by the U. S. Forestry plane from 13,000 feet. The seeding plane flew a circular flight path in the updraft from 1546 to 1556. Metro I (the MRI Cessna 180) entered the updraft at 1546 from the 11,500 foot level and ascended at 1,000 feet per minute in a tight spiral turn. The power setting was adjusted so the plane would not climb with respect to rising air. At 18,800 feet, Metro I entered the cloud base, and continued to spiral upward to 22,200 feet. The ascent rate decreased with elevation. Above 22,000 feet, Metro I was unable to stay in the updraft except for brief periods. From 22,700 feet, Metro I spiraled down outside the cloud.

The thermal structure of the cloud and its environment along this flight path is of interest, and will be reviewed before discussing the particle structure of the cloud. Before Metro I entered the updraft below the cloud, it flew for several minutes at 10,000 to 11,000 feet in air that had a potential temperature (θ) of 1.5C colder than the θ for the cloud base. The mixing ratio of this air was about 6 gr/kg. The mixing ratio of the cloud base was 3.8 gr/kg. This air must have been cooled and moistened by precipitation. Two minutes before entering the updraft the air had a θ of 0.5C less than at the cloud base. The θ of the updraft from 11,500 feet to 18,800 feet was within $\pm$0.3C of cloud base except at elevation 17,500 feet and 18,000 feet. At these levels Metro I strayed towards the edge of the updraft and θ dropped to 0.5C less the cloud base. Above cloud base (Fig. F-7) the θ_{sw}(the pseudo-wet-bulb-potential temperature) transformation is used. The observed θ_{sw} follows the θ_{sw} of cloud base with only minor departures to 20,100 feet. Above this level to 22,700 feet (where Metro I left the cloud) θ_{sw} becomes progressively warmer than cloud base, with a maximum excess of 1C. It is interesting to note that this excess of θ_{sw} coincides with the growth of ice particles and a decrease in number of water droplets. When Metro I left the cloud the θ_{sw} fell sharply to 2.8C below cloud base. This difference drops to 2.0C and then to 1.4C as Metro I descends from 22,700 feet to the cloud base at 18,800 feet.

Fig. F-7 is a time diagram of variables measured on the flight. The height of Metro I vs. time is plotted on the time altitude curve. Differences between the temperature line and the altitude line at a particular time correspond to the departure of the θ_{sw} at altitude from the θ_{sw} of cloud base provided the observation is taken above cloud base. When the observation is taken below cloud base the difference between temperature and altitude corresponds to the difference between θ and θ at altitude of cloud base. The liquid water line shows the amount of liquid water measured on the Johnson-Williams L. W. Meter. The observed and adiabatic liquid water differences are shown by the differences between the L. W. curve and the altitude curve. On the same time scale the concentration and sizes of liquid and frozen cloud particles are shown.

Micrographs of the drop samples at positions a - f shown on Figure F-7 are reproduced on Figure F-8. The evolution of droplet size and the growth of ice crystal size and concentration can be seen. The cloud droplet concentration was 600/cm^3 in what was apparently an unmixed

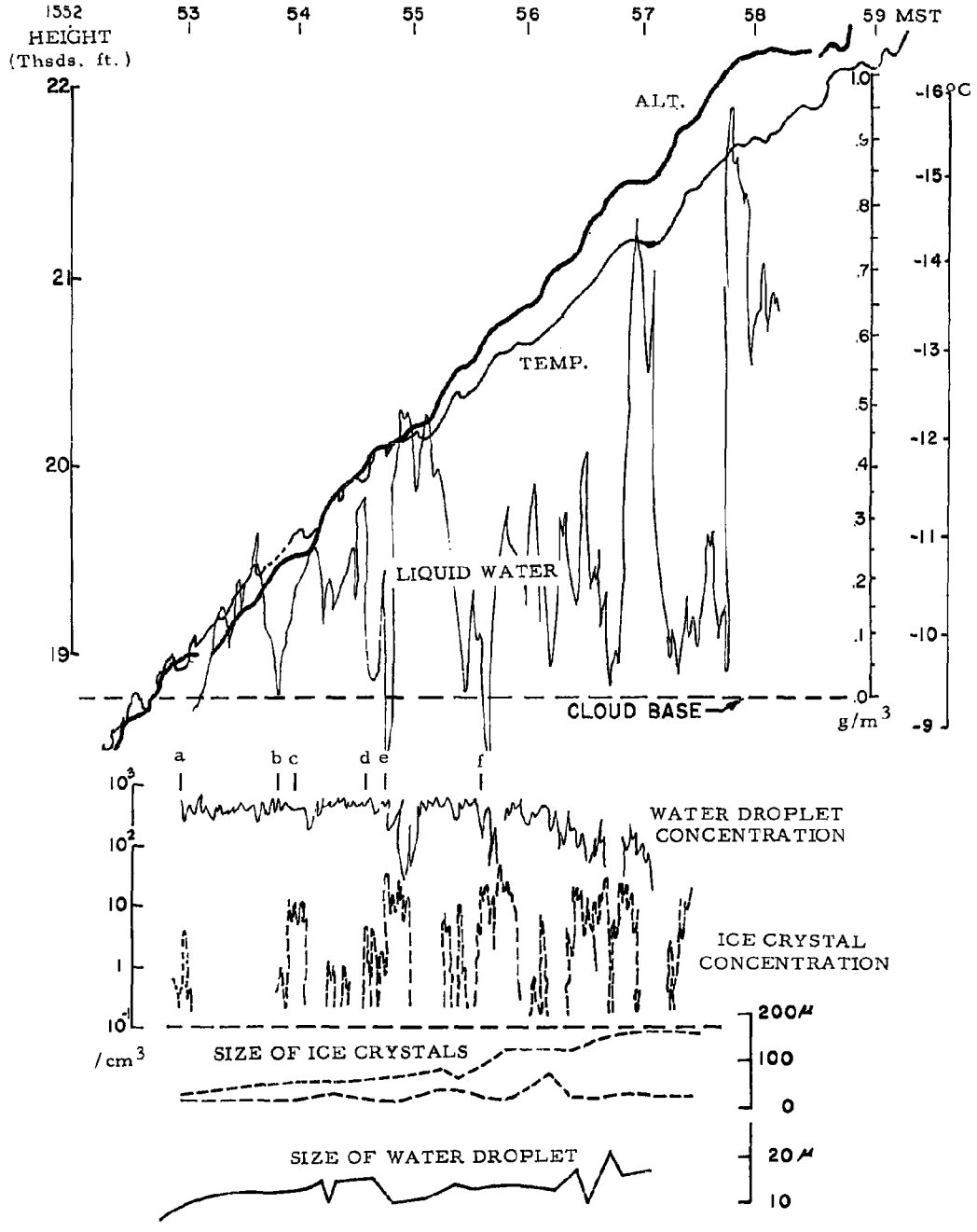

Fig. F-7. FLIGHT TIME SECTION FOR AUGUST 15.

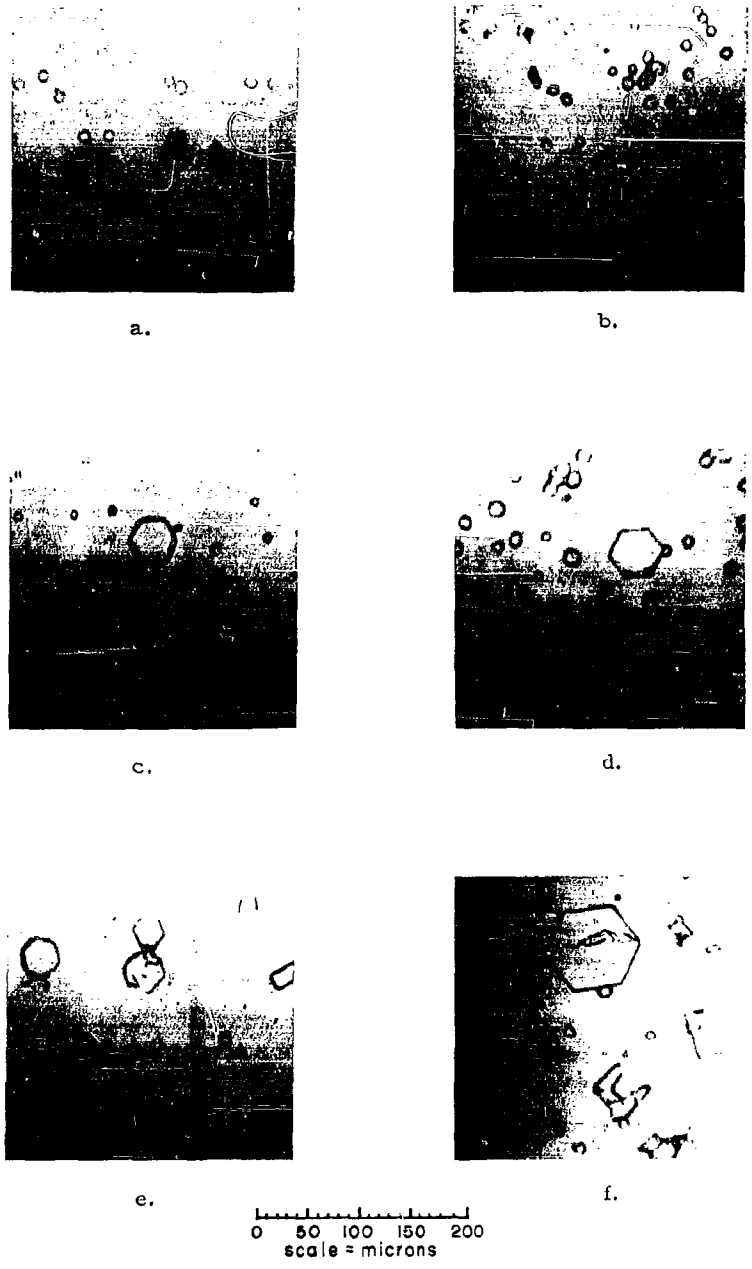

Fig.F8. MICROGRAPHS OF DROP SAMPLES a - f, AUGUST 15, Fig. F-7.

portion of the cloud. The diameter of the droplet increased immediately above cloud base and then increased more slowly as the diameters became larger. In some places, the growth of the ice crystals at the expense of water droplets can be clearly seen as the water droplet size decreases, and finally disappears completely.

Ice crystals 10 to 18 μ in diameter were first observed 225 feet above the cloud base. The replicas were in the form of plates and cubes. Size of the ice crystals increased with height. This increase was most rapid where the water part of the cloud had not been exhausted by increasing numbers and growth of ice crystals. The higher the ice crystals concentration the sooner the water cloud disappeared. In high concentrations the ice crystals compete with each other for moisture and remain small. The largest crystals found were 156 μ at 2,725 feet above cloud base.

Ice crystals were not evenly distributed in the cloud. Their occurrence in clusters, indicated that extensive diffusion of silver iodide, in the updraft had not taken place. This suggests that it may be possible, on occasion, to observe seeding effects and natural water droplet backgrounds in the same cloud at different times during the spiral.

Discussion of Daily Analysis

Certain conclusions can be drawn at this point. Some of these are rather tentative and may change on the basis of additional evidence. Areas of uncertainty will be outlined and needs for additional observation and analysis will be pointed out.

Ice Crystals from Seeding

On July 20, ice crystal concentrations of 20-100/cm^3 were found at temperatures of -5C in a region nucleated by massive dry ice seeding. Ice crystal shapes corresponded to those found in laboratory experiments at a similar temperature. In some regions the ice crystals had consumed all of the cloud water, in others the water and ice still coexisted.

On July 24, ice crystal counts of 500/cm^3 were found when Metro I seeded with dry ice the same cloud that it was observing.

On August 10, ice crystal concentrations of 1-3/cm^3 were found at -14C, 8,000 feet above the silver iodide seeding aircraft.

On August 15, concentrations as high as 10-20 ice crystals/cm^3 were found at -11.5C, 7,000 feet above the aircraft seeding with silver iodide.

The task ahead is to relate the concentration of ice crystals and the volumes they occupy. Sizes and shapes must be studied further in relationship to temperatures, time, and cloud motions and seeding techniques.

Natural Ice Crystals

The ceiling for Metro I was generally 21,000 feet, or -12C. Natural ice crystals formed at this level are in such low concentrations that the sampling technique does not usually record them. However, the cloud particle sampler does collect many ice crystals not associated with seeding. It is assumed that these crystals are carried from higher levels by downdrafts. Crystals may be found on the edges or outside the clouds, and/or in cloud regions where there are downdrafts, but not undiluted cores.

During the summer of 1963 the observational plane should have a ceiling of 27,000 feet, or roughly -22C. Working at this altitude and below, it should be possible to observe the birth and growth of natural ice crystals and follow their migration down the edges of clouds or in downdrafts.

Natural ice crystals formed at high altitudes may remain unevaporated in clean air. In future analysis it may be necessary to include a computation of whether the air is saturated with respect to ice.

Water Droplets

Cumulus clouds measured at Flagstaff show high concentrations of water droplets, 500 to 800/cm^3, in the undiluted portions of the clouds. In most clouds there were no indications of coalescence of water droplets. In some cases where coalescence might have been taking place the droplet sampler was flooded. Droplets, in general, did not approach the 36μ size, which according to Hocking, is the minimum size for coalescence. 15 to 20μ was generally the size of the largest droplets. Some of the samples had replicas of larger droplets, but these usually occurred in badly flocculated samples. It is possible that coalescence occurred after collection. Refinements in collection and replication techniques should clarify this point during the summer of 1963.

Cloud droplet concentration in the undiluted part of the cloud should be a function of: (1) Nuclei distribution, which should be measured in a specific mass, and (2) supersaturations in the first 500 feet above cloud base (which is a function of the rate of ascent) and (3) mixing ratio. Since the concentration is almost directly proportional to the rate of ascent, it should be possible to measure differences due to this factor. This would require quantitative knowledge of the aircraft speed. This data was not available in the 1962 field program. It should be possible to describe the conditions of coalescence precipitation for Flagstaff cumulus in terms of: (1) cloud updraft rate at the cloud base, (2) mixing ratio at the cloud base, (3) depth of the undiluted portion of the cloud, and (4) the condensation nuclei distribution.

Cloud Mixing

The observations analyzed thus far have shown that parts of some clouds have a structure that is in agreement with what might be expected if parcels had been raised unmixed from cloud base. Other parts of the clouds show the characteristics of having been mixed with the environmental air. Cloud B on July 24, as well as the cloud discussed for August 15, are good examples of unmixed clouds, or clouds with large enough unmixed cores for the aircraft to spiral in. Other clouds had some area of unmixed core which the aircraft found intermittently, such as cloud A on July 24 and cloud A and cloud C on July 20. The occurrence of the undiluted cores will be related to the best estimate of: (1) the cloud base dimension, (2) the age of the cloud, (3) the vertical development of the cloud, (4) the wet bulb temperature of the cloud environment, and (5) the wind shears acting on the cloud. In all, 18 clouds are available for analysis of undiluted cores. As the conditions of non-dilution are studied an explanation of how the diluted portions of the cloud acquired their properties must also be sought.

Air External to the Clouds

This part of the analysis has only been touched on so far. The discussion of the flight path on August 15 points out some of the anomalies that are observed, such as: (1) The air is chilled and moistened by precipitation, (2) the up current flowing into the cloud base is warmer than the environment by 0.5C. These anomalies and many others are important to cloud development and can be analyzed from the data now available, as well as explored with new observations.

G. Cell Dynamics: An Evaluation of July 27 and August 15

Introduction

An analysis of cloud development has been made, from ground time-lapse cine film and from aircraft measurements, of two days during the 1962 Flagstaff field studies. The two days, July 27 and August 15, differed in that the former was marked by comparatively low cloud base and strong wind shear while high base and negligible shear existed during the latter.

The pertinent reduced data are presented in this chapter and comparisons are made between:

a. the development of a cell seeded with dry ice and unseeded cells on 27 July,

b. rate of rise and persistence of cloud towers on 27 July and on 15 August,

c. observed values on the two days and those computed using constants obtained from laboratory models.

Main Points

Prior to seeding on July 27 the following features were observed and measured from the time-lapse cine film:

a. The rate of rise of towers emerging from the main cloud mass was 1400 ft/min and the maximum height attained was roughly 30,000 feet.

b. The horizontal speed of the tower cap upon emerging was considerably less than the environmental wind speed.

c. After emerging there was rapid vertical deceleration coupled with horizontal acceleration until the speed reached the environmental wind speed.

d. New cloud growth always formed on the upwind side.

e. Tower trajectories, from any one cell, or cloud mass, tended to originate from roughly the same point source.

f. After glaciation and maximum development there was insignificant new growth in the cell; it would drift downwind and a new preferred area for development would then form.

The seeded cell had the same characteristics as listed above except that the maximum rate of rise of emerging towers exceeded 2000 ft/min and the maximum height attained was approximately 38,000 feet.

On 15 August the vertical velocity was considerably less (750 ft/min upon emerging) than on the 27th, however the velocity was constant for a considerable period of time and the duration of individual towers greater. As a result the development of the cloud mass as a whole was more rapid.

The aircraft data from the two days show:

a. Dry adiabatic lapse rate below cloud base.

b. Maximum values of temperature, mixing ratio, and liquid water that are observed in cloud are equivalent to the pseudo-adiabatic values and indicate a comparatively undiluted core.

c. The temperature difference between cloud and environment at the 20,000-foot level was roughly 4C on 27 July and 2C on 15 August.

d. On the 27th extremely severe turbulence was encountered, notably in the region of rapid mixing on the downwind side.

It is not known for certain if the flight measurements on the 27th were made in the seeded cell, however the aircraft was in the region where the seeding occurred.

When the observed values, obtained from aircraft and time-lapse measurements, are compared with those predicted from laboratory models it is found that there is reasonable correlation considering the assumptions that must be made. The models are obtained from laboratory experiments of isolated masses of buoyant fluid rising in both neutral and unstable, but undisturbed, surroundings and have been reported by Scorer (1957), Woodward (1959) and Turner (1963).

July 27

Time-Lapse Measurements

Measurements of cloud position, height, vertical and horizontal velocities were obtained from three time-lapse cameras:

Site	Distance, Miles, to Mt. Humphreys	Direction to Mt. Humphreys	Lens Focal Length	Frames/min.
Flagstaff Control	14.5	360°	10 mm	~ 2
Rimmy Jim	40.8	202°	5/8 in.	~ 1
Gray Mountain	33.8	295°	5/8 in.	~ 1

The film was projected so that the scale at the peak was 1 inch = 2 miles.

Cloud, or tower, position was obtained by triangulating from two or three cameras and checked, where possible, with radar echo, U-2 film or whole sky camera. Heights were then determined from one or more cameras. The absolute value of the cloud tower height may be assumed to be accurate to within:

± 1000 feet at 20,000 feet
± 1500 feet at 30,000 feet
± 2000 feet at 40,000 feet

Relative accuracy of measurements for any one tower or cloud is greater than the absolute. Vertical velocities are accurate to about ±200 ft/min and horizontal velocities ±300 ft/min.

0715 - 0915 MST

Cumulus were well developed (tops between 22,000 - 28,000 feet) over the peaks by daybreak. Precipitation occurred the previous afternoon and the mixing ratio was comparatively high in the lower levels; cloud base at roughly 12,500 feet was low for the area.

At 0752 rapid development occurred. The cloud outline, from the cine camera at Flagstaff Control, is shown in Fig. G-1a for 0752 (dotted line) and 0800 (solid line). The position of several towers, shown at half minute intervals, gives an indication of rate of rise and strong shear. The maximum height of any tower, between two miles west and three miles east of the peak, is drawn in Fig. G-1b (solid line). The breaks in the trace indicate that the tower has drifted beyond three miles east. Glaciation occurred (observed from cine film) at about 0756 when the cloud tops were at 25,000 feet and where the estimated temperature was -18C. After the

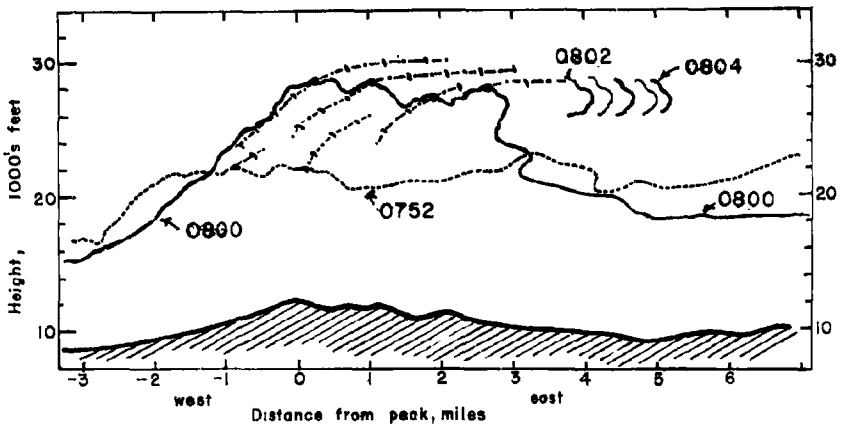

Fig. G-1a. CLOUD OUTLINES

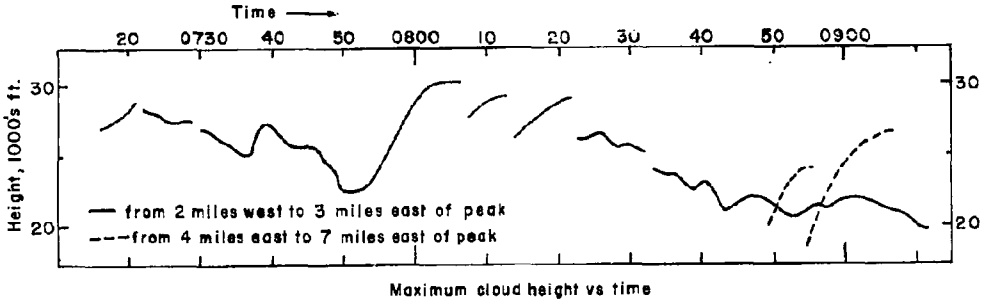

Fig. G-1b. MAXIMUM CLOUD HEIGHTS

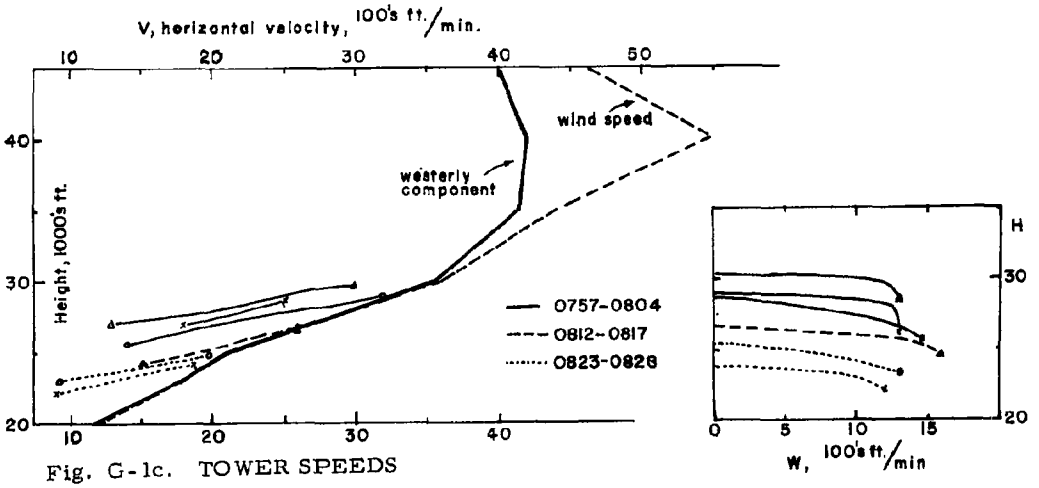

Fig. G-1c. TOWER SPEEDS

Fig. G-1 EARLY JULY 27 CLOUD POSITIONS AND MOVEMENTS.

towers had drifted to the east, the maximum height, to which subsequent towers developed, decreased. At about 0850 a new "preferred area" developed about six miles to the southeast. The height of two towers in this new center are shown as dashed lines in Fig. G-1 b.

Fig. G-1 c shows the horizontal speed, v , and the vertical speed, w , of emerging towers as a function of height. The wind speed, dashed line, and its westerly component, thick solid line, obtained from the 0600 Winslow pibal are drawn. It can be seen that the rate of rise of the emerging towers is about 1400 ft/min and that rapid deceleration occurs. As expected, the horizontal speed upon emerging is less than the wind speed; however, the parcel quickly acquires the velocity of the environment as its vertical speed diminishes. The close agreement on the chart is more than one should expect from the accuracy claimed for the measurements.

Velocities for only six of the towers are shown. Additional measurements gave similar results.

1050 - 1140

At 1052 a cell (Cell I) about six miles WSW of the peak was seeded with dry ice (approximately 500 pounds) from the MRI Aero-Commander. Estimated top was 27,000 feet; seeding was done at roughly 20,000 feet where the temperature was about -12C. The development of this cell is shown in Fig. G-2 a. At 1055 the top of the cloud system, as seen from Gray Mountain, is shown as the hatched solid line in the upper right diagram. Since Gray Mountain is situated NNE of the peak, east is to the left and west to the right. The height and distance scales apply only to the cross section normal to the camera and through the peak. The horizontal position of the cell was determined from radar and this position was taken into account, at one-minute intervals, when computing height and velocities. The cloud approached Gray Mountain at an angle of 35° with respect to the cross section.

The trajectories of two protuberances B and C, on a tower emerging from the cell, are drawn with positions indicated at one-minute intervals. The tower outline is drawn every two minutes. The position at 1110 and 1112 is indicated, at which time glaciation was observed (from cine film). The cloud outline at 1115 is drawn in Fig. G-2 b. A tower, M, from Cell II, emerged below the seeded tower. The center of this new cell, which was distinct from the seeded cell, lay about one-half to one mile north of the track of the first cell. Subsequent trajectories are drawn. The height of the emerging towers in each of Cell I and Cell II is plotted versus time in Fig. G-2 c. Rate of rise is shown on Fig. G-2 d. In both cells the

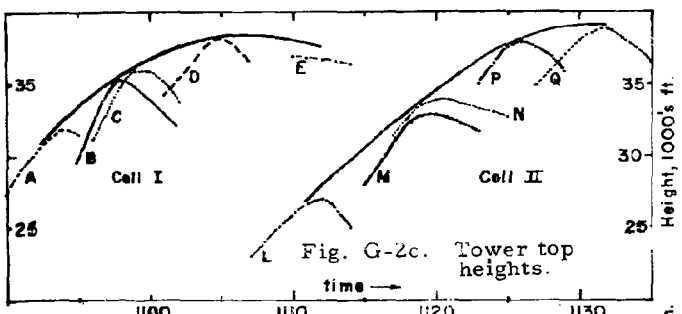

Fig. G-2c. Tower top heights.

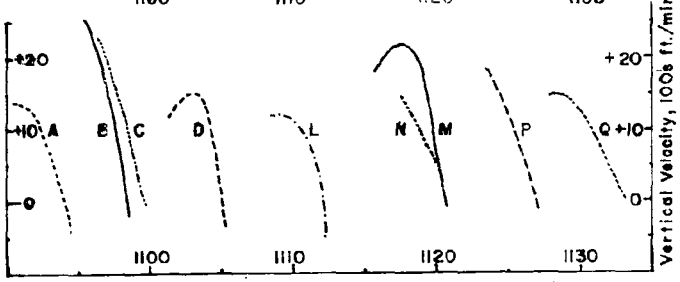

Fig. G-2d. Tower top vertical velocities.

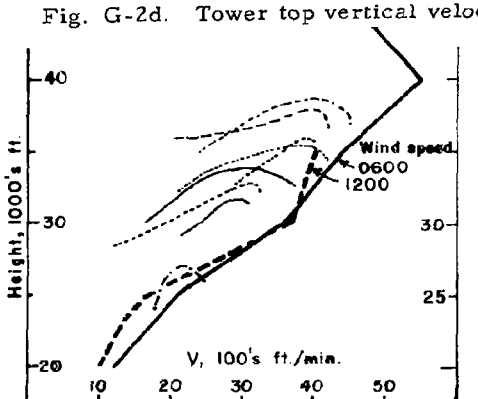

Fig. G-2e. Tower top horizontal velocities.

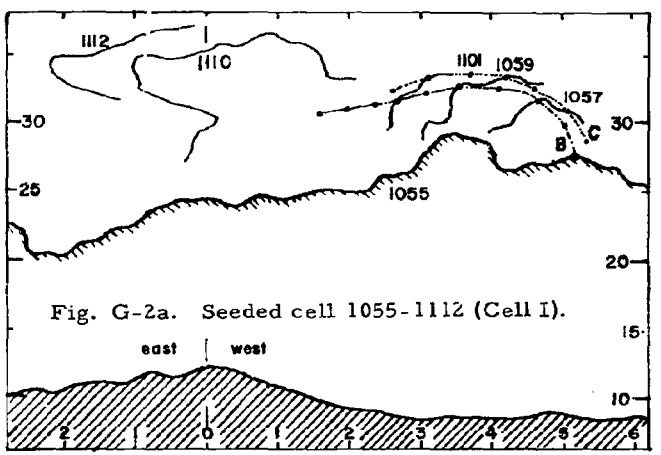

Fig. G-2a. Seeded cell 1055-1112 (Cell I).

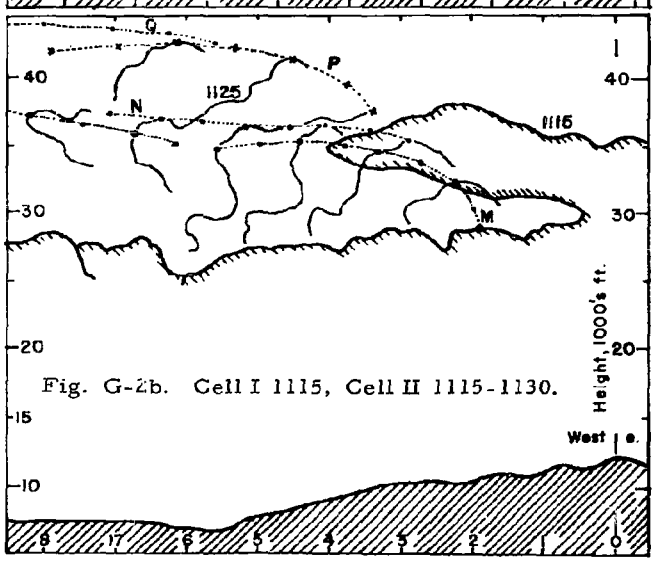

Fig. G-2b. Cell I 1115, Cell II 1115-1130.

Fig. G-2. CHARACTERISTICS OF SEEDED AND SUBSEQUENT CELLS, JULY 27.

velocity was greatest at the 30, 000-foot level where the cloud temperature was probably about -30C. Except for cases D and M, the towers decelerate almost immediately after emerging. Because positions could be plotted only every minute, too much attention should not be paid to these two cases where acceleration is indicated for only two minutes. The horizontal speed is shown versus height in Fig. G-2e. The wind at noon had backed and decreased slightly since the 0600 sounding.

Aircraft Data

The instrumented Cessna entered a cloud in the same region as the seeded cell from below the base at 1048.

The following are among the variables that were recorded:

Altimeter:

The pressure height was read from the Brush recorder chart to the nearest ten feet (chart scale: 1, 000 feet = 4 cm) taking into account the zero drift and change in gain. No scale correction was applied; the altimeter calibration chart gives a change of 100 feet from 8000 to 22, 000 and a change of 30 feet from 12, 000 to 18, 000 feet. A crude test of hysteresis was made at ground level and indicated a difference of 30 feet. It was decided to apply for the height range 12, 000 - 20, 000 feet a correction of 50 feet low when climbing and 50 feet high when descending in addition to a two-second lag. This amounted to a difference of about 150 feet between ascent and descent.

Temperature (Vortex thermometer):

Read to the nearest 0. 1C from the recorder, where 4 cm = 14C. No correction, except for zero and gain, was applied. When a scale change was made adjacent end points had the same value (on the flight in question). The readings presented are probably accurate to the nearest 0. 3C.

Mixing ratio:

A crude calibration of the mixing ratio instrument was obtained by comparing the meter reading while on the ground to the value found by sling psychrometer. The values shown here were obtained from this one point calibration taking appropriate recorder zero and gain into account. The mixing ratio was read to the nearest 0. 1 gr/kg (10 gr/kg = 3. 2 cm).

Liquid Water (Johnson-Williams hot wire type):

Read to the nearest 0. 1 gr/m^3 (1 gr/m^3 = 9 mm on the chart) the value was converted into gr/kg by taking the density into account. A change in the

instrument zero occurs (generally when in cloud), and the appropriate correction for this is not known.

Values of the above variables were read from the chart every 5 mm (12.5 sec) and at every significant point. Fig. G-3 shows temperature, mixing ratio, liquid water content and relative humidity versus height. Ascent was made in cloud, descent in clear. Pseudo-adiabats (for θ_w = 18C, 20C and 22C) are drawn as dashed lines. The appropriate saturation mixing ratio, with respect to water, was determined for each point and the relative humidity computed. The dashed line, originating at 8.3 gr/km, indicates the value of the saturation mixing ratio, with respect to water, along the pseudo-adiabat that passes through cloud base. The pseudo-adiabat selected, rather arbitrarily, was θ_w = 21.5. It should be remembered that the cloud base is usually difficult to define to an accuracy greater than ±100 feet and that there is some discrepancy in the zero of the liquid water. Nevertheless, the "adiabatic value" as drawn can serve as a guide line, and it can be seen that the maximum values of the recorded mixing ratio, though less than the "adiabatic value", follow the same slope. They lie on a line which would be equivalent to a pseudo-adiabatic of 21C. Comparative values of temperature, mixing ratio, liquid water, and RH are as expected. For example, at 1050 (true height of 14,000 feet, pressure height 13,000 feet), there is a temperature decrease of about 1C, a drop in the mixing ratio, little if any liquid water and a relative humidity of only 90%. At this time the rate-of-climb indicator showed a decrease from about +1100 ft/min to +300 ft/min. A similar situation occurred at pressure heights of 15,500, 17,200, and 17,900 feet. The aircraft spiraled up in the cloud, attempting to stay in the "core"; however, one part of the turn may be comparatively close to the cloud edge. This appears to be the case from the recorded data. The estimated diameter of the circle is 2500 feet and the time to complete 360° about one minute.

At 1054:30 the aircraft left the cloud and re-entered at 1057 to make a traverse through it. (Details of this traverse are given in the next figure). Descent was then made in the clear. The horizontal position relative to the cloud is not known. The temperature gradient on the descent is roughly 2.2C/1000 feet and the air comparatively dry, especially at the higher levels where the relative humidity is 50%. The temperature difference, in and out of cloud, will be discussed subsequently.

Traverse Through Cloud

Fig. G-4 shows temperature and moisture values versus time (distance), from 1054 through 1058. At 1054 the Cessna was still spiraling up in the cloud. We do not know at what stage in the growth of cloud the aircraft left, whether it was approaching the top of the cell or whether the pilot deliberately flew out the side. At this time the maximum height of the seeded cloud was 32,000 feet; the aircraft left at 20,500 feet.

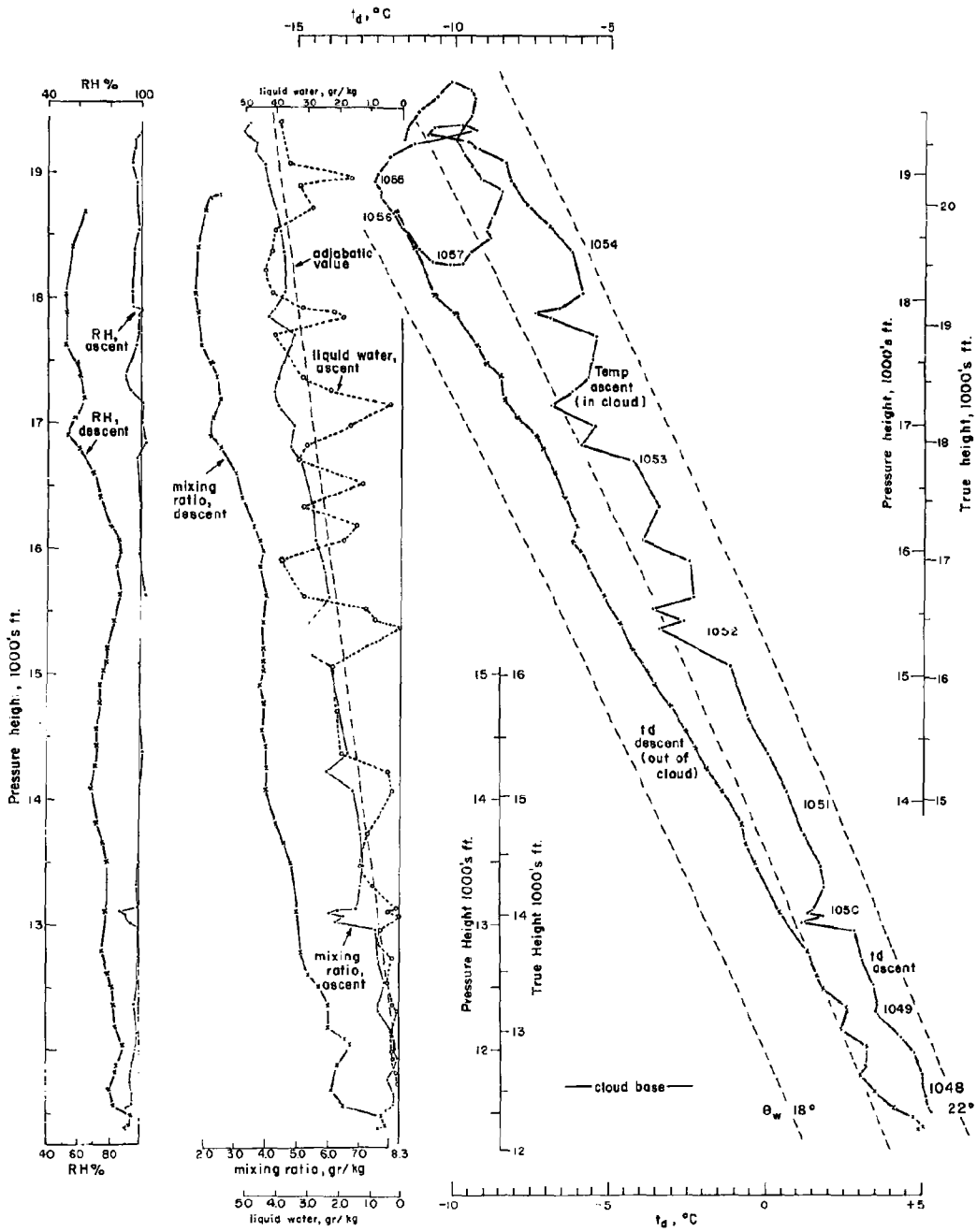

Fig. G-3. AIRPLANE MEASUREMENTS, JULY 27, 1962

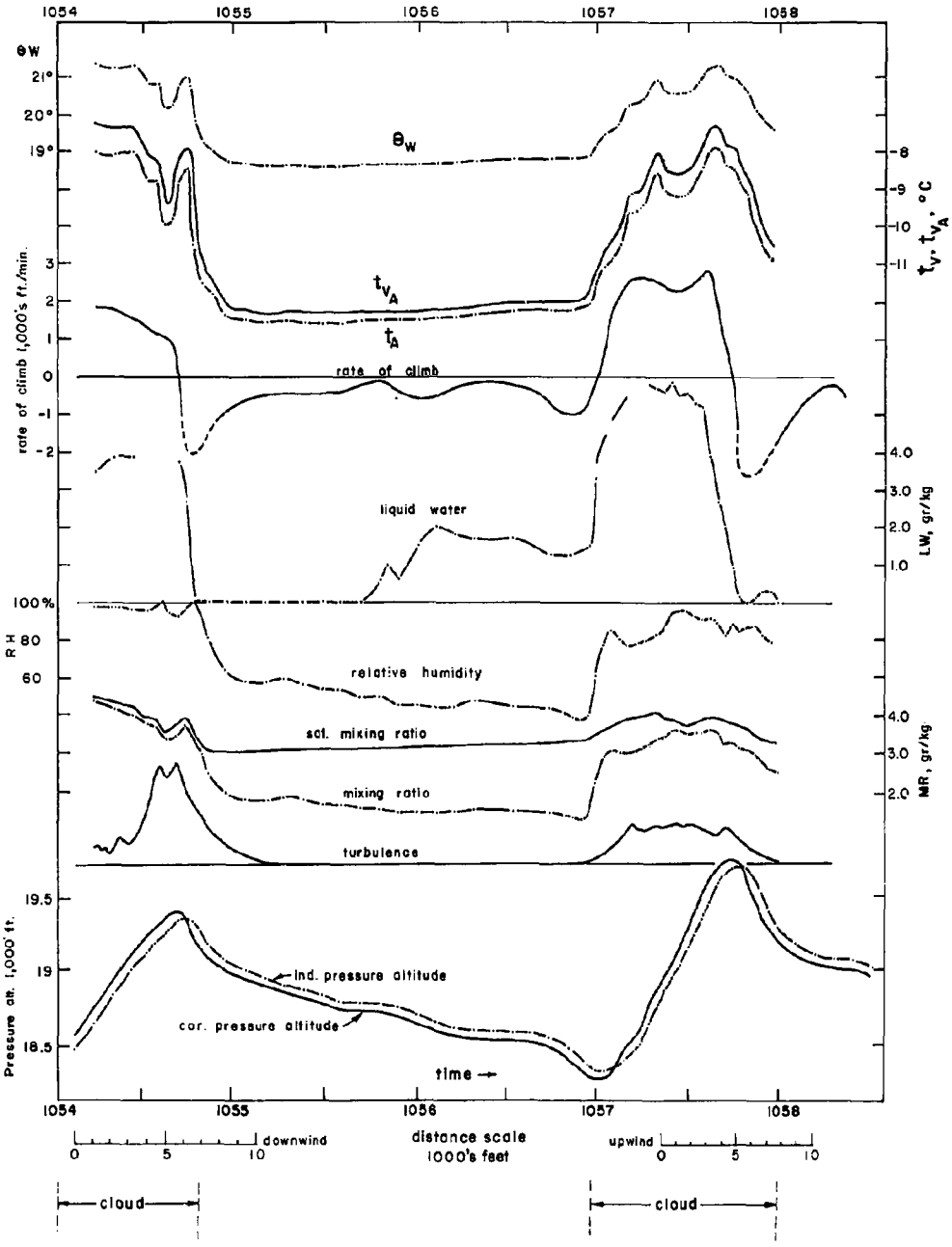

Fig. G-4. CLOUD TRAVERSE, JULY 27, 1962.

The Cessna emerged from the eastern, or downwind, edge of the cloud. At 1054:45, there was a sharp decrease and increase (followed by decrease) in temperature and mixing ratio. At this same time a high reading is recorded on the turbulence meter. (A quantitative value has not been given to this reading; observer's notes state at this time: "extremely severe turbulence". Also at this time there are abrupt changes in the trace of liquid water and rate of climb (Crossfell Variometer) on the Brush recorder chart. These changes are not shown in Fig. G-4; the two chart traces, which overlap, cannot be separated with any confidence. The rate of climb was obtained by differentiating the corrected pressure height obtained from the altimeter. The difference between pressure height and true height was also taken into account, i.e., $\Delta H_{pres.} = 1.06\ \Delta H_{true}$, at this level.

On a day of strong shear one may expect to find a turbulent region on the downwind side of the cumulus. It is logical to assume that the values at 1054:45 were recorded in a region of rapid mixing (between cloud air and dry cooler environmental air). The horizontal dimensions of this region are, very roughly, 2000 feet.

The aircraft turned in the clear and then re-entered the cloud, on the downwind side. Entry was made a few seconds before 1057. The liquid water content indicates 1.5 to 2.0 gr/km prior to this time. In the cloud a value of approximately 5.8 gr/km is roughly 1.8 gr/km above the adiabatic value. We can assume then that the liquid water content in the cloud was approximately the adiabatic value and that this is another case of a change in the zero of the meter.

Turbulence was encountered throughout the traverse of the cloud. Observer noted: "severe turbulence".

The curve designated t_A is the temperature which the air would acquire if brought pseudo-adiabatically to a standard pressure level. The level chosen was 18,875 feet. The virtual temperature increment has been added to the values and the resulting curve, t_{v_A}, drawn. That is,

$$t_{v_A} = t_A + \frac{r}{r_s} (\Delta t_v)_s$$

where r and r_s are the mixing ratio and saturation mixing ratio respectively, and the saturation virtual temperature increment,

$$(\Delta t_v)_s = T\ r_s \left(\frac{1}{\epsilon} - 1 \right) \left(\frac{1}{1 + r_s} \right)$$

The maximum virtual temperature difference in and out of cloud is 5C;

the average virtual temperature difference is roughly 2.5C. When considering cloud density the weight of the dispersed condensate of water or ice should be taken into account. The notation of Saunders (1957) will be used. The "cloud virtual temperature" is the virtual temperature reduced by the amount: $T_v \times r_L$, where r_L is the liquid water content in gr/gr. In the above case this reduction amounts to 1.0C if we let r_L equal 3.8 gr/km, the "adiabatic value" at a pressure height of 18,875 feet.

It is of interest to examine the cloud virtual temperature difference obtained from the spiral in the cloud and the descent in the clear. Values were computed at those heights where higher, i.e., warmer, temperature readings were recorded. (See Fig. G-3) The temperature difference between that obtained inside cloud and that recorded outside at the same level, Δt_d, is shown in Fig. G-5. The virtual temperature increment, Δt_v, decreases with height both in and outside the cloud. The difference between the two remains comparatively constant, i.e., between 0.35 and 0.5C. The effect of the liquid water is plotted on the left side of the diagram; the crosses indicate actual values of $T_v \times r_L$ and the line is the "adiabatic value" of $T_v \times r_L$. The cloud virtual temperature difference ($\Delta T_v'$), is depicted by circles in the figure and

$$\Delta T_v' = \Delta t_d + \Delta t_{v_{in}} - \Delta t_{v_{out}} - T_v \times r_L \quad .$$

The rate of rise of the aircraft ($\Delta H/\Delta t$) where H is the true height and Δt is 30 seconds, is shown. The aircraft was flown in a manner which gave approximately zero rate of climb in still air. The points given in Fig. G-5 are probably accurate to about ± 300 ft/min.

Comparison with Laboratory Models

The data obtained from the above aircraft traverse and spiral may be substituted in the formula (see, for example, Scorer, 1957):

$$W = C(g\ BR)^{1/2}$$

where W is the rate of rise of the thermal cap, or leading edge, B is the average buoyancy ($\overline{\Delta T_v'}/T_v$), and R the radius. Laboratory experiments (of isolated masses of buoyant fluid rising in neutral and undisturbed surrounding) give a value of 1.2 to the constant C. Also:

$$Z = nR$$

$$V = mR^3$$

where Z is the height above the theoretical point source and m and n are constants.

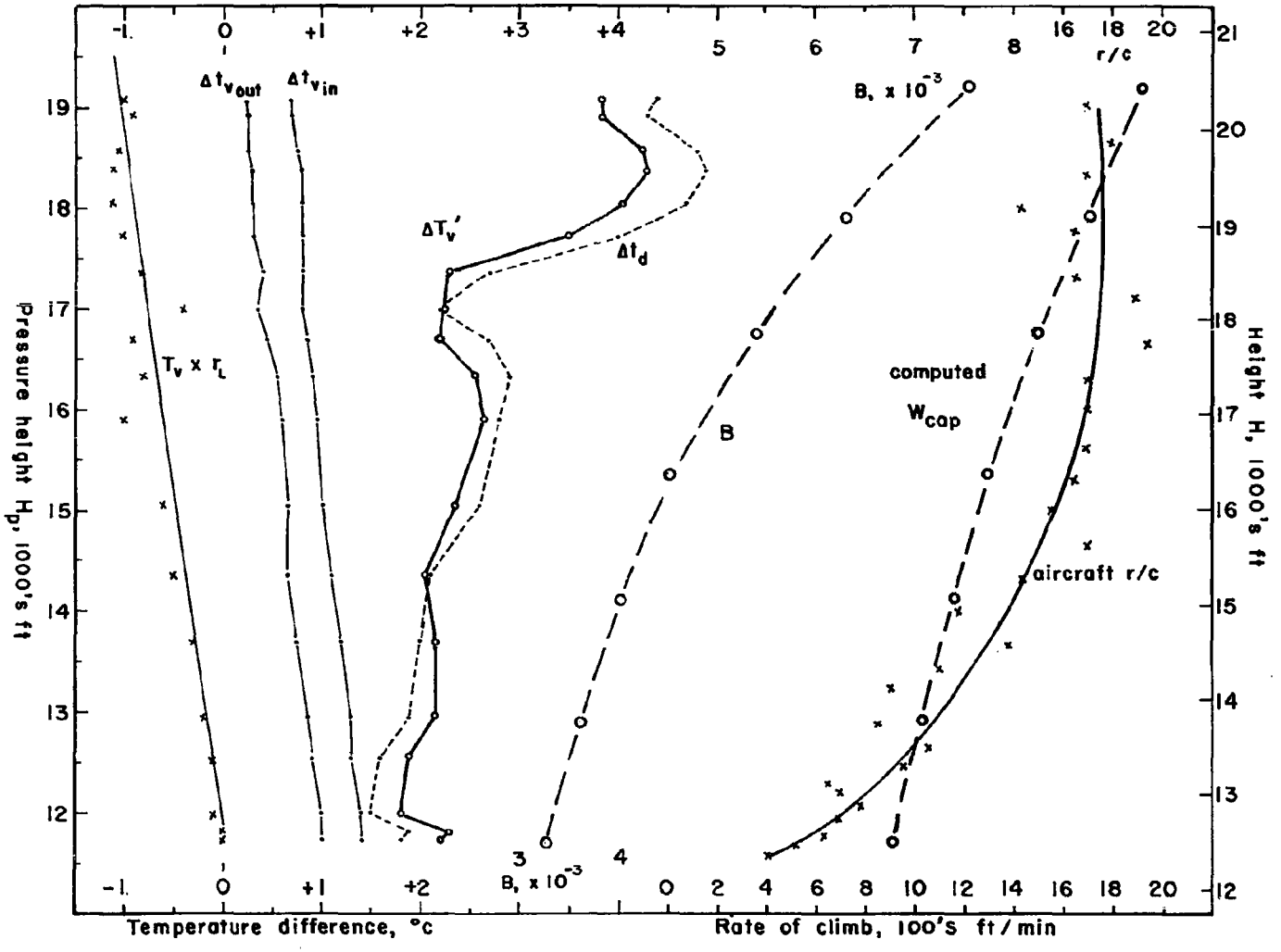

Fig. G-5. CLOUD VERTICAL TEMPERATURE DIFFERENCES, BUOYANCY, AND VERTICAL VELOCITIES.

The experiments gave a value of $n = 4$ and $m = 3$. The total excess buoyancy (BV) remains constant in any one experiment in neutral surroundings. It has also been shown that:

$$Z^3 = kt .$$

where t is the time from release at point source. By writing $dz/dt = W$ and substituting we have

$$k = \frac{2nCg^{1/2}}{m^{1/2}} (BV)^{1/2}$$

It can also be shown that the acceleration

$$- \frac{dw}{dt} = \frac{R}{t^2} = \left(\frac{4C^2 g}{n^2}\right) B$$

and that the rate of entrainment

$$E = \frac{1}{V} \frac{dV}{dz} = \frac{3}{nR} .$$

A nomogram, giving values of R, Z, B, W, t, dw/dt, and R, is presented in Fig. G-6. The value of k remains constant for any given thermal.

As stated above, the values obtained for the constants apply only to neutral surroundings; in unstable surroundings we do not know a value for n or if it is constant. The constant C is probably a function of the stability but it is reasonable to suppose that its value is within about 50% of that obtained for neutral surroundings.

Recent experiments by Turner (1963) dealing with thermals of increasing buoyancy enable us to use most of the above formulae in those cases where the surroundings are unstable. The experiments show that the thermals spread along a cone, i.e., n is constant. In those cases where the acceleration was constant n had a value of 5.0 and where there was constant velocity the mean value was 4.3. As with the neutral case the element acquired a spherical shape; $m = 4.3$ when dw/dt = constant and $m = 2.9$ when w = constant.

Turner calculated upper limits to the constant of proportionality β where

$$\frac{dw}{dt} = \beta B$$

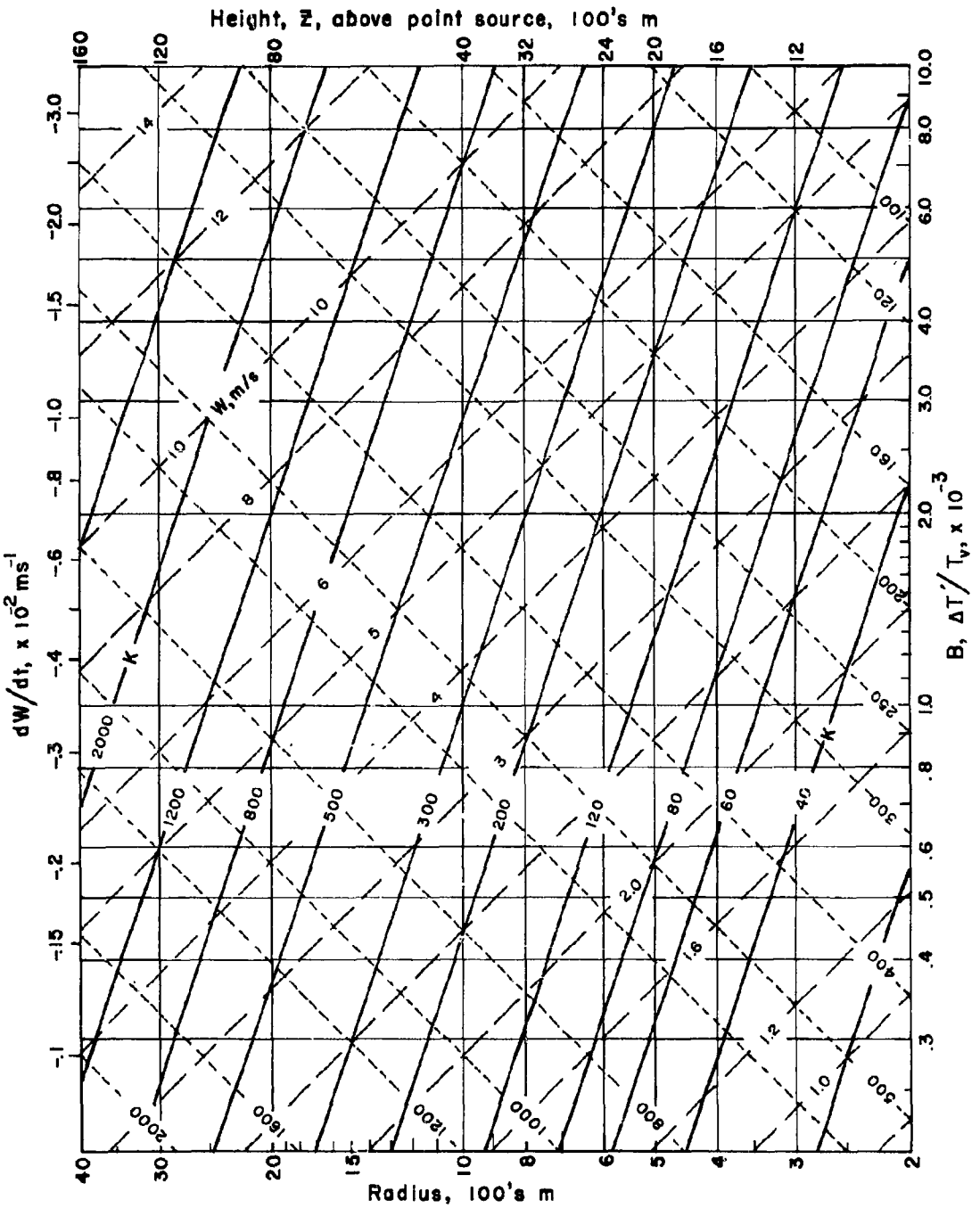

Fig. G-6. NOMOGRAM FOR ISOLATED THERMAL, NEUTRAL STABILITY.

and arrived at a mean experimental value of 3.3. He did however state that the measurement technique and theoretical reasoning, which would be discussed in another paper, suggest that β had been seriously over-estimated by a factor of about 3.

Examining the situation, if $dw/dt = \beta B$, then

$$W = \beta Bt = C(g\ B\ R)^{1/2}$$

and

$$Z = \frac{\beta\ Bt^2}{2} = n\ R\ .$$

Substituting we have

$$\frac{C^2\ g}{2\ n\ \beta} = 1.$$

Taking $n = 5.0$, then $C = 1.8$ if $\beta = 3.3$. A more probable value for C of 1.0 is obtained if we assume the 3 x over-valuation and take $\beta = 1$.

A nomogram where $dw/dt = B$, $n = 5$, and $C = 1.0$ is presented in Fig. G-7. The absolute value of t is of course different than presented in Fig. G-6 for the neutral case. The rate of rise is 20% less.

A radius of approximately 4200 feet (1280 m) is obtained from the aircraft traverse (see Fig. G-4). The maximum cloud virtual temperature difference is 4.0C ($\Delta T_V' = \Delta T_V - r_L \times T_V = 5.0 - 1.0C$). We will, rather arbitrarily, assume that the average is half the maximum value, i.e., $B = 2.0/263 = 7.6 \times 10^{-3}$. Substituting we have $W = 9.75C$ and if we take $C = 1.0$, since we are dealing with unstable surroundings, we arrive at a rate of rise of the cloud top of 9.8 m/s (1950 ft/min). The rate of rise of emerging towers at this time is 1800 ft/min ±600 ft/min. If the aircraft traversed the center of the cell we can expect, from laboratory experiments, theoretical models, and previous flight measurements, that vertical velocities will be encountered that are roughly twice the rate of rise of the thermal cap. In this case the rate of rise of the aircraft was about 2800 ft/min. In view of the observational accuracy and the assumptions which must be made it is felt that there is correlation if the computed and observed values are within 50% and such is the case in this example.

If we make further assumptions we may obtain a set of points for the ascent. The radius is 1280 m at a true height of 6250 m. If we assume this to be the center of mass, H_m and that $H_m = H_{cap} - R$ then $H_{cap} = 7530$ m. The height of the cap above the theoretical point source, $Z_{cap} = 5R$; the

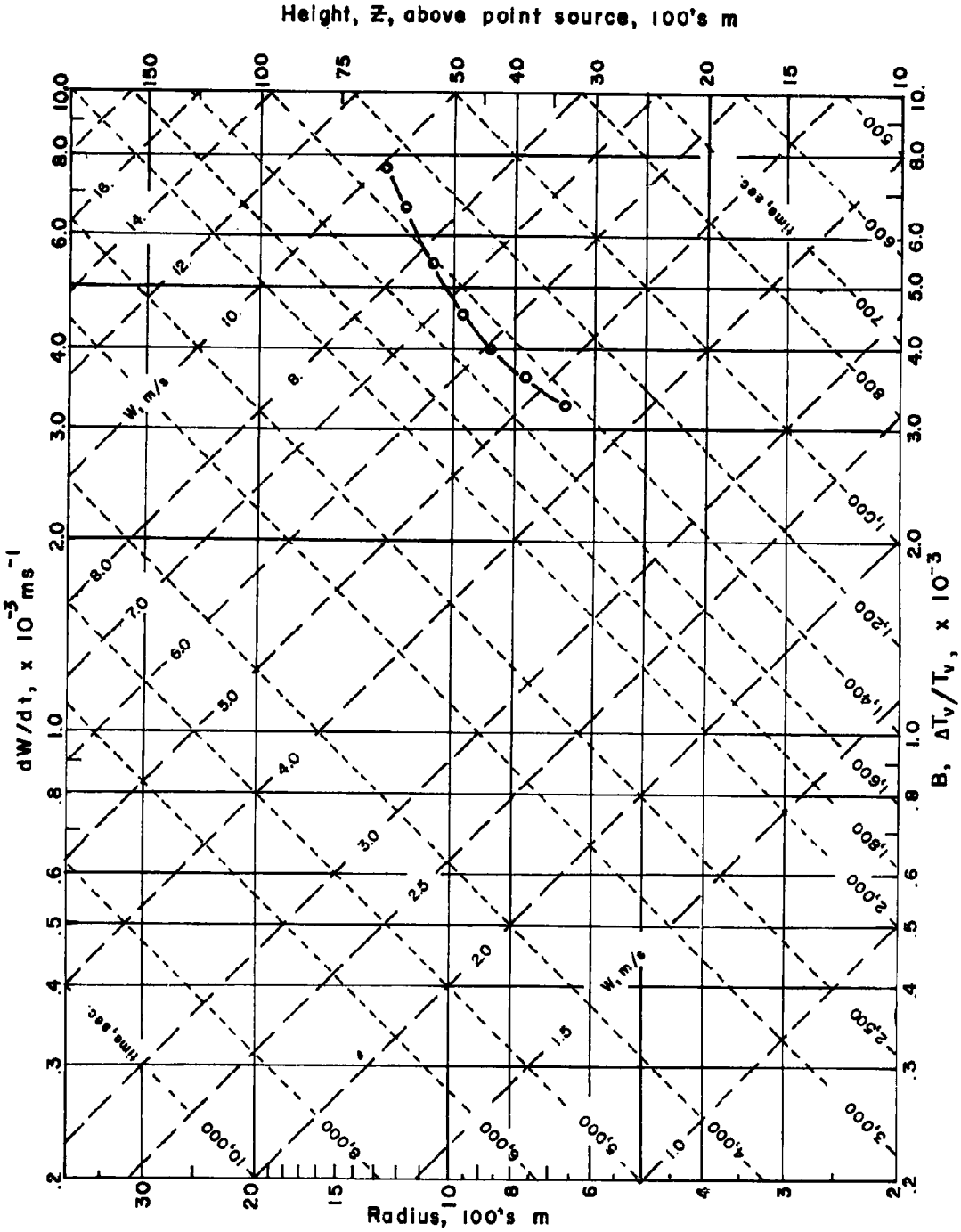

Fig. G-7. NOMOGRAM FOR THERMAL IN UNSTABLE SURROUNDINGS.

point source (Z_o) , is thereiore at a height of 1130 m MSL or, very roughly, 1400 m below the terrain. We may then compute the radius at various heights of H_m . The average buoyancy (B) was obtained by taking one-half the value of $\Delta T_v'$ (see Fig. G-5) and dividing by the appropriate virtual temperature (T_v) . The values are plotted on Fig. G-5. We may then plot these points of H_m and B on the nomogram (Fig. G-7) and read off the resultant value of W_{cap} . It can readily be seen that there is an increase in the vertical acceleration and that the slope exceeds that for t = constant. On first inspection it seems reasonable to assume that this 45° slope should not be exceeded, however it should be noted that the absolute values given to t (which is time from theoretical point source) apply only to the case of dW/dt = constant. If the acceleration is increased the value of t increases.

The computed values of W_{cap} are plotted on Fig. G-5. and can be compared with the rate of climb achieved during the spiral. It is very doubtful that a climb of 2 x W_{cap} can be achieved, for any significant period of time, while spiraling in a thermal. It is obvious, that if this were so the aircraft would soon rise relatively to the cap and then climb at a rate equal to, or more probably, less than, the rise of the cap. If one does not know the aircraft's vertical position relative to the top, it is difficult to make a logical assumption of the actual value of W_{cap} .

The fact that there is significant vertical deceleration in "observed" rate of climb and acceleration in "computed", leads one to look for an explanation. This difference could be accounted for by changing the above assumptions that were made to deduce the radius and average buoyancy, and by assuming that the aircraft has risen relative to the cap, however one is greatly tempted to question the validity of too closely comparing the laboratory models with atmospheric cases.

Note Concerning "Undiluted Core"

During a number of spirals at Flagstaff observed values of temperature and mixing ratio closely resembled the moist pseudo-adiabatic values. It should be pointed out that this correlation does not necessarily mean that the core is undiluted. If the condensate is ice and is retained then there can be significant differences, as far as dynamic studies are concerned, between the two processes. For example, at 30,000 feet there is a difference of several degrees between the ice adiabatic (reversible) process and the pseudo-adiabatic, the former exceeding the latter. Saunders (1957) has discussed the various processes, i.e., moist and ice pseudo-adiabatic (irreversible), water and ice saturation adiabatic (reversible), and shown the temperature differences attained. The program discussed by Wurtele (1961) has been re-written by C. W. Chien, M.R.I., to include values (e.g. pressure level of cloud base, temperature range) that are typical of the

Flagstaff area. This program is currently scheduled for the I. B. M. computer at UCLA. A subsequent report will discuss this program and present the results, that is, revised values of the moist pseudo-adiabatic process, ice pseudo-adiabatic process, and the water saturation adiabatic and ice saturation adiabatic processes for various cloud base heights.

Nevertheless, pseudo-adiabatic values do indicate a relatively undiluted core. Numerous explanations are possible. If there is a fairly continuous updraft into the base, which remains at approximately the same level, then the core can be "undiluted" for some undetermined depth. (On 27 July the aircraft sampled a depth of about 9000 feet). It should be emphasized that if the cloud is large and in the development stage, and if the sampled depth is small compared with the total then a core which was not comparatively undiluted would be unusual, especially considering the fact that in a spiral the aircraft ascends at very roughly the same rate as the parcel.

If, however, one applies isolated thermal theory to the cloud mass, then a comparatively undiluted core can occur over an appreciable depth only if the mass were significently large. As previously shown the entrainment rate is inversely proportional to the radius.

In so far as isolated thermal theory applies to atmospheric clouds it appears that it should be applied to small cumulus or to cells or cloud towers in large cumulus. Large cumulus may be considered as composed of multiple cells. Because of the large entrainment rate when the element is small computations have shown rapid destruction of the cloudy thermal when comparatively dry environmental air is incorporated. The computations assume that there is instantaneous and uniform mixing. This assumption is not representative of the mixing in the isolated thermal model. The writer, in fact, suggests that evaporative cooling on the cloud, or tower, edges can assist in maintaining a relatively undiluted core.

In the isolated thermal model an environmental parcel does not enter the core until after it has descended around the side, been advected in the lower region and then risen relative to the cap. If, however, the element is rising in stable surroundings, with constant density gradient, then the parcel on the edge of the thermal will not be advected in, and subsequently up, the central core. That is, the circulation decreases in the stable case whereas it is constant in the neutral environment case. It is suggested that a similar situation occurs when relatively cool, dry environmental air enters the element. The mixture of cloud and environmental air will advance around and down the element and when evaporation occurs it will continue to descend, relative to the cap, instead of being entrained into the main body of the element at the rear.

August 15

Time-Lapse Measurements

There was a high cirrus cover during the morning and the first small cumulus did not form until shortly before 1100. The duration of the first three or four "puffs", which formed over the peak, was only a few minutes; the first to exceed five minutes was tower "A" shown in Fig. G-8c.

A note should be given concerning evaluation of time-lapse data for this day. Initially it was assumed that time, read from the clock on the film, was correct. The two primary cameras used were Gray Mountain and Rimmy Jim; the view from Flagstaff Control was obscured by both higher cloud and small, but close, cumulus. It became apparent that there were considerable discrepancies in tower positions and velocities, obtained after triangulating from the two primary cameras. Possible reasons for the discrepancies were investigated and the only plausible explanation was that there was a difference in the recorded times. From radar, U-2 photographs, noting first cumulus (difficult from Rimmy Jim because of poor visibility) and by obtaining a "best fit" from the two cameras, it was decided to apply a time difference of four minutes to the Rimmy Jim camera data. Further analysis of U-2 and time-lapse films is planned; at the present time the writer believes that the absolute values of the heights presented here are accurate to 2000 feet and vertical velocities ±300 ft/min.

There were two primary cells: one over the peaks which formed first and one about four miles south which grew more rapidly. Outlines of these two cells at 1116 and 1126 are shown, as viewed from Rimmy Jim, in Fig. G-8a. Subsequent development from 1146 to 1156 is shown in Fig. G-8b. Height scale is applicable only for the plane through peak and normal to the camera.

A plot of height vs. time and rate of rise vs. time is presented in Fig. G-8c. Solid lines denote the northern cell and dashed lines the southern cell. The elapsed time from formation of the southern cell to a height of 40,000 feet is 38 minutes. The emerging velocity of all towers is fairly constant and is 700 ft/min. The unusual feature is the persistence of each tower, notably "D". The height and rate of climb of the Cessna are also shown.

Aircraft Data

There are incomplete data available for dynamic studies since the primary purpose of this flight was to obtain electrical parameters.

Temperature is the only variable shown vs. height in Fig. G-9. The aircraft entered the base at a pressure height of 16,800 feet where the re-

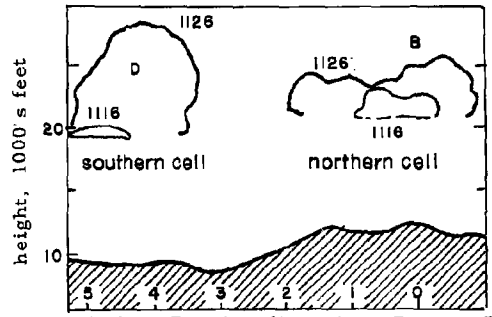

Fig. G-8a. Cloud outlines from Rimmy Jim, 1116-1126.

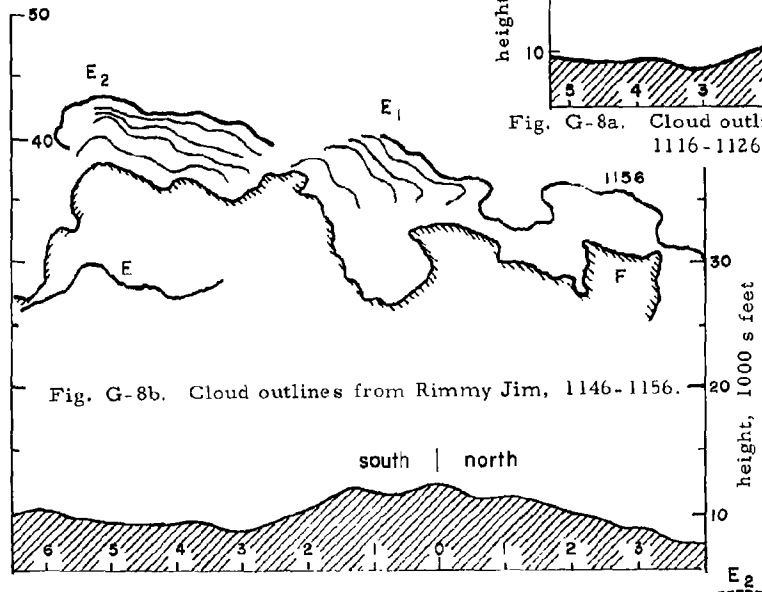

Fig. G-8b. Cloud outlines from Rimmy Jim, 1146-1156.

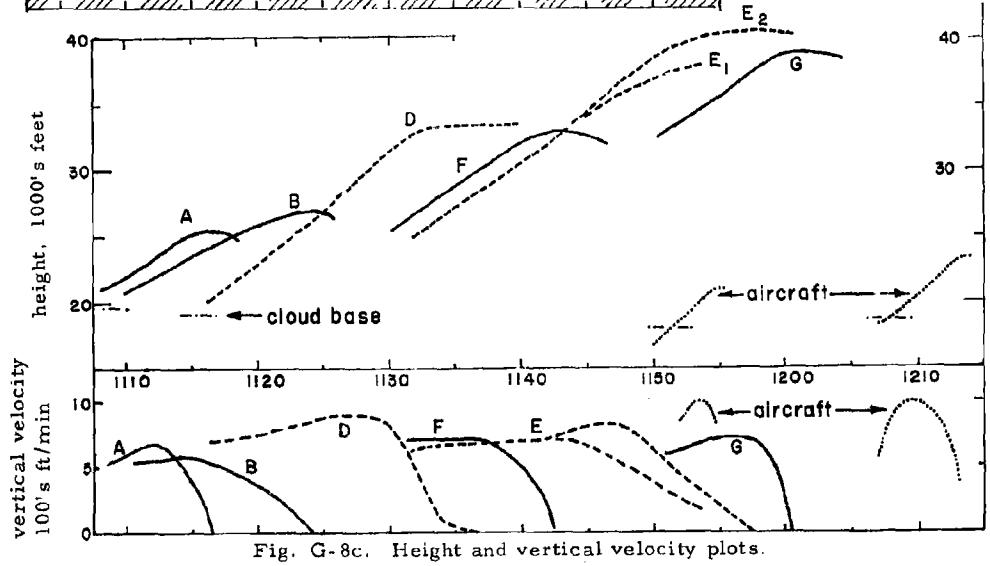

Fig. G-8c. Height and vertical velocity plots.

Fig. G-8. AUGUST 15, DEVELOPMENTS.

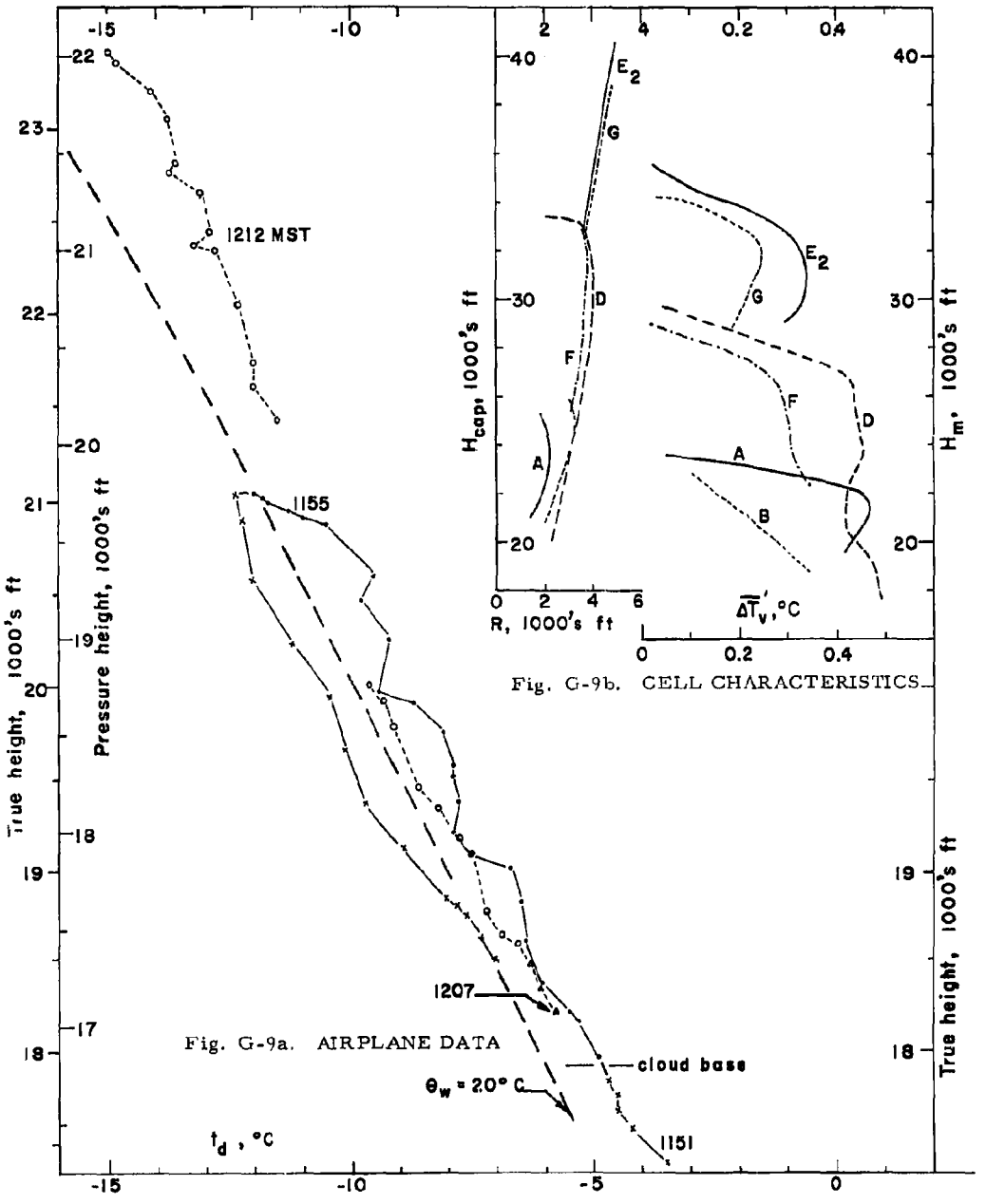

Fig. G-9b. CELL CHARACTERISTICS.

Fig. G-9a. AIRPLANE DATA

Fig. G-9. AUGUST 15 AIRPLANE DATA AND CELL CHARACTERISTICS

corded mixing ratio was 5.0 gr/km which is equivalent to the saturation mixing ratio. However, as the aircraft spiraled up in the cloud the relative humidity increased and approached 120%, when the same mixing ratio calibration scale was used. Several explanations are possible, (e.g. change in recorder gain, zero, etc., the most likely being the instrument gain setting) but rather than presenting values that are questionable this variable is not shown. The values are probably close to the pseudo-adiabatic values. There is considerable variation of the liquid water content; the maximum values are equivalent to the adiabatic.

The aircraft left the cloud at a pressure height of 19,750 feet and then descended in the clear. It re-entered, apparently a different portion, at about 1208, where the ill-defined cloud base was approximately 17,400. It then proceeded to spiral up in the cloud. The lapse rate from 20 to 22,000 feet is less than the pseudo-adiabat; it is probably close to the ice-adiabat (reversible process). The gap in data in the middle of the second ascent was due to the temperature unit being off-scale.

Correlation with Laboratory Model and Comparison with 27 July.

The persistence of the towers enables the slope Z/R to be determined. Radius vs. height is plotted in Fig. G-9b for several towers. The ratio, n , is as follows:

tower	n = Z/R
B	3
D	4.5
F	6
G	5.5
E_2	5.5

The variation is not surprising, and is not significantly greater than that obtained from laboratory experiments when the introduction of the buoyant fluid is not closely controlled. One would expect a value slightly greater than 5, the mean for the unstable case (when dW/dt = constant), which would allow for evaporation.

The cloud virtual temperature difference ($\overline{\Delta T_v'}$), has been computed using the formula

$$W = C\left(g \frac{\overline{\Delta T_v'}}{T_v} R\right)^{1/2} .$$

The constant C has been taken equal to unity and the value of T_v

has been taken from the 0400 Winslow sounding. The temperatures obtained from the sounding are within 1.0C of those recorded by the aircraft, and lie close to the moist pseudo-adiabatic value, above cloud base, up to the 200 mb level (about 40,750 feet). At 25,000 feet θ_w = 20C, at 35,000 feet θ_w = 21C, and at 40,000 feet θ_w = 22C. Computed values of $\overline{\Delta T_v'}$ are plotted in Fig. G-9b vs. height, H_m, where

$$H_m = H_{cap} - R$$

It should be noted that the above computations do not allow positive vertical velocity when the element is negatively buoyant, a fact that is often observed during the latter part of the cloud's growth. The formula is applicable only if the motion is due to buoyancy forces; therefore as $\Delta T_v' \longrightarrow 0$, $W \longrightarrow 0$.

The computed values presented in the figure are significantly less than those for 27 July. (For comparison, one-half $\Delta T_v'$, given in Fig. G-5, should be taken.) We may determine Δt_d and compare with recorded values presented in Fig. G-9a. Again we assume that the average cloud virtual temperature difference is one-half the value in the core, and that the maximum liquid water content is the adiabatic value. The quantity $T_v \times r_L$ was computed after assuming an average cloud base of pressure height 17,000 feet with mixing ratio 4.8 gr/km. The value of $T_v \times r_L$ increases to about 1.0C at a true height of 30,000 feet; from 30 to 40,000 feet it is 1.0C ± 0.05. The difference in the virtual temperature increment. ($\Delta t_{v_{in}} - \Delta t_{v_{out}}$) was determined after taking a relative humidity of 75% for the environment (determined from aircraft and Winslow sounding).

We then arrive at a temperature difference (Δt_d) of 0.9C at pressure height 18,000 (19,200 feet true) and 1.05C at 21,000 (22,400 feet true) by taking $\overline{\Delta T_v'}$ equal to 0.5C and 0.4C respectively. The computed Δt_d is 1.4C at a true height of 30,000 feet.

At the 20,000-foot level Δt_d, computed, is roughly one-half the recorded value. As with 27 July, the discrepancy between recorded and computed values could be reduced if it were assumed that $\overline{\Delta T_v'}$ equals, say, 0.3 times the maximum value. The factor of 0.5 was selected simply because the writer had previously used this value and found remarkable agreement between the laboratory model and measurement of atmospheric thermals below cloud base (dry thermals) in neutral surroundings.

It is realised that the assumptions that must be made when comparing observed values with those predicted by laboratory models are open to question. Indeed it can justifiably be argued that the constants, determined from the experiments, cannot be applied to the atmosphere, particularly when evaporative cooling is taking place, and that the basic formula

$$W = C(g\ B\ R)^{1/2}$$

is valid only if the shape of the buoyant element is roughly spherical.

The writer is fully aware of these limitations; however, it is felt that if enough cases are obtained and compared, then a coherent pattern may emerge.

Conclusions

The measurements of cloud development on July 27 show that there is a considerable increase in the rate of rise of emerging towers after dry ice seeding and that the seeded cell attained a significantly greater height than that reached by previous, unseeded cells. This is, of course, compatible with what would be expected resulting from an increase in the rate of release of latent heat of fusion due to the change of phase from water to ice.

The temperature excess and rate of rise of emerging towers on the 27th are roughly twice the values observed on the 15th, however on the 27th there is rapid deceleration of the towers after emerging while the towers on the 15th maintain a constant velocity for a considerable period of time. It is suggested that the deceleration is caused primarily by more rapid mixing due to the strong shear on the 27th and that on the 15th there was comparatively continuous updraft, probably due to inflow on a "meso-scale".

This is probably the first time that measurements from both aircraft and time-lapse films have been compared with values obtained from laboratory models. The correlation is such that the constants obtained from the experiments, can be applied to these and similar atmospheric cases to predict approximate values of rate of rise, radius, and average temperature excess of cloud towers. If comparisons of this type are made in the future, then the number of assumptions that must be made can be reduced and/or made with greater confidence if the position of the aircraft, relative to both the cloud top and edges, is known.

H. Mountain Wake Studies

Introduction

Cumulus cloud developments in the Flagstaff area are profoundly affected by the presence of the San Francisco Peaks. Not only are the slopes of the peaks strong heat source regions during the forenoon, but dynamic effects of the air flow over and around the mountain apparently create additional influences on the cloud development. For most of the morning the clouds must form, grow and decay under the dynamic effects superimposed by the presence of the peaks, and it is consequently of considerable importance to understand the magnitude and nature of these influences. In addition, the relatively isolated character of the Peaks region makes the area a unique location for observing mountain wakes without major complications from nearby terrain.

The summer of 1962 was an unusually favorable one for investigating mountain wake effects due to the relatively dry and windy conditions which prevailed during most of the field period. Under moist conditions in the low levels, slope heating during the early morning readily causes the formation of cumulus over the peaks which not only obscures the observation of any wake clouds but, in addition, disturbs the flow over the peaks by the release of latent heat and may substantially alter the character of the wake flow. Under drier and windier conditions, condensation frequently does not occur over the peaks and clouds are readily observed forming in the wake.

Although a complete documentation of the mountain wake effects was not feasible during the summer of 1962, sufficient information was obtained to show the general nature of the wake and its relation to cloud breeding areas. Additional work in the future would require a considerable observational effort to obtain the three-dimensional structure of the wake and its variation with time. The advisability of such an effort will have to be judged against the relative value of other possible study programs which can be carried out in the Flagstaff area.

Surface Wind Effects

Since extensive permanent anemometer equipment was not available for a study of the wake during the 1962 summer, the principal observations of surface winds were obtained by automobile traverses around the mountain with principal emphasis on the lee side. Winds were measured during these traverses at intervals of 1 - 2 miles on road systems which formed a near semicircle in the lee of the peaks.

At each observing location, the observer got out of the car, faced into the wind and observed wind direction and velocity with a Dwyer hand-held anemometer. These automobile traverses were made each day during the period August 4 through August 14 to determine if deviations in the wake pattern could be associated with observed weather factors.

Fig. H-1 shows traverses made in the lee of the peaks on August 4, 1962. Fig. H-1a shows all wind observations made from 1000 - 1100 along a 20 - 25 mile path. Winds aloft at 12,000 feet are shown over the top of the peaks area as obtained from observations at Navajo Ordnance Depot at 0600. Features of interest in the surface wind pattern are: 1) southerly wind in the lee of Mt. Elden, turning to southwesterly as air passes through the lower elevations of Schultz Pass, 2) northeasterly winds in the immediate lee of the peaks, 3) southwesterly winds north of the peaks where the undisturbed flow pattern again prevails. Winds recorded at Cinder Lake by the Signal Corps anemometer are shown as southerly at 1000 shifting to southwesterly by 1100.

Fig. H-1 b shows the surface wind observations made in the lee during the period 1100 - 1200. It is to be noted that southwesterly winds prevail over a much wider region of the mountain wake and only a small 3 - 5 mile portion of the surface wake still remains. Fig. H-1c gives wind observations made between 1200 and 1219 and shows southwesterly winds at all locations where the surface wake had previously been observed.

This sequence of events was observed on a number of days with only slight variations. It appears probable that the wake is usually destroyed about noon by surface heating and increased convective activity. This would ultimately result in exchange of momentum between the airflow over the top of the peaks and the ground layers and the southwesterly winds aloft would lead to similar directions at surface levels. It is clear also that the wake decreases steadily in width during the morning because its vertical depth decreases as a function of crosswind distance from the immediate lee of the highest peaks. Only in this most protected area is the surface wake able to last until noon. In other areas a smaller degree of surface heating is required to create the convective activity necessary to destroy the wake. Surface observations of temperature related to the existing vertical air temperature structure and aircraft observations of the top of the convective layer on August 10 suggest that surface heating effects must extend to approximately 14,000 feet MSL to complete the destruction of the wake. This amounts to about 2000 feet above the highest peak. Fujita has discussed inflow into a thermal low on the east slope of the peaks in the morning of July 22, 1960. Although the inflow characteristics may be similar, the wake low generally forms in stronger winds.

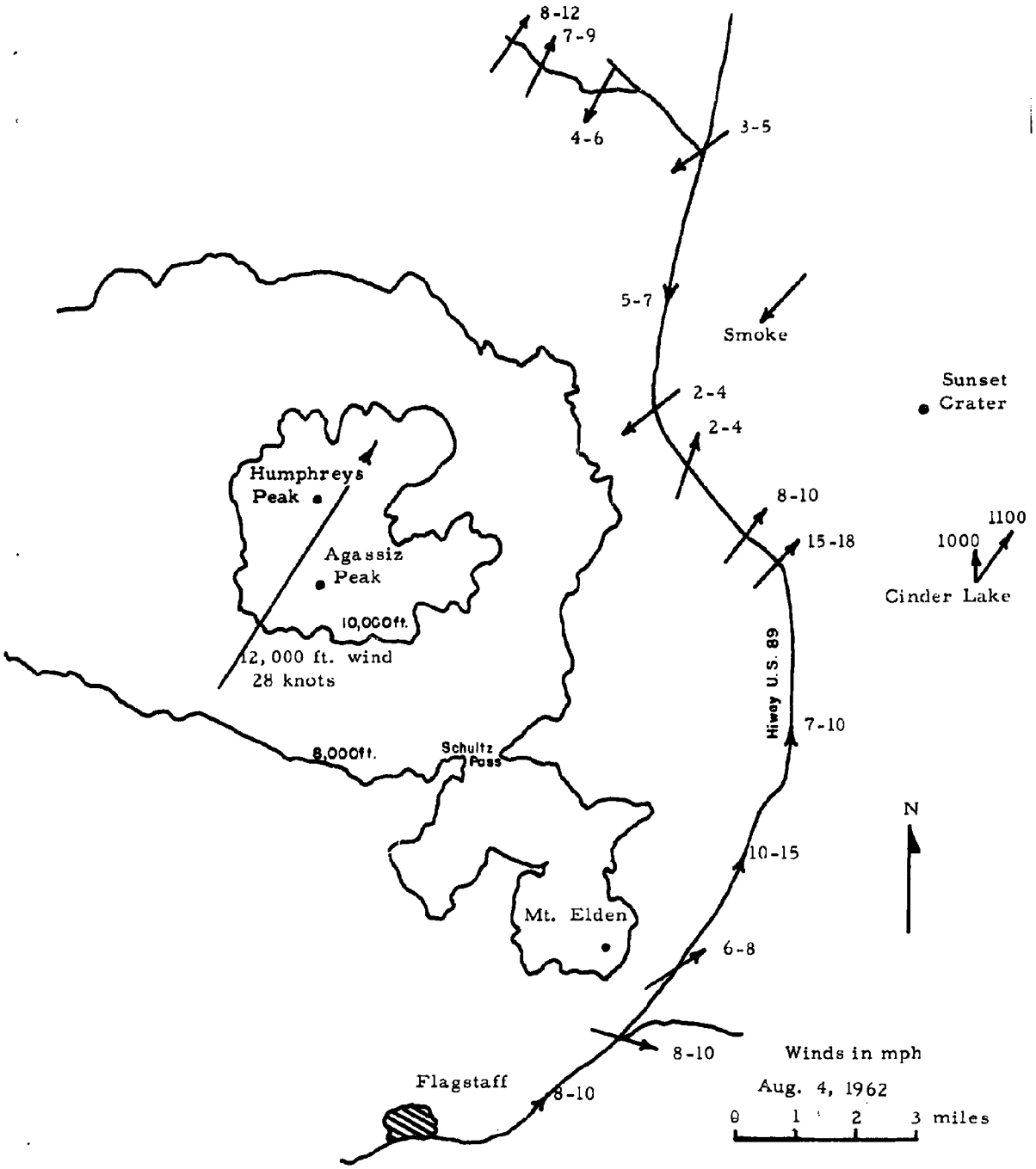

Fig. H-1 (a). SURFACE WIND OBSERVATIONS (1000-1100 MST).

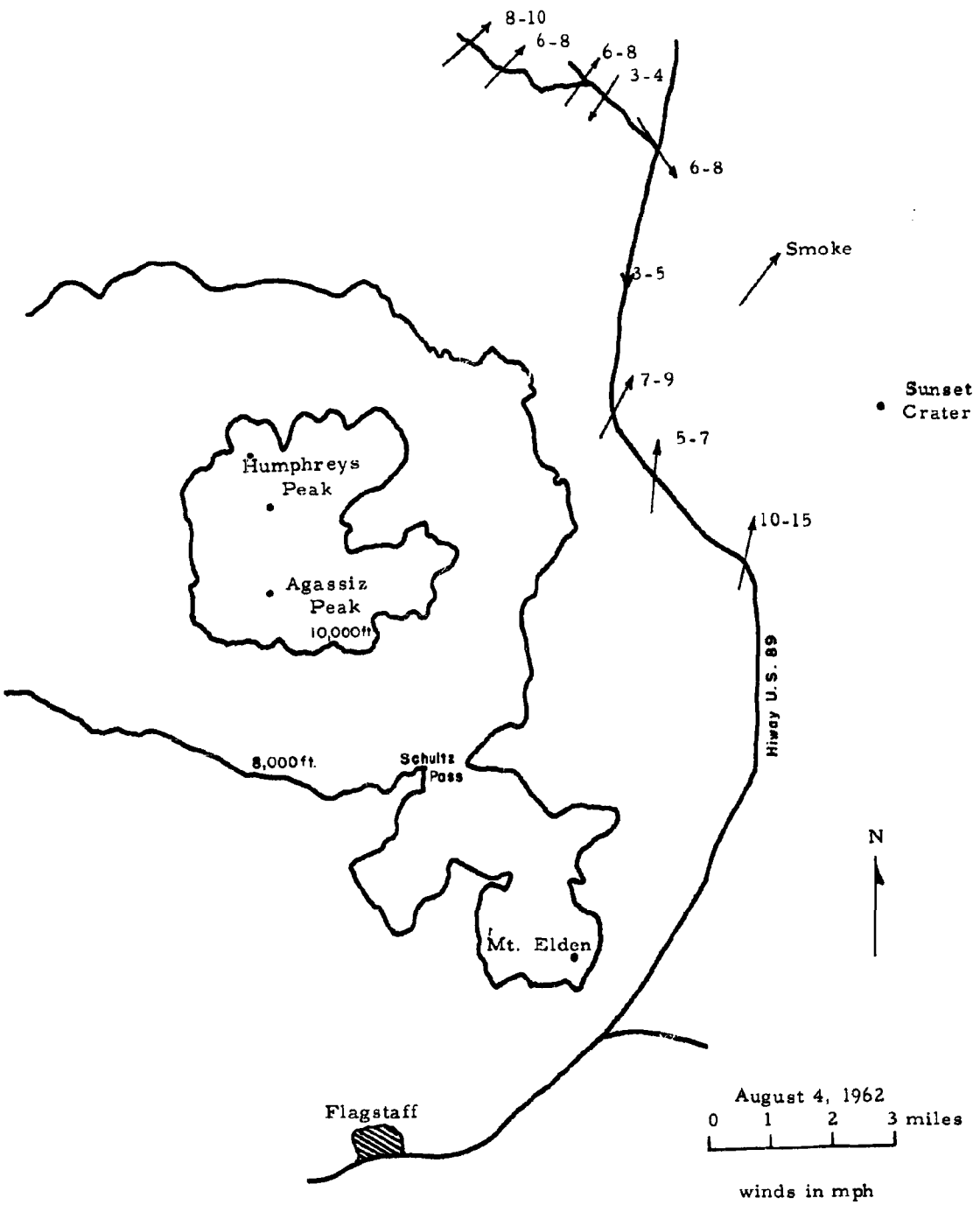

Fig. H-1 (b). SURFACE WIND OBSERVATIONS (1100-1200 MST).

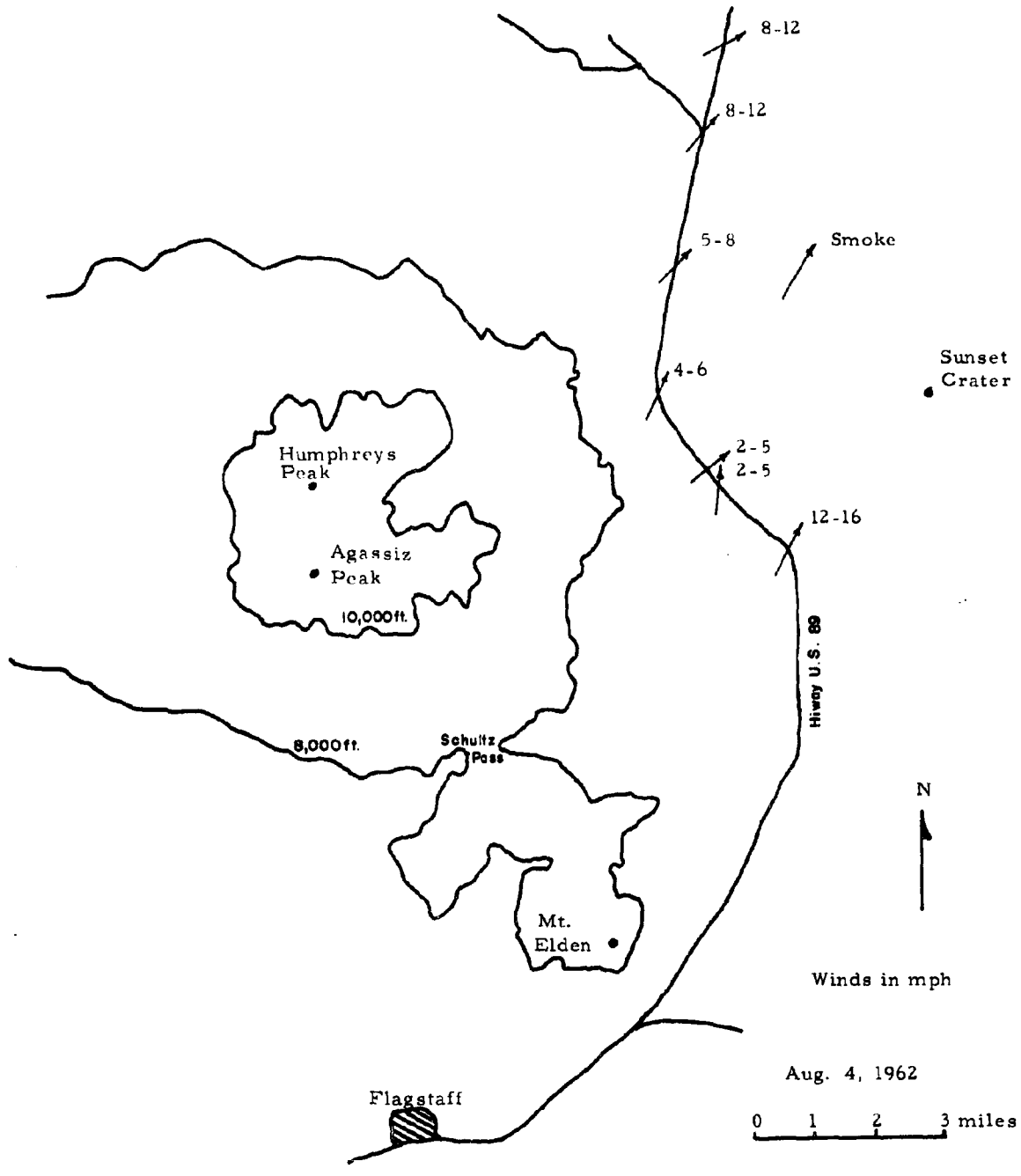

Fig. H-1 (c). SURFACE WIND OBSERVATIONS (1200-1220 MST).

Vertical Structure of the Wake

A more detailed study of the vertical structure of the wake was made possible on August 10 by a number of crosswind and upwind-downwind flights through the wake by the Cessna 180. Temperature, turbulence, vertical air velocity and altitude were recorded continuously in the aircraft. It was not possible to delineate clearly the lateral extent of the wake through crosswind flight measurements of temperature, turbulence or vertical air velocity. However, the upwind and downwind traverses produced a very informative picture of the vertical structure of the wake along the mean wind direction.

Fig. H-2 shows the terrain on the lee slope of the peaks and the flow patterns which have been constructed from potential temperature and vertical air velocity measurements made by the aircraft at the two indicated levels. Surface wind observations in the lee have been used to construct the flow pattern in the lower levels.

Principal features of interest in Fig. H-2 are: 1) the strong downslope flow in the immediate lee of the peaks and 2) the convergent region and associated updraft area which appeared to be connected with the surface flow as measured at the indicated location. The principal cloud area at the time of the two traverses is shown in the figure and is clearly related to the convergent area at lower levels. Most of the clouds appearing in this general region during the morning were relatively short-lived and showed the shredded characteristics resulting from strong turbulent zones. Heavy turbulence regions encountered by the aircraft during the traverses are shown in the figure and are closely associated with the convergent area.

This type of flow pattern is typical of stable air flow over isolated ridges or peaks. Previous flows of this nature have been reviewed by P. Queney et al (1960). Kuettner (1958) called particular attention to the rotor (reverse) flow apparent in Fig. H-2. The flow pattern is also similar to that observed in the Bear Mountain area by Halitsky (1961).

Cloud Generation in the Wake

A particularly interesting example of cloud generation in the wake occurred on July 31 when nearly continual generation could be observed in the lee of the mountain for a period of nearly three hours from 0730 to 1026. Principal area of cloud development was between Sunset Crater and Doyle Peak.

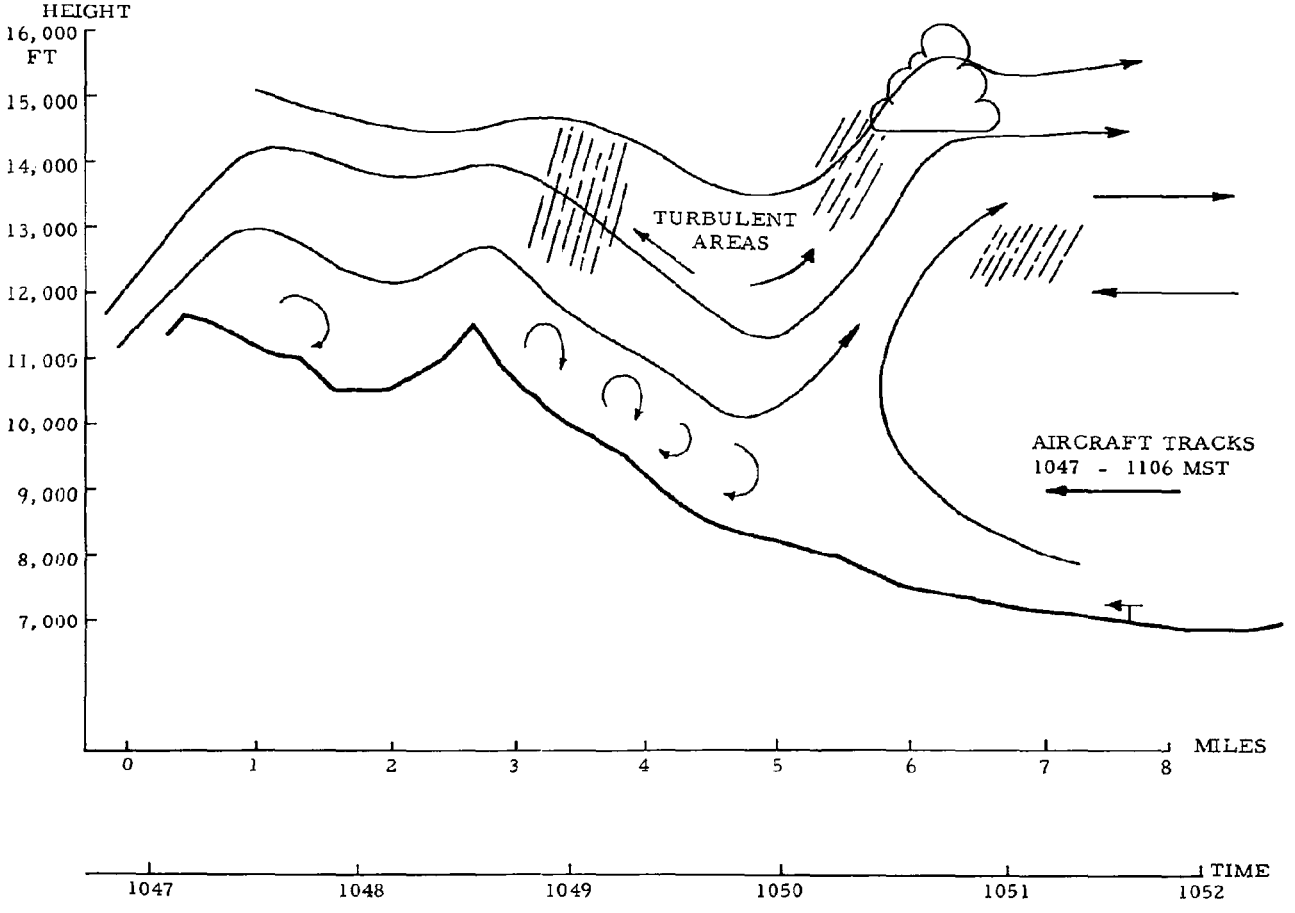

Fig. H-2. VERTICAL STRUCTURE OF MOUNTAIN WAKE, AUGUST 10, 1962

The cloud development in the time-lapse photo appeared to be composed of a succession of small cells which had been organized into a mean updraft area due to the convergent effects of the wake. Ground heat sources, particularly prior to 0800, are generally insufficient to cause large scale cumulus development but, caught in the convergent area of the wake, they appear as small scale variations superimposed on the mean updraft flow pattern.

Fig. H-3 shows cloud tops measured on July 31 in the wake area during the period 0745 - 0805 and from 0905 to 0929. The character of the cumulus tower growth shows a general lack of deceleration in vertical motion for a considerable period of time after emergence from the main cloud body. This is similar to the tower growths discussed in the previous chapter for August 15 which were also suggested as being associated with a larger meso-scale flow pattern. There is little doubt, from the time-lapse photos of July 31, that considerable erosion of the individual towers occurred but, since the buoyancy of the individual elements is not a major factor in creating the updraft area, little deceleration of the cloud tower takes place.

Conditions for Wake Formation

A survey of all days from July 12 through August 15 has been made to determine the prevalence of wake conditions. A list of the days follows:

Wake Observed or Highly Probable	Wake Not Present	Insufficient Data
July 12-14	July 20 (AM)	July 15
16-19	26	22
21	28	24
23	30	27
25	Aug 1	29
31	2	
Aug 3- 7	8	
9-14	15	

It is seen from the table above that the conditions prevailing during the summer of 1962 were quite conducive to wake formation.

The principal factors expected to control wake formation might be considered to be air stability and wind flow over the peaks. The stability requirement was satisfied on all mornings in the July 12 - August 15 period, and it did not appear that degrees of stability were of any great

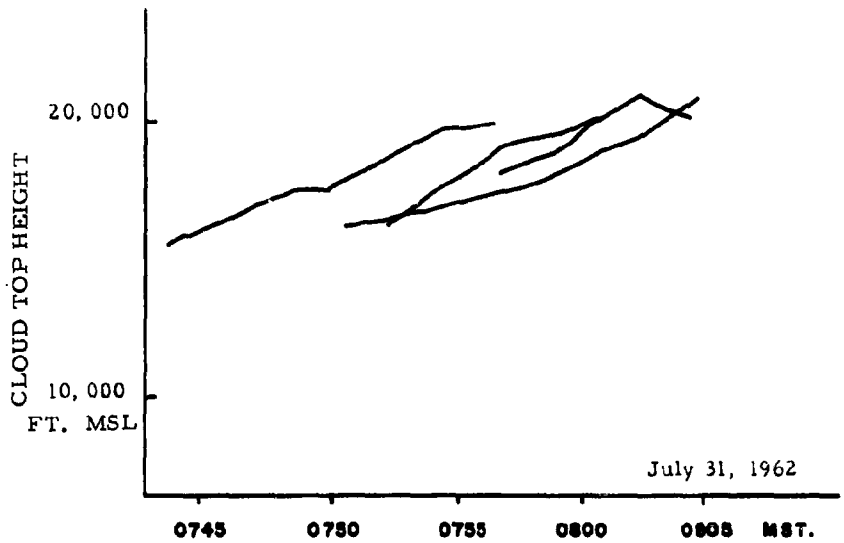

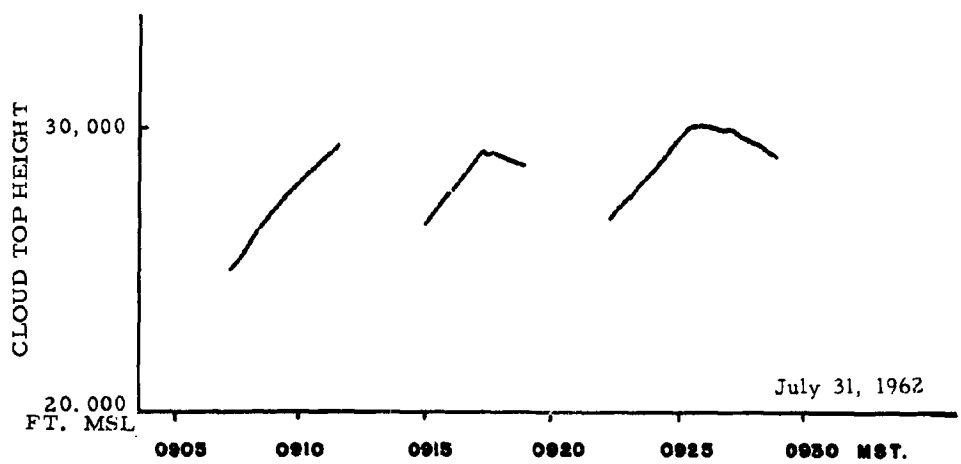

Fig. H-3. GROWTH OF CLOUD TOWERS IN LEE WAKE.

importance in determining wake formation. Wind flow, however, contributed markedly to the wake development. Of the days when a wake was not present, all days except August 2 and 8 were associated with light winds over the top of the peaks, i. e. 10 - 15 knots or less.

August 2 and 8 had extensive cloud cover during the morning and little surface heating in the wake area. Surface winds on August 8 in the lee of the peaks, for example, showed no deviation from the southwesterly direction prevailing aloft. These days suggest that release of buoyancy in the surface layers must play an important role in helping to initiate the low-level convergence patterns observed in the wake.

Extensive cloud development occurred in the lee of the peaks after 1500 on August 8 in spite of the lack of such an effect during the morning. This late afternoon development occurred on numerous other days during the summer when wakes had been observed in the morning. This effect is clearly the result of stabilization after the peak of the surface heating has been reached. The same factors of wind flow, stability and surface heating operate in the same manner as during the morning to produce the wake effects. On many days of the 1962 summer, it was only the intense heating near noon and in the early afternoon which could destroy the wake by exchange of momentum between the ground layers and the air flow above the level of the peaks.

Afternoon cloud developments in the wake are different from the morning characteristics in one important aspect. Considerable heating has been taking place during midday and very much larger sources of heat are available at ground levels than in the morning. If the wake is able to organize this heat supply by means of convergent flow patterns, the clouds in the lee during the late afternoon can develop into major storm areas. Such was the case, particularly, on August 8 and 10.

Conclusions

Sufficient observations on cloud developments in the wake of the San Francisco Peaks have been made to demonstrate the outstanding importance of the Peaks in conditions of relatively dry environments such as occurred during the summer of 1962. Under these conditions the flow pattern produced in the wake serves to collect the available heat supply from the lower layers into a localized convergent area where near-continuous updraft regions may exist for periods of 1 - 2 hours. The wake which frequently occurs during the morning is usually destroyed about noon due to increased convective activity which serves

to exchange momentum between the surface layers and the air passing above the tops of the peaks. Frequently the wake returns during the late afternoon when surface heating decreases and the flow patterns again become similar to the morning regime. Very extensive storm areas are observed to develop during the late afternoon under these conditions.

In moister environments and with lighter winds than were observed during the summer of 1962 the wake effects can be expected to be much less pronounced.

I. Slope Studies

Introduction

In the absence of dry environmental conditions and moderate winds over the peaks, the slope heating effects of the San Francisco Peaks area control the primary cloud developments during the morning, at least. The manner of organization of the flow on the heated slope, culminating usually in one predominant cloud area, is not well understood and deserves further study. Due to the isolated nature of the San Francisco Peaks, such studies may be more easily made than in other locations with more complicated terrain.

Isolated observations on the slope, with small pressure gradient forces in the area, show pulsing upslope flows. During the early portions of the morning these upslope flows usually last for short intervals of around 5 minutes. As the slope becomes more strongly heated during late morning hours, the flows frequently persist for periods of about 15 minutes before being interrupted. Since a large area of the slope must contribute to the upslope flow, such isolated studies have limited usefulness in providing an understanding of the influence of the entire slope. More extensive coverage of the slope appears to be needed.

Through the cooperation of Dr. Vincent Schaefer and eight student members of the NSF- State University of New York program, it was possible to provide greater coverage of the slope by stationing personnel at seven locations along the Doyle Saddle Road on the southeast slope of Fremont Peak. Elevations ranged from 8200 feet to near 10,000 feet MSL. Observations of winds and temperatures were made at each location and attempts made to correlate the various readings.

The slope study program during the summer of 1962 was largely an exploratory one involving a number of days of isolated slope observations and two days of more intensive observations with the entire group. Of the two days, July 28 proved to be a much better slope heating day than July 21 and is discussed in the following paragraphs. Detailed results from the program were limited but an appreciation of the broad aspects of the slope flow was obtained and considerable progress was made in developing appropriate observational techniques.

Observational Program

The observations made during the intensive periods of study were composed of the following:

1. Surface wind and temperature readings at each of seven locations on the slope at 2-minute intervals from approximately 0900 - 1130. Temperatures were read by thermistor units and winds by Dwyer anemometers.

2. A 30-foot meteorological tower near the middle of the observational line which recorded temperature and wind.

3. Tethered balloons at about 1000 feet above ground level. These were moored at the bottom position of the observation line, at the tower and at the top position of the line. Azimuth and elevation angles of the balloons were measured or estimated at 1 - 2 minute intervals during the morning.

4. The Cessna 180 aircraft made traverses over the slope below cloud base continuously from 0915 - 1130. Temperature, turbulence and altitude were recorded in the aircraft. The track of the aircraft was plotted from radar positioning and photographs made in the aircraft from a forward-pointing time-lapse camera.

Tower Observations - July 28

Fig. I-1 shows the sequence of meteorological events which occurred at the tower location during the morning of July 28. Two marked periods of upslope (southeast) flow are shown at around 1030 - 1045 and again from about 1100 - 1125. Both of these are associated with warm surges. The end of the heated flow period is generally marked by a decrease in wind velocity to a very small value. Prior to 1030 no organized upslope flow of any great significance was present at the tower location.

Similar data are available from six other locations on the slope as a result of observations made by NSF - State University of New York personnel. Examination of these data suggests considerable local influence on the measurements made at other locations. Correlations between the various locations are not as clear as had been anticipated, and it is usually very difficult to trace the passage of one heated upslope pulse from one location to other adjacent regions. For this reason the major emphasis in the following paragraphs is placed on data obtained from the tethered balloons, responding to a flow field which must be much less influenced by small scale terrain features.

Convective Slope Flows - July 28

The Cessna 180 aircraft made nearly 50 passes over the slope region during the period 0915 - 1130 when the intensive ground observations

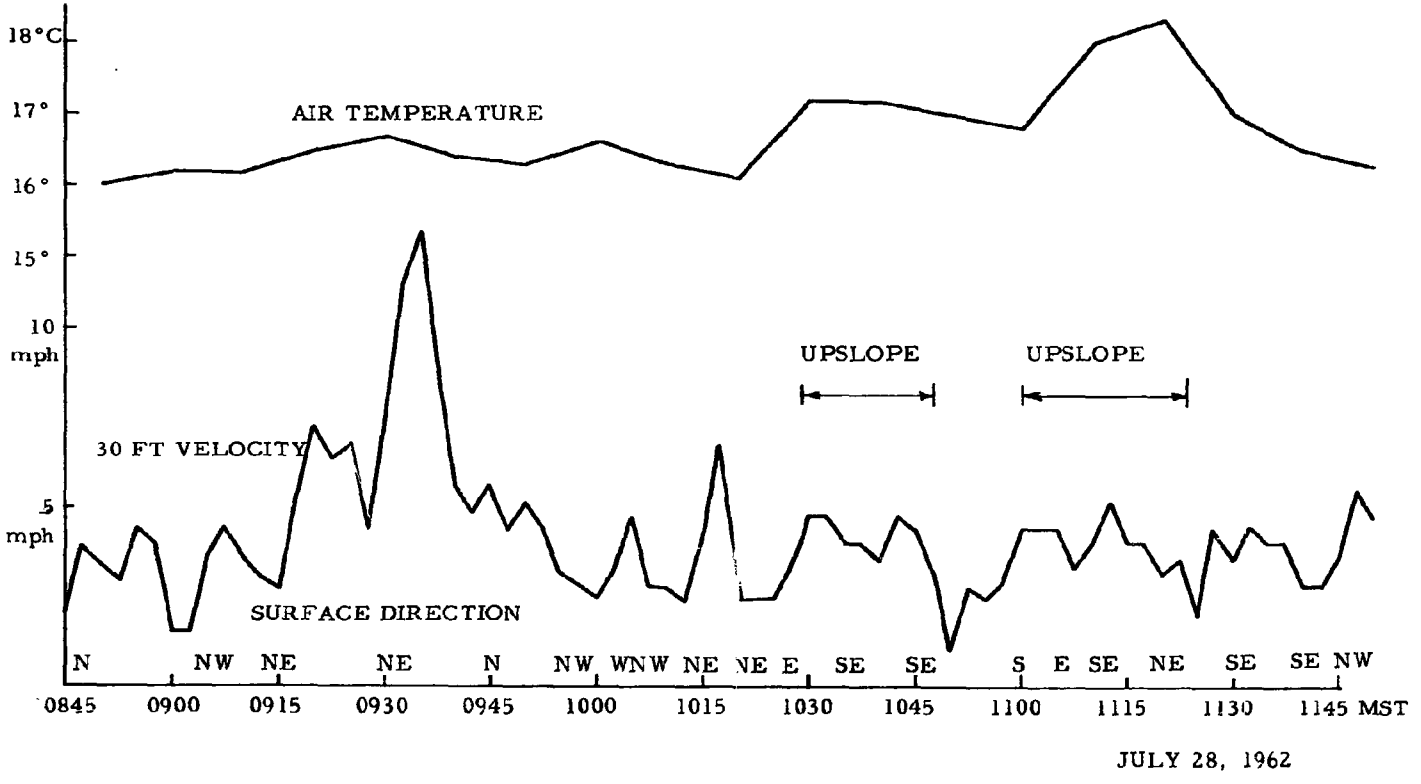

Fig. I-1. METEOROLOGICAL OBSERVATIONS (0845-1145 MST) 30 FT TOWER

were being collected. These traverses generally were confined to an area approximately 3 miles by 2 miles with the longer axis being oriented in a northwest - southeast direction. The flight level was maintained generally at about 13,000 feet MSL. On occasions the aircraft released smoke and this proved to be an effective method of marking the convective flow regions during the early part of the morning before extensive convective activity had commenced.

Vertical velocities encountered by the aircraft were marked at appropriate locations along the plotted flight track and areas of consistent updrafts were outlined. Primary requirements for outlining the horizontal extent of the updraft regions were 1) observation of the region on two or more traverses and 2) a maximum updraft of 300 ft/min or more.

Updraft areas obtained from the aircraft traverses are shown in Fig. I-2 for the period 1020 - 1045. Prior to this time the updraft areas were smaller, less well organized and more difficult to identify for any appreciable length of time. Also shown in Fig. I-2 as vectors are the relative positions of the tethered balloons with respect to their mooring locations on the slope. Ends of the vectors represent pictorially the balloon position. Longer vectors indicate a lower elevation angle and hence a stronger wind.

In Fig. I-2 updraft area A, outlined for the period 1024 - 1035, apparently moved westward along the southern slope of Doyle Peak to its new outlined location at 1039 - 1044. This is shown in marked fashion by the gradual counter-clockwise rotation of the upper balloon without any significant interruption in the strength of the flow. Area B apparently started in the vicinity of the tower about 1037 and is associated with the first period of upslope flow shown in Fig. I-1. Aircraft traverse data make it clear that areas A and B are not connected at flight level and the balloon positions also suggest this. The position of the lower balloon indicates that it was not responding to either updraft area.

In Fig. I-3 area B has expanded in size as indicated in the 1055 - 1100 position and subsequently moved toward the northwest in the 1107-1112 position. At 1056 the upper balloon was still responding to a weak flow into area A but by 1102 had come under the influence of area B and a downslope flow continued through 1112. The upper balloon did not continue to follow the movement of updraft area B after 1112 due to the generation of a new, more vigorous updraft area to be described in the next paragraph. At the tower location, the end of the 30-foot upslope flow at 1050 apparently signifies the end of the area B influence. At the lower balloon location the flow was apparently not influenced by area B through 1105.

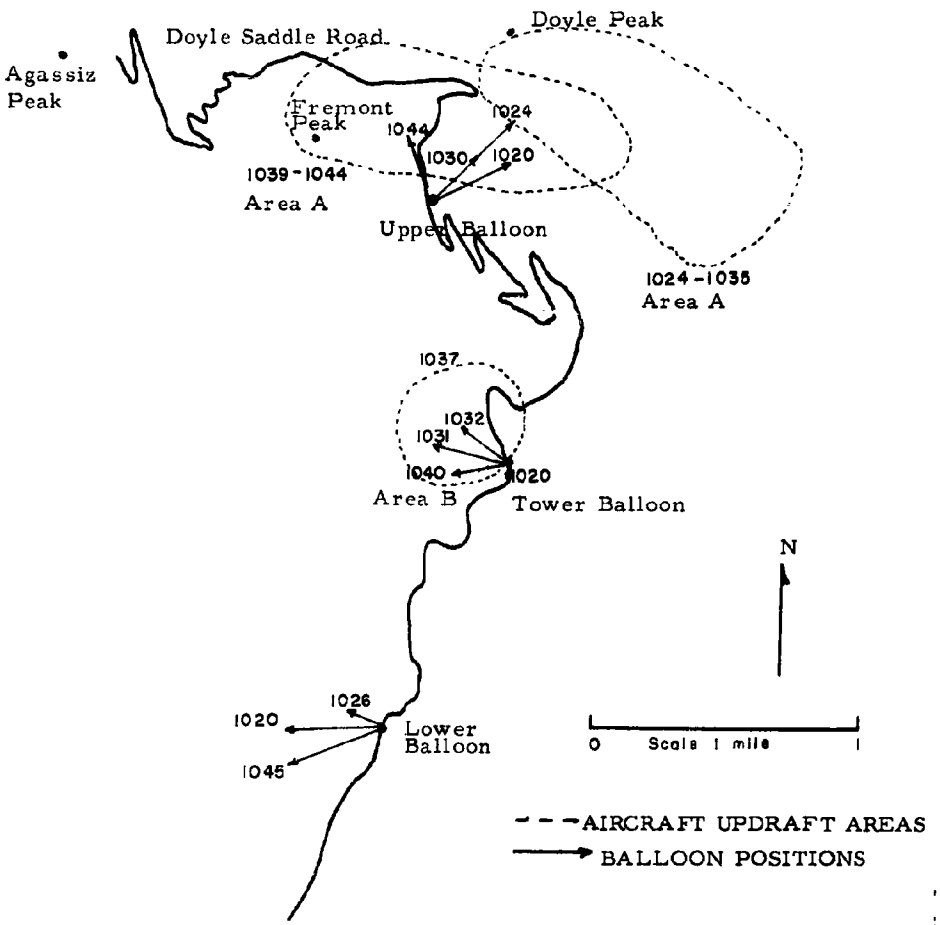

Fig. I-2. CONVECTIVE SLOPE FLOWS (1020 - 1045 MST) JULY 28, 1962

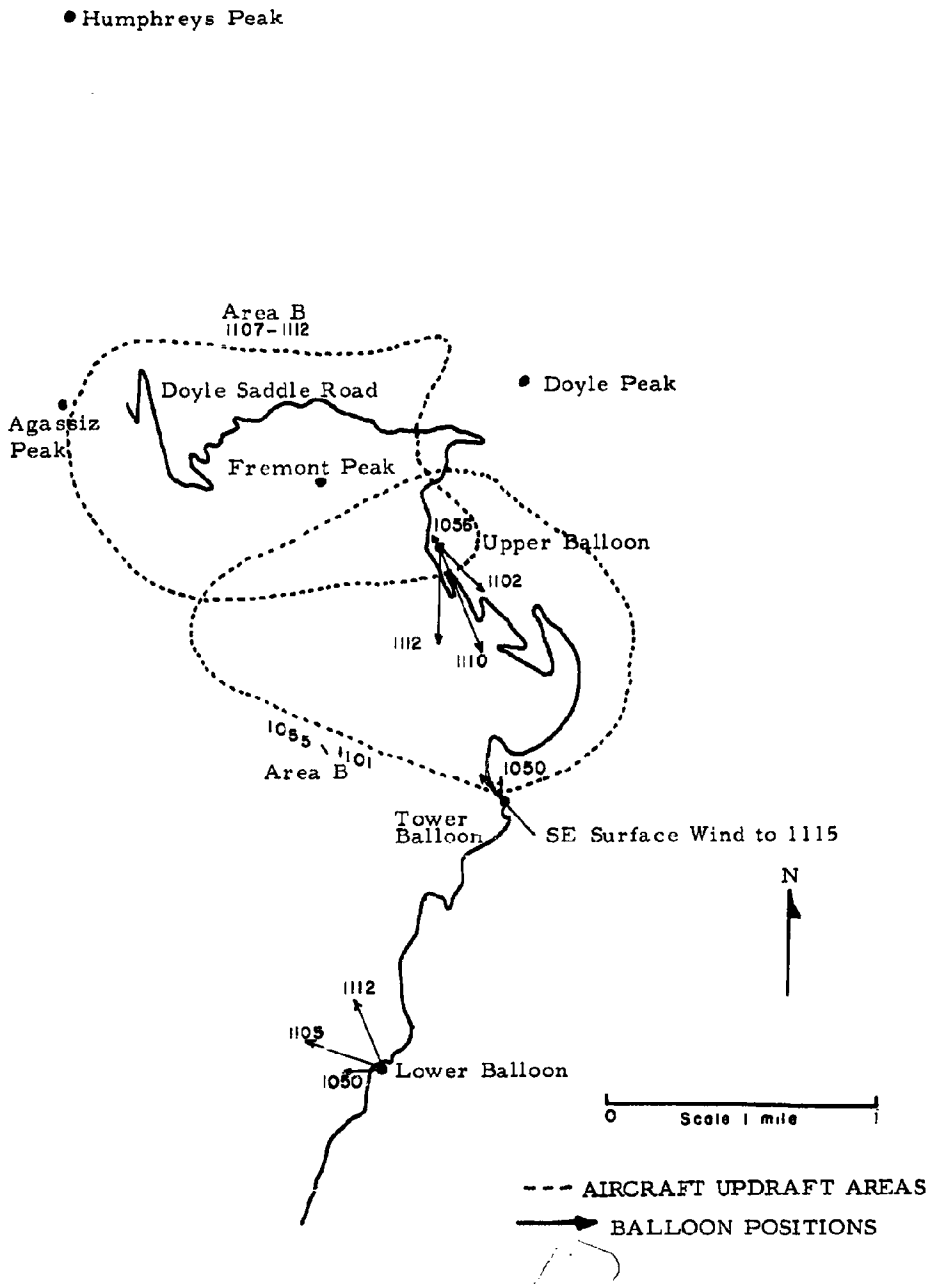

Fig. I-3. CONVECTIVE SLOPE FLOWS (1055 - 1112 MST) JULY 28, 1962

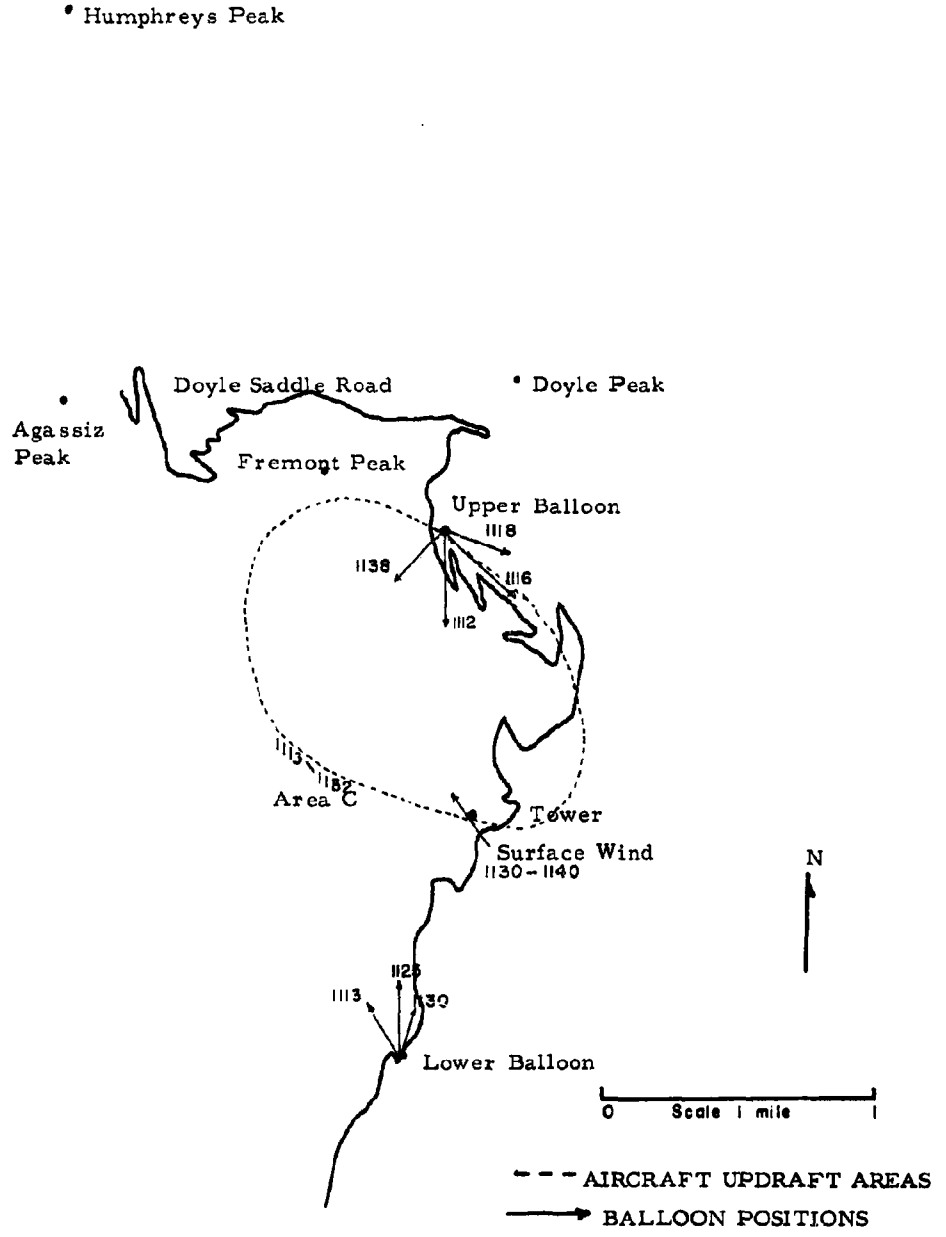

Fig. I-4. CONVECTIVE SLOPE FLOWS (1113 - 1140 MST) JULY 28, 1962

The second upslope flow at the tower commenced at 1100. The updraft area (area C) was first noticed in the aircraft at 1106 slightly north of the tower and, again, distinctly separated at flight level from area B. This area developed rapidly, fed by warm air as shown in Fig. I-1 from 1100 - 1123 and is outlined in Fig. I-3 for the time interval 1113 - 1132. The effect of the area C development on the upper balloon was to overcome the effect of area B after 1112. During the period 1112 - 1118 the upper balloon swung counter-clockwise (toward the southeast) in response to area C updraft intensification. Thereafter until 1138 the upper balloon rotated clockwise as area C drifted slowly northwestward up the slope. At the tower location, balloon data for this period were not available but the 30-foot flow shows inflow into area C until around 1120. At the lower balloon site, the balloon began to respond to area C developments between 1105 and 1112 and the influences continued through 1130. Thus, for the period 1112 - 1130 the entire observational line (about 2 miles in length) appears to have been under the influence of one major updraft area (area C). Rain was reported by the aircraft from this cloud system at 1136. No other rain had occurred with the previous updraft areas.

Conclusions

The combination of continual aircraft traverses and tethered balloons along the slope appears to be a very powerful technique for studying the organization of convective slope flows. A grid of 6 - 8 tethered balloons on the slope would be required to show the lateral extent of the convective flows in addition to the upslope - downslope character.

A comparable grid of low-level wind observations (e. g. 30 feet) would apparently not give as useful results as balloons tethered at 500 - 1000 feet. More consistent and longer duration flows are observed by the balloons than in the ground observations, presumably because of small scale terrain effects in the low levels.

The data obtained on July 28 show consistent updraft areas which exist for considerable periods of time and drift slowly upslope. These apparently can be recognized as separate entities with each successive area being somewhat more extensive and influencing a larger portion of the slope. The lifetime of the areas is longer than would be judged from observations at one location since the updraft area merely moves into a new region of the slope.

Additional studies with only slight changes in observational techniques would yield considerable information on the character of convective slope flows.

J. Atmospheric Electricity

General

One of the continuing aims of the long range Flagstaff program has been the probing of the dominant mechanisms by which nature separates charge to the point where lightning can occur. This research has advanced along various avenues of field measurement of potential gradients and hydrometeor charges on the ground and in the air during both natural and artificially seeded conditions. It has necessarily entailed development of techniques and instrumentation. The initial work, sponsored in 1958 by the AEC*, verified that strong charging could be generated in small, previously uncharged supercooled clouds, by seeding to create ice hydrometeors. Subsequent studies were performed by Atmospheric Research Group from 1959 to the present**, which continued the same sort of measurements but went further with potential gradient and hydrometeor charge measurements from aircraft and with some associated laboratory studies and instrumentation developments. The main MRI-ARG atmospheric electricity work which went on during the 1962 season was related to the NSF-sponsored program. The work took place primarily at the end of the field season after the main USAERDL program, and it was performed with personnel, equipment, and the aircraft sponsored by the NSF. Therefore the results are considered to pertain to the NSF grants. However, all phases of the Flagstaff operation are necessarily interrelated, and the important role of the USAERDL sponsorship in the atmospheric electricity studies must be acknowledged. Thus it seems appropriate here to review the main results of the 1962 NSF investigation but not duplicate the details which have been or will be presented elsewhere. The follow-up on these items in the 1963 season are to be included in the continuing USAERDL-sponsored program; the technique details are given later in this section.

MRI did provide for Dr. Kasemir of USAERDL some relatively crude ground potential gradient measurements. These were taken continuously at three sites, associated with time-lapse cameras, between June 14 and August 14. The chart recorders were battery powered and did not have

---

*MacCready, Beesmer, and Lockhart, MRI Final Complete Report, Cloud Electrification Study, AEC Contract No. AT(04-3)-236 and supplemental agreements, July 1959.

**Grants NSF G8334 and G11969.

accurate time scales. However, by various calibrations the record times could usually be rectified to within a few minutes and, when there were lightning strikes nearby, exact time rectification could often be obtained. The data are of some help in interpreting the significance of Dr. Kasemir's gradient change records. For 1963 similar radioactive probe units will be employed, but in at least two of the sites the charts will be a.c. driven and provide exact time information.

Hydrometeor Charge Evolution

This subject is best summarized by presenting the latest version of the abstract of a paper "Hydrometeor Charge Evolution in Thunderstorms"*.

"Systematic measurements of hydrometeor charges associated with electrified clouds and thunderstorms at Flagstaff, Arizona, have shown a rather consistent picture: a) charges on graupel and hail within the supercooled clouds were positive, b) below the cloud at the +2 and +8C level, just where the melting of the hydrometeors was apparently complete, the hydrometeors became abruptly negative, c) at still lower, warmer levels the charge magnitudes were considerably smaller, with both signs represented but predominantly negative. The data suggest that a strong negative hydrometeor charging mechanism is associated with the melting of the ice hydrometeors outside the cloud. The maximum charge magnitudes were comparable to the amounts which would be limited by breakdown gradients at the hydrometeor surface. These measurements were made from a light plane by the standard induced-charge method, and other pertinent variables were recorded simultaneously. The aircraft would spiral within the central upcurrent up into the cloud, and then later spiral down through precipitation shafts.

"The charge measurements are consistent with a model derived by Kuettner to account for the observed cloud charge dipole with consideration of hydrometeor charge, droplet charge, and cloud dynamics, although many details of the possible charge distribution mechanism remain obscure. The magnitudes of the charges appear adequate to produce the over-all charge values leading to the first lightning strike."

The main point of this paper is graphically illustrated by Fig. J-1, taken from the paper, which shows hydrometeor charges measured during a spiral descent through a hail shaft below cloud base.

These field investigations were followed up by a laboratory investigation in Altadena in which ice particles were melted in a wind tunnel to see if the

---

*Presented by P. B. MacCready, Jr., ARG, at AMS-AGU Meetings, Washington, D. C., April 1963.

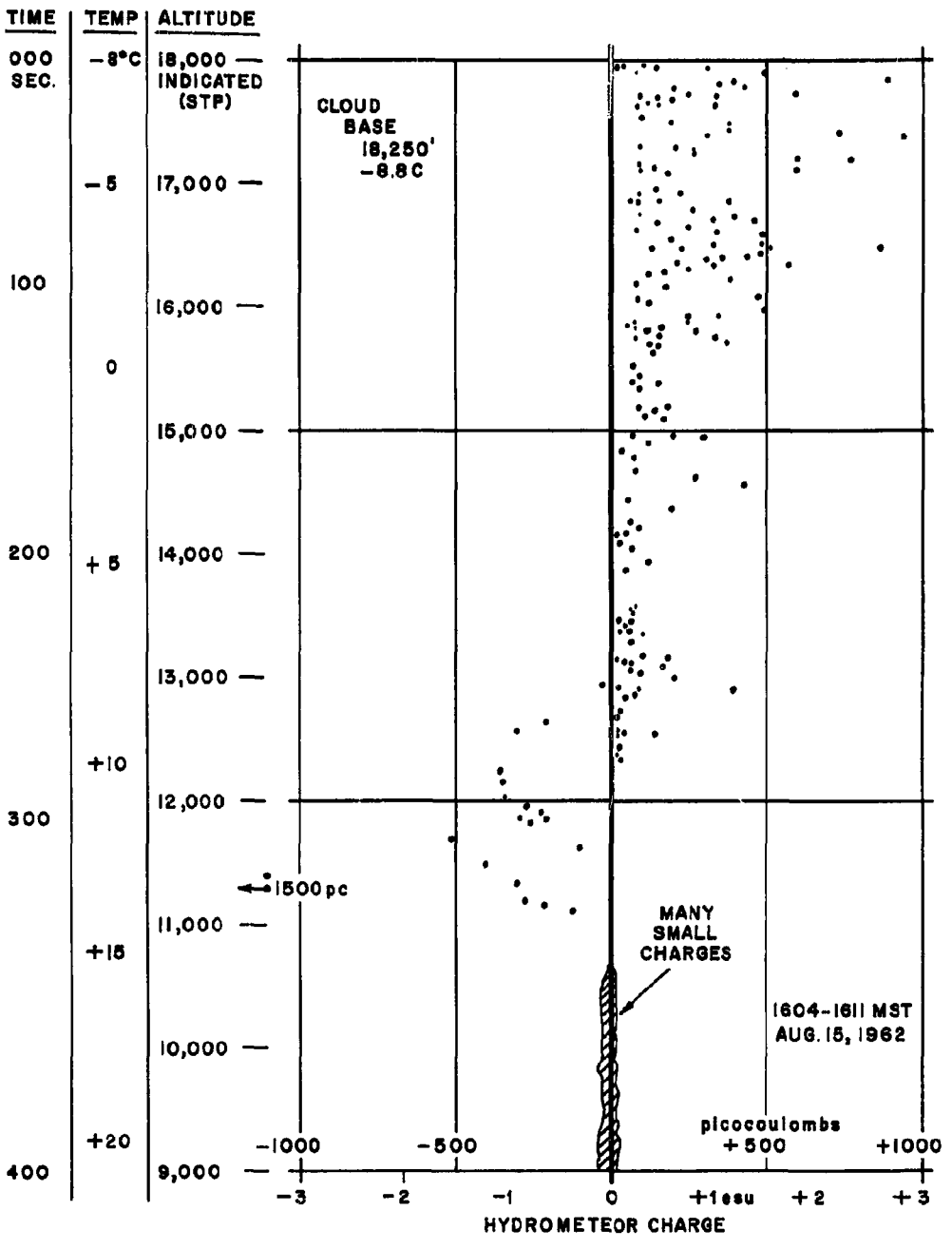

Fig. J-1. Hydrometeor charge measurements during spiral descent., 8/15

phenomenon observed in the field could be duplicated. The results of this study are best summarized by presenting the abstract of a paper* on the subject.

"A laboratory investigation was initiated to try to duplicate a phenomenon which had been repeatedly observed in flight measurements during the Flagstaff cumulus studies: the apparent strong negative charging of ice hydrometeors at the final stage of melting during their fall outside of the cloud. Using distilled water sample ice structures of approximately 1 cc were melted in an 8 mps air stream at ambient temperature. Regardless of the shape of the ice structure (spherical or cubical), and regardless of the technique of measurement used (current into the sample, charge into the sample, or charge into an open Faraday cage around the sample), certain features were observed consistently:

1. A positive charge was acquired by the sample.
2. The magnitude of the charge was on the order of 30 picocoulombs (0.1 esu).
3. The acquisition of charge occurred primarily during the later portion of the melting process.

"The sign of the charging was opposite to that observed in the flight measurements, and the magnitude of the charging was far less, but the correlation of the charging with the final stage of melting agreed with the flight tests. It is felt that the charging effect is real, and is probably associated with effects from bubbles during melting, but that the laboratory measurements cannot be expected to agree in detail with the flight results until the atmospheric conditions and hydrometeor structure are duplicated more realistically in the laboratory. Laboratory tests by Dinger and Gunn also showed positive charging during melting."

Further Investigations

The electrification research depends primarily on the development of appropriate equipment and the development of the operational techniques for its use. The main developments and plans have been presented in the Atmospheric Electricity portion of the Instrumentation section. The salient features for 1963 are:

Improved potential gradient and airplane charge units are available. The probe positions available on the Apache for 1963 make data interpretation easier than in 1962 on the single engine plane.

---

*By A. Proudfit and P. B. MacCready, Jr., unpublished, for inclusion in 1963 final report to NSF.

The hydrometeor charge unit is being refined, and in some cases is to be used in conjunction with the capacitance type hydrometeor sizing device.

Improvements in space charge and simulated hydrometeor charging are underway. Use of an oscilloscope in the aircraft can greatly assist the development of the space charge unit. Conductivity will be measured with existing MRI equipment.

An attempt will be made to duplicate the laboratory melting-charging experiments in the aircraft, with newly captured ice hydrometeors and ambient air.

Some ground measurements on hydrometeor charging vs. gradient and hydrometeor type can be undertaken with the above equipment. Comparison of the aircraft hydrometeor charging unit and a ground measurement technique is to be made.

The routine airborne atmospheric electricity measurements are to be included throughout the whole 1963 field season. There will also be special flights devoted primarily to atmospheric electricity investigations.

K. References

Farlow, N.H. and French, F.A., 1956: Calibration of Liquid Aerosol Collectors by Droplets Containing Uniform Size Particles, J. of Colloid Science, 11, 177.

Fujita, T., et al., 1961: On the Mesometeorological Field Studies near Flagstaff, Arizona, The University of Chicago, Dept. of Met., March.

Fuquay, D.M., 1960: Generator Technology for Cloud Seeding, J. of Irrigation and Drainage Div., Proc. of Am. Soc. of Civil Engineers, IR-1, March.

Halitsky, J., 1961: Wind Turbulence in the Lee of a Low Conical Mountain, NYU Quart. Prog. Rept. No. 4, Contract DA-36-039 SC-84939.

Hocking, L.M., 1959: The Collision Efficiency of Small Drops, Quart. J. Roy. Met. Soc., 85, 44.

Kuettner, J., 1958: The Rotor Flow in the Lee of Mountains, Schweizer Aero-Revue, Bern, 33.

Langmuir, Irving and Blodgett, Katherine B., 1949: Mathematical Investigation of Water Droplet Trajectories, Final Report, General Electric Research Laboratory, Rept. No. RL225.

MacCready, Jr., P.B., 1962: The Continuous Particle Sampler at the Puy de Dome Comparison Conference, Bull. de l'Observatoire du Puy de Dome, 1.

_____, 1963a: The Mixing Ratio Indicator, paper presented at the 1963 International Symposium on Humidity and Moisture, Washington, D.C., May 22. Proceedings to be published.

_____, 1963b: Standardization of Gustiness Values from Aircraft, paper submitted to Astronautics and Aerospace Engineering, January.

Queney, P., et al., 1958: The Airflow over Mountains. Tech. Note No. 34, W.M.O.

Saunders, P.M., 1957: The Thermodynamics of Saturated Air: A Contribution to the Classical Theory, Quart. J. of Roy. Met. Soc., 83, 342.

Scorer, R.S., 1957: Experiments on Convection of Isolated Masses of Buoyant Fluid, J. Fluid Mech., 2, 583.

Todd, C.J., 1961: A Study of Cloud Composition, Proc. of the 9th Weather Radar Conf., Kansas City, October.

Turner, J. S., 1963: Thermals with Increasing Buoyancy, Quart. J. Roy. Met. Soc., 89, 62.

Woodward, B., 1959: The Motion in and around Isolated Thermals, Quart. J. Roy. Met. Soc., 85, 144.

Wurtele, M. G., and B. Finke, 1961: A Note on the Computation of the Saturation and Pseudo-Adiabatic Processes, J. of Met., 18, 6.

OVER-ALL CONCLUSIONS

The basic conclusions have been presented in the individual sections and a resume given in the abstract, and so these results will not be duplicated again here. Rather, an over-all conclusion of the program to date will be presented in perspective.

The project aim has been to gain significant understanding of the physical mechanisms which go toward causing the development of convective clouds, and their flow fields, precipitation, and lightning. Even in the relatively simple outdoor cloud laboratory at Flagstaff the interrelations between all these factors are extremely complex. Individual problems can be studied somewhat separately, but the secrets to the dominant factors can only be uncovered by paying attention to the whole cloud dynamics - cloud microphysics system. Thus the project aims necessitate a broad program, involving an extensive ground and air data acquisition capability and, even more vital, a data processing and analysis capability that can flexibly handle the details comprising the complex meteorological situation.

Cloud dynamics have received special attention because this subject provides the link between the microphysics effects by which typical cloud seeding is performed, and the gross storm effects which are of economic significance. An introductory understanding has been developed concerning the role of the isolated peaks in controlling the development of convective cells (the slope studies and the mountain wake effects). The aircraft probings have been quantitatively examined to show the detailed microphysics of seeding effects and precipitation initiation. The aircraft data have also been interpreted to show dynamics details of dilution and buoyancy, and the results have been related to gross cloud motions found by photography.

The over-all program conclusion can be presented as follows:

"The program results to date demonstrate that appropriate physical concepts and research methods have been developed leading toward a physical understanding of modified and unmodified convective storms".

RECOMMENDATIONS

The detailed recommendations on specific subjects have already been presented in the separate sections. Much care is required to put all the desires within the practical framework dictated by time, economics, and the capabilities of the analysis methods now available.

The procedure for data collection in the summer of 1963 and the analysis during the months to follow is believed to be the best possible on the basis of present knowledge, the scope of the problem, and the resources available for the effort. One of the new tactical problems is to maximize the use of the M-33 radar during the field program. Generally the techniques for 1963 will be those already developed in 1962 and earlier. The 1963 effort will thus emphasize the application of the techniques to specific tasks. In future years studies should be directed towards understanding the effects of massive seeding as might be done by seeding a number of clouds at the same time by airborne or ground based generators, specialized experiment designing to understand the total cloud dynamics, and very localized field studies directed at understanding the detailed microphysics of clouds.

The larger seeding events mentioned above should provide more detailed information on the effects of seeding on clouds in different stages of their life cycle. It is also important to continue to look at the natural seeding processes, i. e., when one cloud seeds another.

As the project progresses more detailed objectives can be specified. As one example, the discrepancy between the sign of charging during ice measurement in the laboratory and under the clouds at Flagstaff can at this stage best be resolved by putting the laboratory gear in the aircraft and testing hailstones collected right then in flight. It is possible then to duplicate in the flying laboratory almost all the natural conditions. To duplicate conditions as well in a ground laboratory would not be possible, even if the important parameters were known.

There are several items not receiving emphasis in 1962 which are deemed critical for the completeness of future work. One is the more complete measurement of natural freezing nuclei to provide knowledge of the background into which artificial seeding is introduced. The other is the investigation of cumulus edge and top dynamics, especially the horizontal motions near the upper portions of the clouds. These details are of great importance for the understanding of dilution, cloud dynamics, and perhaps also of over-all electrification. The M-33 radar capability can considerably assist this investigation. Eventually the knowledge and techniques learned in the Flagstaff operations should be applied to other areas for the purpose of comparison and the hoped for eventual understanding of how to modify clouds for practical aims.

PERSONNEL

Field Program

Name	Role
Dr. P. B. MacCready, Jr.	Principal Investigator & Aircraft Operations
Dr. T. B. Smith	Project Scientist
Dr. H. Selvidge	Project Scientist
Mr. C. J. Todd	Test Conductor, Research Meteorologist
Mr. T. J. Lockhart	Project Coordinator
Mr. F. E. Clark	Ground Instrumentation, Logistics

Others participating in a significant way to the project included:

Instrumentation: C. F. Rothrock, R. Beesmer, D. Sanders, J. Gretta, A. Frost, R. Bunton, R. Ellingwood, D. Evans, B. Bowmar, H. Hutchinson, W. Gregge, W. Wilson

Data Reduction: N. Smith, K. Beesmer, R. Crabtree, R. Sloane

Pilots: B. McManus, H. McHenry

Flagstaff, local: M. Driscoll, D. Jones

Various of the above personnel also aided in the overall program with the support of NSF through ARG. Mr. R. Schley (Flagstaff operations) and Mr. A. Proudfit (atmospheric electricity equipment and measurements) were supported primarily by this NSF grant.

Mr. E. Hindman assisted with the development and use of the continuous droplet collector, through the support of NRL.

Dr. V. J. Schaefer, in addition to assisting the program in his consulting capacity to MRI - ARG, organized and handled the eight student-trainees from the Atmospheric Science Center of New York State University, supported by grant from the Army. The students were:

Edson Blackman	Richard Hadsell	Garland Lala
Robert Singer	Edmund Holroyd	Douglas Robins
Alan Carlton	Alan Michalowski	

PERSONNEL

Analysis and Research Program

Name	Role	Principal Contribution
Dr. P. B. MacCready, Jr.	Principal Investigator	Instrumentation & Atmospheric Electricity
Dr. T. B. Smith	Senior Scientist	Slope and Wake Studies
Dr. J. R. Stinson	Senior Scientist	Consultant
Dr. C. W. Chien	Research Scientist	Cloud Particles
Mr. C. J. Todd	Research Meteorologist	Cloud Modification
Miss E. W. Woodward	Meteorologist	Cell Dynamics
Mr. K. Beesmer	Meteorologist	Analysis
Mrs. C. A. Stersic	Research Assistant	Documentation
Mr. R. B. Sloane	Junior Analyst	Drop Particles
Mr. D. D. Smith	Junior Analyst	Analysis

Appendix A

SAMPLING ERRORS AND CALIBRATION OF THE CONTINUOUS CLOUD PARTICLE SAMPLER

Background

This instrument is still in the process of basic development, and both analytical and empirical calibrations are still being worked out. During the summer of 1962 its stage of development did not warrant a high degree of sophistication in calibration. Refinements incorporated in the instrument for the 1963 Flagstaff program, however, promise higher quantitative results with emphasis being placed on the instrument's calibration. This program is now well under way.

A detailed report is forthcoming in conjunction with NRL Contract No. Nonr 3819(00)(X) covering continuous cloud particle sampler research.

Sampling Exposure

After the film has been coated with the plastic solvent solution it moves up through a tube and past the sampling window. The section of the tube that contains the sampling window narrows down to an outside diameter of 12 mm to make the collection efficiency high. This 12 mm diameter is less than the 16 mm width of the film so the film must be curled into a semi-cylinder to pass through the sampling window tube. This curvature is forward so that the center coated part of the film passes 1 mm behind the window. 180° of the forward facing part of the tube is open for 2 mm along its length. This allows the whole width of the film to be exposed to the air blast for 2 mm as it passes up the tube.

Sampling Volume

As the film runs at a constant rate while sampling, the duration of the exposure of any sample on the film is $t = \ell / v_f$. t is time in seconds, v_f is film speed, 75 mm sec^{-1}, ℓ is length of the window, 2 mm. Here $t = .0267$ sec.

Distance flown in t is $D = v_a t$, where D is distance flown while a point on the film passes the open sampler window. v_a is velocity of aircraft. Here $v_a = 50$ m sec^{-1}. $D = 1333$ mm.

Volume of air, V, sampled on an area A of film is $V = A D$. The maximum A that can be viewed at one time when projected by 16 mm stop motion projector or one frame is 10 $7.5\ mm^2$. The sample on this area is from a volume $V = 100\ cm^3$. The projection can be magnified to 1000 X through a microscope lens with a field of vision of $A = \pi (75/2)^2 = .44\ mm^2$. For this case $V = .586\ cm^3$.

Errors of Estimating Sampling Volume

In the 1962 Flagstaff data, all factors involved in computing the sampling volume can be measured with desired precision except for the airspeed. It was not recorded in flight, but an attempt was made to fly all sampling runs at 50 m sec^{-1}. The observer estimates that this airspeed is held to ± 20% of this speed during cloud flying. For this reason, there is an uncertainty of ± 20% in all estimates of the sampling volume. In 1963 the true airspeed will be recorded on the flight record, and high accuracy and high resolution of cloud particle concentration counts will be possible.

Collection Efficiency

Collection efficiency has not been analyzed empirically, but a first-order analytical study has been made. It is assumed that the sampling window section has nearly the aerodynamic characteristics of an infinitely long cylinder 12 mm in diameter suspended with the major axis perpendicular to the wind. From Langmuir and Blodgett (1949) the collection efficiencies at the stagnation point are found for the cloud range of droplet sizes through flying speeds from 30 to 100 m sec^{-1}. These are graphed in Fig. Appendix-1.

The sampling window section is designed to be a close approximation to an ideal cylinder. Distortions at the window have not yet been studied in detail.

Calibration of Droplet Diameter to Replica Diameter

The microphysics of the replication is complicated and not completely understood. A final replica is a product of the processes of collision and capture in the fluid plastic solvent coating and the shrinking and hardening of this plastic.

After impact the plastic solution flows over the droplet encapsulating it. Then the surface forces come to equilibrium. If the droplet is small compared to the thickness of the plastic solution, the encapsulating covering pulls it below the surface where it comes to equilibrium as a sphere. If the droplet diameter is large compared to the thickness of the plastic solution coating, the encapsulating covering pulls the droplet against the film base and forces it into an oblique spheroid. The larger the ratio of droplet diameter to plastic coating thickness the more oblique the spheroid.

Solvent evaporates out of the plastic solution rapidly and the solution shrinks and becomes hard, distorting the captured droplet. A theoretical study of droplet distortions have been made using machine computation to solve for the equilibrium shape produced by the surface forces. This analysis showed the importance of accurate control of the solvent concentration and of the thickness of the plastic coating. These two controls are

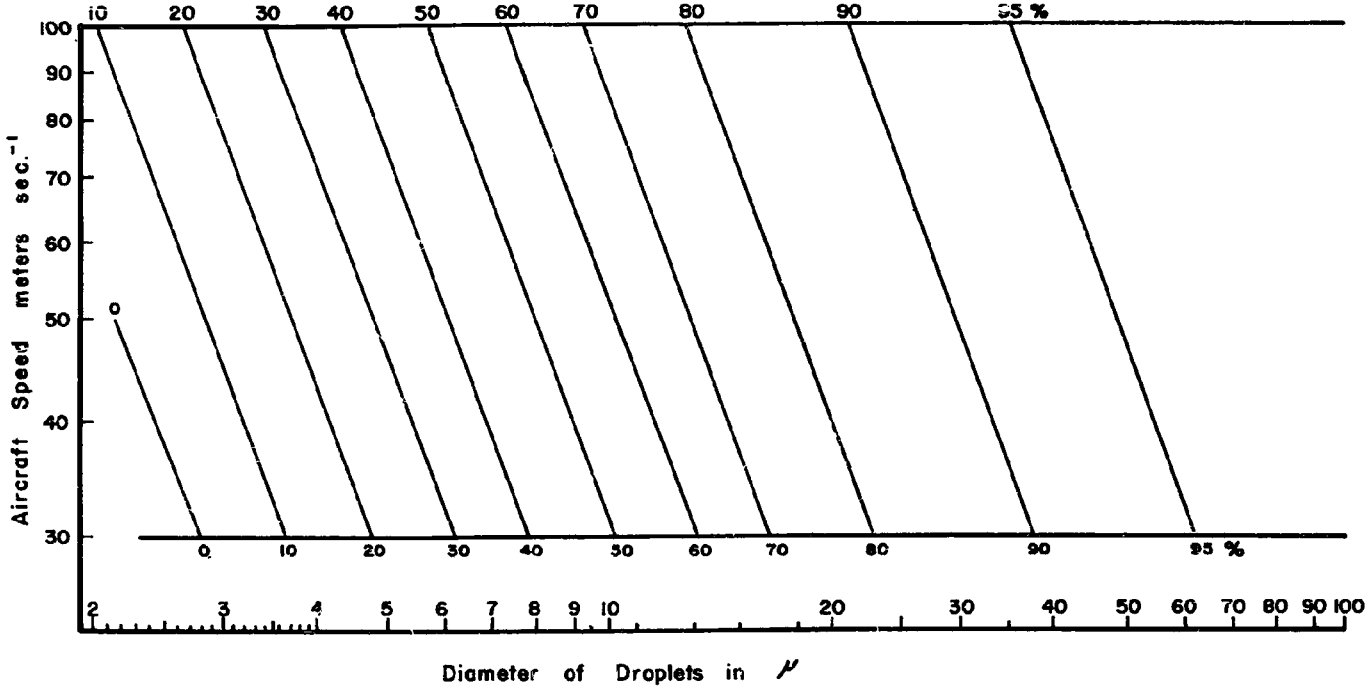

Fig. Appendix-1. % COLLECTION EFFICIENCY ON A 12 mm CYLINDER AT STAGNATION POINT.

being incorporated in the 1963 sampler. They were not in the 1962 version and because of this lack, there are several examples showing variations of a factor of two in replica diameter where ripples produced variations in the plastic coating thickness.

At the Puy de Dome Meeting on the Comparison of Droplet Collectors, November 1961, simultaneous samples taken on the MRI continuous cloud particle sampler (MacCready 1962) and others indicated that the droplet to replica ratio is about 1 to 1.5 for the MRI sampler. Another check for the rough calibration is the comparison of a conversion of the total droplet concentration to liquid water and this with measured liquid water contents. Here also the 1 to 1.5 ratio seems to be a good first approximation for the cloud droplet size range.

Empirical calibrations, using a technique reported by Farlow and French (1956), are now underway at MRI. Here a spray of water containing a suspension of 3 μ spores is blown on the film. The spores can be seen and counted in the droplet replicas. From these counts the volume of the droplet can be deduced and the calibration curve worked out. Some curves have been worked out and compared with the analytically derived curves. It is yet too early to generalize on these results.

Ice Crystal Replication

Clear, sharp, high-resolution replicas of ice crystal faces are produced in the plastic. Replicas show that the crystals crack on impact with the film if they are larger than 100 μ in diameter. They break apart on impact if they are larger than 200 μ in diameter. Large crystals, snowflakes, and soft graupel shatter on impact with the film but leave replicas of broken pieces that reveal a great deal about the original particle.

Summary

In 1962, the version of the continuous cloud particle sampler was unrefined in some respects and the calibration was coarse, yet it produced better quality cloud particle data than has ever been collected before. The 1963 version and the calibration to go with it promise to be much more refined and quantitative. However, the process of replicating cloud particles continuously while in flight has so many second-order complications that a substantial amount of additional development can be anticipated before the full potential of the technique is achieved.

Div. 2/7

Meteorology Research, Inc., Altadena, Calif.

STUDY AND MODIFICATION OF CONVECTIVE STORMS.

P. B. MacCready, Jr., T. B. Smith, C. J. Todd, C. W. Chien, E. Woodward

Rept. No. 2 for 1 Apr. 1962 - 30 Mar. 1963. 129 p.

incl. illus. tables photographs (Rept. No. MRI63 FR-77)

(Contract DA-36-039 SC-89066, Proj. No. 3A99-27-005-06)

(ARPA Order No. 265-62) Unclassified report.

This report describes objectives, instrumentation, analysis techniques, conclusions, and recommendations of the first year of a basic research field investigation of cloud physics, cloud dynamics, and cloud modification at Flagstaff, Ariz., July-August 1962. Two instrumented aircraft, two ground radars, and a photographic network measured microphysics and cloud dynamics parameters of natural and seeded cumulus clouds of various sizes. Results include: (a) the new field measurement and analysis techniques proved adequate for meeting the program aims; (b) ice crystals introduced by dry ice and silver iodide seeding were found at appropriate cloud locations; (c) cloud droplets were numerous (300 to 700/cm^3), and small (< 20 microns diameter) and did not grow significantly by coalescence; (d) aircraft measurements in spirals in upcurrent cores to as high as 9000 feet above cloud base showed air could be undiluted at such heights; (e) the heating effect of glaciation on buoyancy was found by in-cloud temperature measurements and time-lapse cloud growth studies; (f) cloud cell rise rates compared satisfactorily with buoyancy measurements and laboratory tests and theory; (g) a distinct wake effect was often observed downwind of the mountain, which interacted with surface heating effects to generate long lasting upcurrent areas in midmorning and again in midafternoon; (h) consistent, long lasting, large updraft charges were observed, predominantly positive in the ice phase switching rather abruptly to negative at the level where melting was complete.

UNCLASSIFIED

1. Clouds-Physical properties.
2. Clouds-Electrical properties.
3. Cumulus clouds-Growth
I. Title: Project Baton
II. MacCready, Jr., P. B.
III. U. S. Army Electronic R&D Lab Ft. Monmouth, N. J.
IV. Contract DA-36-039 SC-89066

Div. 2/7

Meteorology Research, Inc., Altadena, Calif.

STUDY AND MODIFICATION OF CONVECTIVE STORMS.

P. B. MacCready, Jr., T. B. Smith, C. J. Todd, C. W. Chien, E. Woodward

Rept. No. 2 for 1 Apr. 1962 - 30 Mar. 1963. 129 p.

incl. illus. tables photographs (Rept. No. MRI63 FR-77)

(Contract DA-36-039 SC-89066, Proj. No. 3A99-27-005-06)

(ARPA Order No. 265-62) Unclassified report.

This report describes objectives, instrumentation, analysis techniques, conclusions, and recommendations of the first year of a basic research field investigation of cloud physics, cloud dynamics, and cloud modification at Flagstaff, Ariz., July-August 1962. Two instrumented aircraft, two ground radars, and a photographic network measured microphysics and cloud dynamics parameters of natural and seeded cumulus clouds of various sizes. Results include: (a) the new field measurement and analysis techniques proved adequate for meeting the program aims; (b) ice crystals introduced by dry ice and silver iodide seeding were found at appropriate cloud locations; (c) cloud droplets were numerous (300 to 700/cm^3), and small (< 20 microns diameter) and did not grow significantly by coalescence; (d) aircraft measurements in spirals in upcurrent cores to as high as 9000 feet above cloud base showed air could be undiluted at such heights; (e) the heating effect of glaciation on buoyancy was found by in-cloud temperature measurements and time-lapse cloud growth studies; (f) cloud cell rise rates compared satisfactorily with buoyancy measurements and laboratory tests and theory; (g) a distinct wake effect was often observed downwind of the mountain, which interacted with surface heating effects to generate long lasting upcurrent areas in midmorning and again in midafternoon; (h) consistent, long lasting, large updraft charges were observed, predominantly positive in the ice phase switching rather abruptly to negative at the level where melting was complete.

UNCLASSIFIED

1. Clouds-Physical properties.
2. Clouds-Electrical properties.
3. Cumulus clouds-Growth
I. Title: Project Baton
II. MacCready, Jr., P. B.
III. U. S. Army Electronic R&D Lab. Ft. Monmouth, N. J.
IV. Contract DA-36-039 SC-89066

Contract DA 36-039 SC-89066
Meteorology Research, Inc.

DISTRIBUTION LIST

Address	No. of Copies
ARDC Liaison Office, U. S. Army Electronics Research and Development Laboratory, ATTN: SELRA/SL-LSW, Fort Monmouth, New Jersey	1
U. S. Navy Electronics Liaison Office, U. S. Army Electronics Research & Development Laboratory, ATTN: SELRA/SL-LNS, Fort Monmouth, New Jersey	1
USCOMARC Liaison Office, U. S. Army Electronics Research & Development Laboratory, ATTN: SELRA/SL-LNP, Fort Monmouth, New Jersey	1
Commanding Officer, U. S. Army Electronics Research & Development Laboratory, ATTN: SELRA/SL-DR, Fort Monmouth, New Jersey	1
Commanding Officer, U. S. Army Electronics Research & Development Laboratory, Fort Monmouth, New Jersey, ATTN: SELRA/SL-ADT	1
Commanding Officer, U. S. Army Electronics Research & Development Laboratory, ATTN: SELRA/SL-ADJ (Responsible File & Record Unit), Fort Monmouth, New Jersey	1
Commanding Officer, U. S. Army Electronics Research & Development Laboratory, ATTN: SELRA/SL-TWR, Fort Monmouth, New Jersey	17
OASD(B&E), Rm 3E1065, The Pentagon, ATTN: Technical Library, Washington 25, D. C.	1
Office of the Chief Research & Development, Department of the Army, ATTN: CRD/M, Washington 25, D. C.	1
Commanding General, U. S. Army Electronics Command, ATTN: ANSEL-RE, Fort Monmouth, New Jersey	1
Commanding General, U. S. Army Material Command, ATTN: AMCRD-RS-ES-A, Dept. of the Army, Washington 25, D. C.	1

Distribution List (Contd)

Address	No. of Copies
Director, U. S. Naval Research Laboratory, ATTN: Code 2027, Washington 25, D. C.	1
Director, Advanced Research Project Agency, ATTN: Colonel A. P. Gagge, Washington 25, D. C.	1
Commander, WADD (WCOSI-3), Wright-Patterson Air Force Base, Ohio	2
Commanding Officer and Director, U. S. Navy Electronics Laboratory, San Diego 52, California	1
Commander, Air Force Cambridge Research Laboratories, ATTN: CRIL-R, L. G. Hanscom Field, Bedford, Mass.	1
RADC (RAALD), Griffiss AFB, New York, ATTN: Documents Library	1
Commanding Officer, U. S. Army Electronics Research & Development Activity, ATTN: Technical Library, Fort Huachuca, Arizona	1
Commander, Armed Services Technical Information Agency ATTN: TIPDR, Arlington Hall Station, Arlington 12, Virginia	10
Commander, Air Force Cambridge Research Laboratories ATTN: CRZC, L. G. Hanscom Field, Bedford, Mass.	1
Chairman, U. S. Army Chemical Corps Meteorological Committee, Fort Detrick, Frederick, Maryland	1
Chief, Meteorology Division, U. S. Army Chemical Corps Proving Ground, Dugway, Utah	1
Chemical Research & Development Laboratories, Technical Library, Army Chemical Center, Edgewood, Maryland	1
Director, Atmospheric Sciences Programs, National Science Foundation, Washington 25, D. C.	1
Director, Bureau of Research & Development, Federal Aviation Agency, Washington 25, D. C.	1
Chief, Bureau of Naval Weapons (FANE), U. S. Navy Dept., Washington 25, D. C.	1

Distribution List (Contd)

Address	No. of Copies
Chief, Fallout Studies Branch, Division of Biology and Medicine, Atomic Energy Commission, Washington 25, D. C.	1
Officer-in-Charge, Meteorological Curriculum, U. S. Naval Post Graduate School, Monterey, California	1
Chief of Naval Operations (OP 07), U. S. Navy Department, Washington 25, D. C.	1
Office of Naval Research, U. S. Navy Department, Washington 25, D. C.	1
Director, U. S. Naval Weather Service, U. S. Naval Station, Washington 25, D. C.	1
Officer-in-Charge, U. S. Naval Weather Research Facility, U. S. Naval Air Station, Bldg. R48, Norfolk, Virginia	1
U. S. Army Cold Regions Research Engineering Laboratory, Hanover, New Hampshire	1
U. S. Army Corps of Engineers, Waterways Experiment Station, P. O. Box 631, Vicksburg, Mississippi	1
Office of the Chief of Ordnance, Department of the Army, Washington 25, D. C.	1
Commanding General, Army Missile Command, Physical Sciences Lab., ATTN: AMSMIRRA, Dr. O. M. Essenwanger, Redstone Arsenal, Ala.	1
Commanding Officer, U. S. Army Electronics Research & Development Activity, ATTN: Missile Geophysics Division, White Sands Missile Range, New Mexico	1
Chief, West Coast Office, U. S. Army Research & Development Laboratory, 75 South Grand Avenue, Bldg. 6, Pasadena 2, Calif.	1
The American Meteorological Society, Abstracts & Bibliography, P. O. 1736, ATTN: Mr. M. Rigley, Washington 13, D. C.	1
Office of Technical Services, Department of Commerce, Washington 25, D. C.	1
Mr. K. W. Johnson, Johnson-Williams, Inc., P. O. Box 1307, Station A, Palo Alto, California	1

Distribution List (Contd)

Address	No. of Copies
Library, National Bureau of Standards, Washington 25, D. C.	1
U. S. Naval Air Missile Test Center, ATTN: Mr. Masterson Meteorological Division, Point Mugu, California	1
Director, National Weather Records Center, Arcade Building ATTN: Mr. Fox, Asheville, North Carolina	1
Director, Federal Aviation Agency, ATTN: Mr. Nilsenrod, Pomona, New Jersey	1
U. S. Army Electronics RD Laboratory Liaison Office, ATTN: Mr. A. D. Bedrosian, Massachusetts Institute of Technology, 77 Massachusetts Avenue, Room 26-131, Cambridge, Mass.	1
Library, U. S. Weather Bureau, Washington 25, D. C.	1
Brookhaven National Laboratories, Camp Upton, New York	1
Climatic Center, U. S. Air Force, Annex 2, 225 D Street, SE, Washington 25, D. C.	1
Director of Meteorology Research, Weather Bureau, Washington 25, D. C.	1
Mr. C. Gentry, National Hurricane Research Project, Aviation Bldg., Rm 517, 3240 N. W. 27th Avenue, Miami 42, Florida	1
Stanford Research Institute, Menlo Park, California	1
The University of Texas, Electrical Engineering Research Laboratory, Austin, Texas, ATTN: Mr. Gerhardt	1
Department of Meteorology, University of Wisconsin, Madison, Wisconsin	1
Institute for Geophysics, University of California, Los Angeles, California, ATTN: Dr. C. Palmer	1
Department of Meteorology, University of Washington, Seattle, Washington, ATTN: Dr. Buettner	1
Department of Meteorology, Texas A&M College, College Station, Texas, ATTN: Dr. W. Clayton	1

Distribution List (Contd)

Address	No. of Copies
Meteorology Department, Florida State University ATTN: Dr. La Seur, Tallahassee, Florida	1
Meteorology Department, University of Chicago, ATTN: Dr. Fujita, Chicago, Illinois	1
Meteorology Department, University of Chicago, ATTN: Dr. A. R. Braham, Jr., Chicago, Illinois	1
Illinois State Water Survey, University of Illinois, ATTN: Mr. G. Stout, Urbana, Illinois	1
Department of Meteorology and Oceanography, New York University, College of Engineering, University Heights, New York 53, New York	1
Meteorology Department, Pennsylvania State College, State College, Pennsylvania	1
Mr. H. Hiser, Radar Met Section, University of Miami, Miami, Florida	1
Dr. E. B. Kraus, Woods Hole Oceanographic Institute, Woods Hole, Massachusetts	1
Dr. A. Belmont, General Mills Electronics Group, 2003 E. Hennepin Avenue, Minneapolis 13, Minnesota	1
Dr. H. Riehl, Department of Atmospheric Science, Colorado State University, Fort Collins, Colorado	1
Dr. E. Kessler, Travelers Research Center, 650 Main Street, Hartford 3, Connecticut	1
Dr. W. Saucier, University of Oklahoma, Norman, Oklahoma	1
Dr. C. Ramage, Department of Meteorology and Oceanography, University of Hawaii, Honolulu 44, Hawaii	1
Department of Meteorology, Massachusetts Institute of Technology, Cambridge 39, Massachusetts	1